國立臺灣大學生命科學院生態學與演化生物學研究所

博士論文

Institute of Ecology and Evolutionary Biology

College of Life Science

National Taiwan University

Doctoral dissertation

臺灣欒樹的抗張材在傾斜苗木與枝條的
解剖構造與生物力學功能

Anatomical Structure and Biomechanical Function of
Tension Wood in Inclined Seedlings and Branches
of *Koelreuteria henryi* Dummer

洪麗分

Li-Fen Hung

指導教授：黃玲瓏 博士

Advisor: Ling-Long Kuo-Huang Ph.D.

中華民國 106 年 6 月

June, 2017

國立臺灣大學博士學位論文
口試委員會審定書

臺灣欒樹的抗張材在傾斜苗木與枝條的
解剖構造與生物力學功能

Anatomical Structure and Biomechanical Function of Tension Wood in Inclined Seedlings and Branches of *Koelreuteria henryi* Dummer

本論文係洪麗分君（學號D97B44007）在國立臺灣大學生態學與演化生物學研究所完成之博士學位論文，於民國106年1月5日承下列考試委員審查通過及口試及格，特此證明

口試委員：

國立中興大學森林學系	黃彥三博士	
行政院農業委員會林業試驗所育林組	簡慶德博士	
國立自然科學博物館生物學組	邱少婷博士	
國立中興大學生命科學系	蕭淑娟博士	
國立臺灣大學醫學工程學研究所	王兆麟博士	
國立臺灣大學森林環境暨資源學系	林法勤博士	
國立臺灣大學生態學與演化生物學研究所	黃玲瓏博士	

所長　高文媛

中華民國 106 年 1 月 5 日

i

致謝

　　能在不惑之年結束之前完成博士學位，真的要歸功於老天爺的安排以及身邊師長親友的鼓勵與陪伴。首先要感謝我的指導教授黃玲瓏老師，我們的師生緣起於 1991 年，有幸成為黃老師的第一個碩士生，感受到老師亦師亦母的指導與照顧。畢業之後，不忘師恩教誨，努力在學業、家業與事業中取得平衡。因緣際會之下，2008 年回到實驗室，成了黃老師的第一個博士生，亦師亦友的黃老師除了傳道、授業與解惑外，更帶著我成長並分享生活中的喜怒哀樂，衷心感謝您對我的愛護與付出。我也要謝謝黃彥三老師在我論文研究期間的諄諄教誨與耐心指導，感謝您帶我進入生物力學的世界，讓我的論文研究得以順利進行。謝謝高文媛老師、邱少婷老師與簡慶德老師擔任我的資格考口試委員，提供寶貴的意見，引導我建立完整的研究計畫；更要感謝邱少婷老師、蕭淑娟老師、簡慶德老師、王兆麟老師與林法勤老師在百忙之中，擔任我的口試委員，細心審查並協助我修正論文的細節，讓我的博士論文得以完成。也謝謝陳淑華老師在課業上的教授與生活上的關懷，李鳳鳴老師在我擔任普植實驗助教時的協助與鼓勵。

　　感謝植物解剖研究室的大學姊陳香君老師，您給予的不只是研究技術與材料的支持，還有生活上點點滴滴的協助。有了您，生活變得更容易。謝謝萬能學長與秋容的鼓勵、金梅的技術協助，以及學弟妹們的支援與陪伴：沒有馨竹，我的論文難以產生，謝謝你一路陪著我做研究,寫論文；感謝瑋育和育銘陪著我採樣與切片；謝謝資棟、瑋庭、彥佑、靖玫、哲瑜、綱祐、恬君和名偉，是你們讓我跟得上時代，保持青春與活力。感謝高家的學弟妹們，雅倫、孟穎、泰中、佳娟、顯淳、怡清、譯泯、麗智、渼晨、昆松、彥治⋯讓我有地方串門子，調劑生活。

　　要特別感謝所辦月鈴助教協助打理從入學到畢業過程中的學業與生活瑣事。也要感謝博班的同學們，妤馨、欣怡、孟穎、冠霆、敬舒、勵婉，相伴一起走過博班生活的酸甜苦澀。感謝和我一起帶實驗課的所有助教們，特別是月鈴、聖傑、英超、馨儀、玉玲和小米，我從你們的教學方式中獲得啟發，勇於嘗試新方法；也謝謝亞臻、以君和佩穎支援生物電顯實驗；更要謝謝被我帶過實驗課的學生們，是你們活化我的教學細胞，讓我發揮所長，享受工作的樂趣。

　　感謝我的家人，謝謝爸爸媽媽無為而治的教育方式，讓我得以適性發展；謝謝大哥大嫂的厚愛，也謝謝麗雀、麗文兩個妹妹的陪伴與分享。我把最深沉的感激留給與我相依相伴的先生耀銘和兒女俐安與柏宇，是你們無限的包容、支持與愛，讓我得以實現自我，謝謝。最後，給在天上的弟弟源倉，願與你一起分享這份成就與喜悅。

中文摘要及關鍵詞

抗張材在維持被子植物的生物力學穩定上扮演重要的角色，因此在研究傾斜主幹恢復直立以及枝條角度變化的機制時，必須同時關注抗張材的生物與物理特性。本論文以台灣欒樹為材料，研究在恢復直立的傾斜樹苗主幹中以及樹冠不同角度的枝條內，抗張材的形成、構造與分布等生物特徵以及應變分布的物理特徵，以期了解抗張材在傾斜主幹與不同角度枝條中所扮演的角色。

在人為傾倒的兩年生台灣欒樹樹苗主幹中，抗張材的生成與恢復直立的過程歷時約三個月。透過插針法，我們確認：當樹苗傾倒時，主幹上側的形成層區包含形成層與發育中的木質部纖維細胞均感受到力學變化（相對位置的改變），開始形成抗張材，其中的膠質纖維可產生強烈的收縮應變，將主幹拉回到直立的位置。在傾斜主幹之基部形成的抗張材比在半株高處者多，產生的收縮應變也較大，顯示在台灣欒樹樹苗傾斜主幹恢復直立的過程中，主幹基部扮演較關鍵的角色。此外，傾斜主幹伴隨上側抗張材形成的偏心生長有助於主幹恢復直立，而在主幹下側部分測量點所量到的壓縮應變亦可靠著推力協助主幹恢復直立。針對樹冠之不同角度枝條的研究則顯示，台灣欒樹枝條內存在著和傾斜主幹不同的應變分布、抗張材分布與偏心生長。枝條之生長應變參數隨著木材細胞次生細胞壁的成熟而有季節性的變化；角度大的傾斜枝條上下側可能具有收縮或壓縮應變，然而角度較小的近直立枝條的上下側多為收縮應變，顯示這兩種枝條可能具有不同的功能。抗張材可能分布在枝條的各個位置，和抗張材主要分布在傾斜樹苗主幹的上側不同，因此，抗張材有助於枝條角度的動態調整。枝條的偏心生長位於枝條下方，可能阻礙枝條的上揚，甚至促進枝條的下壓。枝條上多樣的應變分布與抗張材分布，顯示各枝條可能為了因應環境因子如重力和光線的差異，而有不同的生物力學需求。
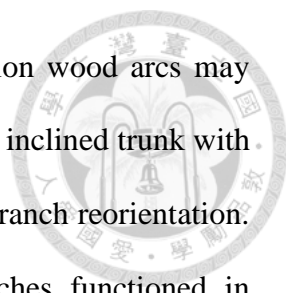

關鍵詞 台灣欒樹、生長應力、生長應變、生物力學、抗張材、枝條、偏心生長、插針法、傾斜主幹、彎曲傾向

英文摘要及關鍵詞

Abstract

Tension wood plays a role in maintaining the mechanical stability of angiosperm trees. Both biological and physical aspects of tension wood are essential in understanding the mechanism of trunk or branch reorientation. In this dissertation, we first worked on both the tension wood formation and its biomechanical function in artificially inclined 2-year-old *Koelreuteria henryi* seedlings. The tension wood formation and reorientation process of the trunk last for about 3 months. With pinning method, we confirmed that at the beginning of inclination the cambial zone including the vascular cambium and the developing normal wood fibers on the upper side of the inclined trunk perceives the onset of mechanical change and starts to produce G-fibers that generate a strong contractile released growth strain (RGS) for gravitropic correction. Stronger contractile RGS and more tension wood were found at the trunk base than at the half-height, suggesting that the trunk base plays a key role in trunk uprighting of *K. henryi* seedlings. The eccentric cambial growth in the tension wood side increases the efficiency of gravitropic correction and the compressive strains measured in the opposite wood of some inclined seedlings also help the upright movement. Then we further discriminated the biomechanical behavior of branches from leaning trunks. We thus investigated the development of growth strains, distribution of tension wood, and eccentricity on the branchwood of *K. henryi*. The results revealed the unusual distribution of released growth strain and tension wood as well as growth eccentricity. The growth strain parameter showed seasonal changes, possibly due to the maturation of secondary cell wall. Both sides of the plagiotropic branches exhibited either contractive or extensive growth strains, whereas the orthotropic branches exhibited mostly contractive strains on both sides, which implied
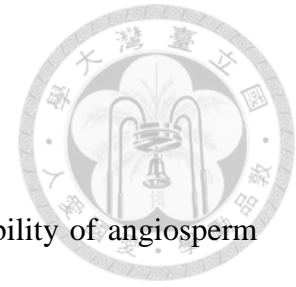
different physiological function of the two branch types. The tension wood arcs may occur in any direction of the branchwood which is different from the inclined trunk with tension wood on the upper side, suggesting dynamic adjustment in branch reorientation. In contrast to trunks, the hypotrophic eccentric growth in branches functioned in obstructing upward movement and even facilitates downward movement, probably because the dissociation between tension wood and eccentric growth. Diversified growth strain and tension wood distribution on the branches may reflect the individual biomechanical requirements for each branch depending on the environmental factors, possibly gravitropic and phototropic stimuli.
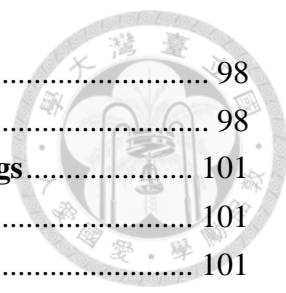
目錄

Index of Figures

x

Index of Tables

Introduction

Trees keep the mechanical stability by adjusting the position of their trunk and branches in response to various environmental disturbances and gravitational stimulus (Ewart and Mason-Jones 1906; Fisher and Stevenson 1981; Gardiner et al. 2014; Sinnott 1952; Wilson and Archer 1979). Leaning tree trunks and branches could reorient to an equilibrium position by producing reaction wood accompanying increased cambial growth. The characteristics of the reaction wood including anatomical and physical aspects are different in gymnosperms and angiosperms. In gymnosperms, compressive growth stress induced by compression wood is generated on the lower side to push the leaning trunk and branches upward. However, in angiosperms, tension wood generally develops on the upper side and produces tensile stress to pull the leaning trunk or branches upward (Onaka 1949; Scurfield 1973; Sinnott 1952; Wilson and Archer 1977).

Anatomical characteristics of reaction wood

Macroscopic Appearance

Compression wood in gymnosperms is usually darker in color, from brown to dark reddish brown depending on species, which leads the name "Rotholz (red wood)" in the German literature. It is an extremely hard and brittle wood with a higher density than normal wood (Timell 1986a; Wardrop and Dadswell 1950). The occurrence of compression wood is associated with hypotrophic eccentric growth, i.e., the promoted growth increment on the lower side and the pith toward the upper side of the leaning trunk and branches. Therefore the growth ring is normally wider on the lower side. (Gardiner et al. 2014; Timell 1986b)

When sawed in the green condition tension wood is likely to leave a rough, woolly

1

surface (Clarke 1939; Gardiner et al. 2014). Because of the silvery appearance tension wood in temperate hardwood is called "Weissholz (white wood)" in the German literature. However, dark streaks are sometimes visible in the tension wood of tropical species. The occurrence of tension wood is generally accompanied with epitrophic eccentric growth, i.e., the promoted growth increment on the upper side and the pith toward the lower side of the leaning trunk (Gardiner et al. 2014; Timell 1986b). Nevertheless, the association of tension wood and growth eccentricity is ambiguous in branches of angiosperms (Kučera and Philipson 1977a; Patel et al. 1984; Tsai et al. 2012; Wang et al. 2009) and awaits further investigation to understand the effect of growth eccentricity on the bending of branches.

By the shiny appearance under a low-angle natural light on the fleshly saw disks of poplar cultivars, tension wood areas can be quickly identified, and made it possible for a large scale research (Badia et al. 2005). Besides, brushing the surface of a wood disc with zinc chloro-iodide solution (Herzberg's reagent) is an efficient and popular method for investigating tension wood areas. Because the chlorine destroys hydrogen bonds between macro-polymers of cellulose and thus facilitates the accumulation of iodine molecules which colors tension wood to be light purple to violet (Doğu and Grabner 2010; Grzeskowiak et al. 1996; Wardrop and Dadswell 1948).

Cellular Structure

Comparing to the more rectangular to hexagonal normal wood tracheids without intercellular space, the tracheids of compression wood are shorter in length and round in cross section with intercellular spaces. The cell wall of a normal wood tracheid or fiber is composed of a primary wall (P) and a secondary wall consisting S1, S2, and / or S3 layers. The secondary wall of compression wood tracheids possesses a relative thick S2 layer

2

with larger microfibril angle (MFA) and a higher lignin content but lacks S3 layer. The thick and heavily lignified cell wall of compression wood tracheids often shows cracks. (Timell 1986a; Wardrop and Dadswell 1950).
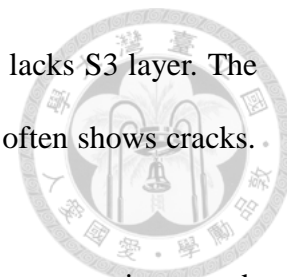
The structure of tension wood is not as consistent as that of compression wood. Typical tension wood is featured by the gelatinous fibers (G-fibers) with the S2 and/or S3 layers replaced by a special gelatinous layer (G-layer) which consists of highly crystalline cellulose fibrils that are almost parallel to the fiber axis, i.e., with smaller MFA (Scurfield 1973; Wardrop and Dadswell 1948). The G-layer has been presumed to be composed of nearly pure crystalline cellulose (Norberg and Meier 1966), however, some authors (Araki et al. 1983; Pilate et al. 2004; Scurfield and Wardrop 1963) have reported a slight deposition of lignin in the G-layer, especially in transitional regions between normal and tension wood. Besides, in addition to cellulose, the G-layer may also contain other polysaccharides including pectin and hemicellulose (Bowling and Vaughn 2008).

In angiosperms, not all of them produce typical tension wood with G-fibers. Onaka (1949) found that 79 % of 346 angiosperms produce G-fibers. Höster and Liese (1966) examined 266 trees/shrubs and found only ca. 50% of the investigated species exhibit G-fibers in branchwood and ca. 25 % in root wood. Fisher and Stevenson (1981) detected G-fibers on the upper side of the branches in 46% of 122 dicotyledonous species in 46 families. Besides, *Buxus microphylla* var. *insularis* Nakai even produces compression wood on the lower side of the leaning trunks, exemplifying the considerable diversified reaction anatomy in angiosperms (Yoshizawa et al. 1993a; Yoshizawa et al. 1993b).

Among species producing G-fibers, there are variations existing in their cell wall structure. G-fibers may contain cell walls consisting P+S1+G, P+S1+S2+G, or P+S1+S2+S3+G (Scurfield 1973; Wardrop and Dadswell 1955). Besides, a special polylaminate secondary wall structure with an alternate of lightly lignified thick layers

3
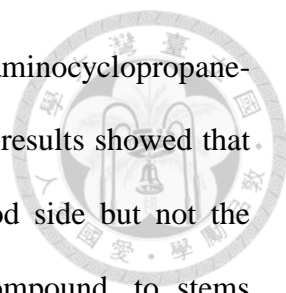
and more lignified thin layers was found in tension wood of *Casearia javitensis* (Clair et al. 2006c) and *Laetia procera* (Poepp.) Eichl (Ruelle et al. 2007b) in Flacourtiaceae family. In the species producing tension wood without G-fibers, the decreasing of vessel frequency seems to be a general feature among quantitative anatomical criteria (Ruelle et al. 2006).

The role of plant hormones in reaction wood formation

Plant hormones including auxin, ethylene, and gibberellin were involved in the formation of reaction wood. The regulatory role of hormone in reaction wood formation have been studied by both locally applying the hormone and/or its inhibitors and by quantifying endogenous hormone during reaction wood formation (for review, see Du and Yamamoto 2007; Gardiner et al. 2014; Hellgren et al. 2004)

The results of application experiments suggested that a high level of IAA is associated with the induction of compression wood in gymnosperms and a low level of auxin for tension wood in angiosperms (for review, see Du and Yamamoto 2007; Gardiner et al. 2014). On the other hand, the studies concerning endogenous IAA quantification often yielded contradictory results (Funada et al. 1990; Wilson et al. 1989). These early experiments can hardly be explained or compared due to coarse and incongruous sampling criterion. Until the high spatial-resolution quantification of endogenous IAA was carried out across the cambial region, Hellgren et al. (2004) disproved the regulatory role of IAA level in reaction wood formation. They suggested that other factors such as auxin perception mechanisms or additional signals are involved in reaction wood formation.

While there is no report of G-layer induction by ethylene treatments (Gardiner et al 2014), the hormone has been associated with compression wood differentiation. Savidge

4
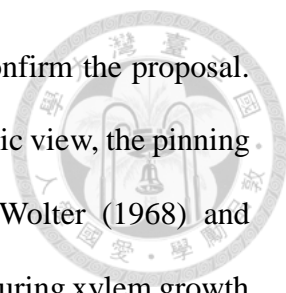
et al. (1983) measured the endogenous ethylene precursor (ACC, 1-aminocyclopropane-1-carboxylic acid) in the vascular cambium of *Pinus* branches. The results showed that the endogenous ACC was only detected on the compression wood side but not the opposite wood side. Applying ethrel, an ethylene–generating compound, to stems stimulated wood production in both woody gymnosperms (Yamamoto and Kozlowski, 1987) and angiosperms (Yamamoto et al. 1987); however, the anatomical features of the induced wood tissue are different from compression wood and tension wood (Gardiner et al. 2014). The regulatory role of ethylene in reaction wood formation need to be confirmed with further investigation.

In gymnosperms, the possibility of a role of gibberellins in compression wood formation has not yet been demonstrated (Gardiner et al. 2014). However, GAs have been suggested to play an important role in tension wood formation. Applying gibberellin promotes the formation of well-defined tension wood in artificially-tilted angiosperm seedlings (Baba et al. 1995; Nugroho et al. 2012; Yoshida et al. 1999). Moreover, the exogenous gibberellin induces the tension wood formation on vertical stems without gravitational stimulus (Funada et al. 2008). Besides, the application of inhibitors of gibberellin biosynthesis suppresses the increases in the thickness of gelatinous layers and the elongation of gelatinous fibers (Nugroho et al. 2013). These results suggested that GAs, at least, mediate the development of gelatinous fibers.

The onset and formation of reaction wood and the pinning method

Scurfield (1972) and Jourez and Avella-Shaw (2003) have proposed that at the onset of tilting, the differentiating xylary fiber cells in different stages may react to gravitational stimulus and add a G-layer in the innermost cell wall. The quick transformation from developing cells to G-fibers allows the plant to promptly recover to an equilibrium

position. However, the authors did not provide direct evidence to confirm the proposal. For studying the onset and formation of reaction wood in a microscopic view, the pinning method could be helpful. This method was first introduced by Wolter (1968) and improved by Yoshimura et al. (1981) and is a precise method for measuring xylem growth by marking the position of cambial zone at the time of pinning. Practically, a pin or a needle is inserted through the bark, the cambium zone to the xylem tissue for inducing the wound reaction of the cambial cells by the minute mechanical injury (Seo et al. 2007; Wolter 1968; Yoshimura et al. 1981). Since it can be difficult to gain good sections from the center region of the tiny wound, some authors (Kuroda and Kiyono 1997; Veenin et al. 2006) used knife incision instead of needle or pin insertion, and thus called it as the wounding method.

The pinning technique has been employed to monitor seasonal dynamics of cambial activity or wood formation in *Picea abies* (L.) Karst. (Gričar et al. 2007; Mäkinen et al. 2003; Nocetti and Romagnoli 2008), *Pinus sylvestris* and *Betula* spp. (Schmitt et al. 2004), *Hevea brasiliensis* (Ohashi et al. 2001) and *Eucalyptus camaldulensis* Dehnh (Veenin et al. 2006); as well as intra-seasonal growth of *Toona ciliata* (Heinrich and Banks 2002). It was also used to investigate the secondary growth via successive cambia in mangrove species *Avicennia marina* (Schmitz et al. 2008). The pinning method has been also applied in the study on compression wood formation of Japanese larch (Yamaguchi et al. 1983) and slash pine (Nix and Brown 1987). In the research of tension wood formation, Mukogawa et al. (2003) marked the vascular cambium with a knife instead of a pin to observe the eccentric growth of leaning trees in a macroscopic view. To study the phototropic and negative gravitropic bending, Matsuzaki et al. (2007) used the pinning method to mark the radial direction and measured possible torsion of the main stem. To distinguish the tension wood produced after the inclination treatment, Jourez et al. (2001)

6

bent the pot and the shoot in the opposite direction of natural incline. In this study, we attempted to identify the origin of G-fiber by the pinning method.
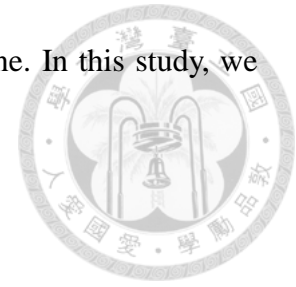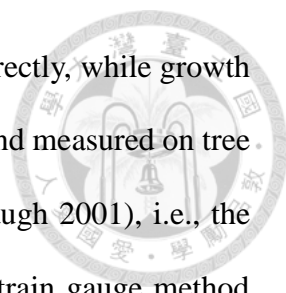
Physical characteristics of reaction wood

Growth stress and growth strain

The growth stress originates in the cambial zone when growing wood cells contract in the longitudinal direction and expand in the transverse direction during differentiation and maturation. Since the contraction is impeded by older cells, the new cells generate longitudinal tensile stress; and the obstruction of the lateral expansion by neighbor cells results in tangential compressive stress (Kubler 1987; Münch 1938). In a vertical trunk, there is a longitudinal stress gradient from the periphery inward along the radius, i.e., tensile stresses in the newly formed wood and compressive stresses near the pith (Archer 1986; Dinwoodie 1966; Jacobs 1945). In gymnosperms, a strong compressive stress occurs on the lower side of the leaning stem; whereas in angiosperms, a strong tensile stress on the upper side (Onaka 1949; Scurfield 1973). These growth stresses perform essential biomechanical functions related to the curvature change of the trunk and branches, which ultimately affecting the tree architecture and its survival strategy. (Alméras and Fournier 2009; Huang et al. 2010; Moulia et al. 2006; Washusen et al. 2003b; Wilson and Archer 1977). However, when trees are felled or wood is processed, these growth stresses are released and the resultant splits, cracks, and warp cause the loss of potential economic value (Clarke 1939).

The growth strain, a consequence of relief of growth stresses, is the dimensional change per unit original length. Within the proportional limit of elasticity, level of growth stress is a function of growth strain and the elastic modulus of the wood (MOE). Growth

7
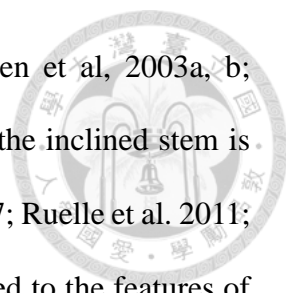
stresses, the force per unit area, are usually impossible to measure directly, while growth strains can be readily measured. The growth strains can be released and measured on tree or log surface by three major methods (Archer 1986; Yang and Waugh 2001), i.e., the Nicholson method (Nicholson 1971), the French method, and the strain gauge method (Yoshida et al. 1999). By measuring the strain, the corresponding stress can be calculated (Yang and Waugh 2001).

Generation of reaction stresses

The dispute about the generation of growth stress is based on the lignin swelling (Boyd 1972, 1973) and the cellulose tension (Bamber 1987, 2001) hypotheses. Boyd (1972, 1973) proposed that the lignification and associated transverse swelling of the cell wall induce the strains and growth stresses in normal wood and compression wood. However, the hypothesis cannot explain the generation of high tensile stress in tension wood, especially in G-fiber tension wood. As an alternative, Bamber (1987, 2001) proposed the cellulose tension hypothesis in which the stress of the both reaction woods arises from the spring-like cellulosic component of the wood. In compression wood, the S2 layer acts as compressed helical springs and thus exerting an extensive force to push the stem upright or to stabilize it. In tension wood, the microfibrils of the secondary wall and/or the G-layer are considered as stretched linear springs and thus developing a tensile stress to pull the stem upright or stabilize it. The role of lignin is to consolidate the compressive strength of compression wood rather than contribute to the generation of growth stress (Bamber, 2001). Besides, an idea that unifies the lignin swelling (Boyd, 1972) and the cellulose tension (Bamber 1987, 2001) hypotheses was proposed by Okuyama (1994).

In the past decade, many researches have been focused on the stress generation in

8
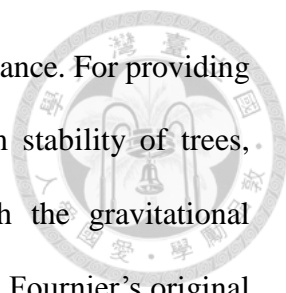
tension wood (Clair et al., 2006b; Goswami et al., 2008; Washusen et al, 2003a, b; Yoshida et al, 2002). The presence of G-fibers on the upper side of the inclined stem is correlated with high tensile growth strains or stresses (Fang et al. 2007; Ruelle et al. 2011; Washusen et al. 2003a). The mechanism of stress generation is related to the features of G-fibers including small MFA (Donaldson 2008; Okuyama et al. 1994), increased cellulose lattice spacing (Clair et al. 2011; Clair et al. 2006b) and high content of xyloglucan (Baba et al. 2009; Mellerowicz and Gorshkova 2012; Mellerowicz et al. 2008; Nishikubo et al. 2011). Besides, the magnitude of growth stress is influenced by the thickness of G-layer and the ratio of G-fiber area (Fang et al. 2008).

The study of growth strain distribution in angiosperm trees

Growth strains on naturally leaning or artificially tilted trunks (Alméras et al. 2005; Clair et al. 2006a, c; Dassot et al. 2012; Kuo-Huang et al. 2007; Ruelle et al. 2007b; Wang et al. 2009; Yamamoto et al. 2005; Yoshida et al. 2002) and branches (Kuo-Huang et al. 2007; Tsai et al. 2012; Wang et al. 2010; Wang et al. 2009; Yoshida et al. 1999; Yoshida et al. 2000b) have been investigated in several angiosperms. These studies revealed that on the upper side of both tilted trunks and branches exhibited contractive strains; however, on the lower side of the leaning trunks exhibited mostly contractive strains but the branches mostly extensive strains.

Biomechanical models

To explain the mechanism of upward bending process, Fournier et al. (1994a) presented a simple biomechanical model according the maturation strain asymmetry of a leaning trunk. Coutand et al. (2007) applied the model to investigate the gravitropic
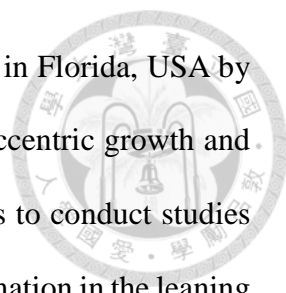
response of poplar trunks and found it limited to explain the total variance. For providing the theoretical predictions on biomechanical design and long-term stability of trees, Alméras and Fournier (2009) expanded the original model with the gravitational disturbance, eccentric growth, and heterogeneous stiffness. Based on Fournier's original model, Huang et al. (2010) developed an equivalent model by using spring-back strain (SBS) to evaluate self-weight bending moment and made the model practical and easy to follow. Huang's model has been successfully applied in the prediction of bending dynamics of broadleaf tree branches (Tsai et al. 2012).

Goals of this dissertation

The investigation of strain distribution, tension wood formation, growth eccentricity, and/or the physiological function in angiosperm trunks have received more attention and reached a consensus (Alméras et al. 2009; Coutand et al. 2014; Mukogawa et al. 2003; Washusen et al. 2003a, b; Yoshida et al. 2000a). In contrast, there are substantial controversies in studies of branches. Comprehensive studies concerning physical and anatomical properties in both trunk and branches of angiosperm trees are rare in the literature.

Koelreuteria henryi Dummer (synonym: *K. elegans* ssp. *formosana*) in Sapindaceae family is a deciduous tropical tree species with meandering branches. In Taipei, the tree starts to change leaf color and to lose leaves from late December and then flushes in next February in Taipei. Flowering and fruiting of *K. henryi* occurs for a relatively brief period from September to December. The terminal panicle florescence (up to 25 cm long) contains many flowers. The fruit is an inflated papery capsule (4 cm long) containing 6 globose seeds (5 mm across). It is endemic to Taiwan but is listed as an invasive species

10

in south-east Queensland, Australia (Batianoff and Butler 2002) and in Florida, USA by Florida Exotic Pest Plant Council (2015). The findings of unusual eccentric growth and released growth strain (RGS) distribution in its branches have led us to conduct studies for having a comprehensive insight into the role of reaction wood formation in the leaning trunk and branches during the tree form adjustment.

In the dissertation, we first monitored the reorientation process of the artificially inclined trunks of *K henryi* seedlings. The growth strain distribution and related eccentric growth were surveyed. Besides, we used the pinning method to directly identify the onset of G-fiber formation. The cell wall structure and distribution of G-fibers were also investigated. Huang's model (Huang et al. 2010) was applied for analyzing the bending dynamics of the inclined trunks. Then we measured the seasonal strain distribution of branches. To verify the physiological function of branches in building the tree architecture, we further investigated the bending tendency and its relationships with growth eccentricity and tension wood in orthotropic and plagiotropic branches. We proposed that strains on the branch may change seasonally. Furthermore, the branches of different angles or locations may have different bending tendency and the consequent physiological functions that are distinguished from the trunk.

Materials and Methods

Plant material and experimental design

Study on the reorientation process of the artificially inclined seedlings

To study the trunk reorientation process of *Koelreuteria henryi* seedlings, two greenhouse experiments were conducted. On Feb 18 2009, twenty-four 2-year-old seedlings germinated from seeds were purchased from a nursery in Changhua (central Taiwan). The naturally defoliated seedlings were transplanted in a 5-liter pot with Yang-Ming-Shan soil, perlite, vermiculite, and peat moss (1:1:1:1) and acclimated in the greenhouse of National Taiwan University (25°00′N, 121°27′E). On Apr. 23, the average height of seedlings was 82.9 ± 18.8 cm and the average basal diameter was 8.44 ± 0.94 mm. Twelve seedlings (T1~T12) were randomly selected and artificially inclined at an angle of about 30° (28.8 ± 2.7° (SD)) from vertical by placing the pots on fixed PVC pipes (Fig. 1a) and the other 12 seedlings (C1~C12) were kept upright as controls. The height and diameter growth of all seedlings were monitored during the experiment (Appendix Ⅰ). The trunk base (at 10 cm above the soil) and the half-height of all seedlings were pre-marked with white-out for subsequent RGS measurement. The bark of each seedling at 1 cm below the measuring site was pinned by an insect needle (0.4 mm in diameter) on the upper and the lower sides of the inclined seedlings and the corresponding A and B sides of the control seedlings. By pinning, the cambial zone was wounded and triangular callus tissue was formed and thus marked the location of vascular cambium at the pinning time (Yoshimura et al. 1981) (Appendix Ⅱ). We monitored the uprighting process of the inclined seedlings. Seasonally, we measured RGSs of the seedlings and investigated the related anatomical structures. We also applied Huang's model (Huang et al. 2010) to analyze the bending dynamics.

12

On Apr. 25, 2012 we started a similar experiment with monthly sampling for three months. The nine studied seedlings (C13~15 for control and T13~T18 for inclination) were obtained through pruning the stems of the seedlings above the soil in 2011 and left one epicormic shoot to become the main stem. The average height was 103.2 ± 12.6 cm and the average basal diameter was 9.54 ± 0.92 mm. One control and two inclined seedlings were sampled monthly for measuring RGSs, examining the tension wood formation, and then predicting the bending tendency.
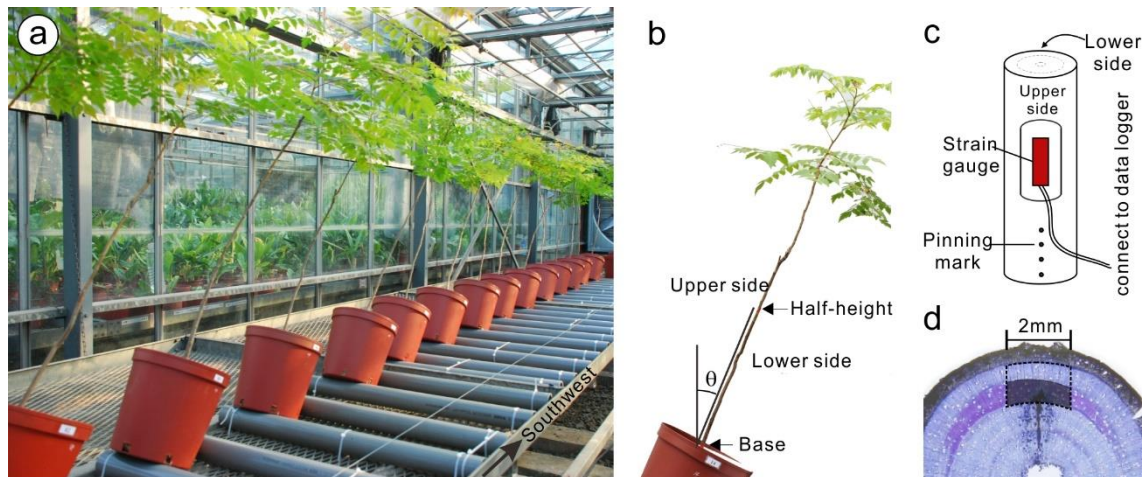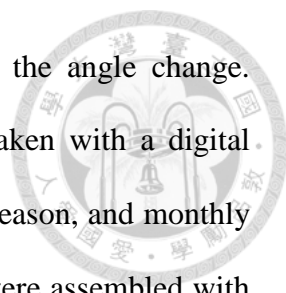
Figure 1. Experimental design for studying reaction wood formation in inclined *Koelreuteria henryi* seedlings.

a Photograph of the inclined seedlings at the beginning of inclination. The experiment was conducted in the green house and each pot was placed on a pair of fixed PVC pipes to set the tilting angle. **b** Picture showing the RGS measuring sites (the base and the half-height of the trunk) and the positions (the upper and the lower sides of the inclined trunk). Pictures of each inclined seedling were taken weekly to monthly and from which the proximal angles (θ) (the angle of the line joining the trunk base and the half-height to the vertical) were measured. **c** Illustration of the locations of pinning marks and RGS measurement. **d** Illustration of tension wood ratio measurement: dotted line outlining the measured whole wood area and grey area marking the area of tension wood

13

To study the dynamics of uprighting process, we monitored the angle change. Pictures of each inclined seedling of the 2009-experiment were taken with a digital camera (Nikon D3) weekly for the 1st season, biweekly for the 2nd season, and monthly for the 3rd and 4th seasons (Fig. 1b). Photographs of each seedling were assembled with Photoshop CS5 to examine the trunk shape evolution during the uprighting process. Because the radius of curvature is large in the inclined trunk of *K. henryi* seedlings, the proximal angle (θ) (Fig. 1b) of each seedling was measured from the pictures using Image J and then used to analyze the uprighting process.

Study on the distribution of growth strain and reaction wood of the branches

The studied 13 plagiotropic and 8 orthotropic branches were randomly selected from *Koelreuteria henryi* trees (with a DBH from 12 to 24 cm) on the main campus of National Taiwan University (25°00′N, 121°27′E). For studying the seasonal biomechanical behavior of branches, 3 to 4 plagiotropic branches, with an angle of 60° to 90° from vertical near the lower tree crown, were sampled in mid-August (summer; branches B1-4), mid-November 2008 (autumn; B5-7), mid-February (winter; ND1-3), and mid-May 2009 (spring; B8-10). In this study, the data in winter were discussed separately because the strains of branches are complicated by defoliation effects. The mean length of the 10 plagiotropic branches was 329 (SD 48) cm and the mean diameter at 10 cm from the trunk was 5.1 (SD 0.8) cm.

For comparing biomechanical behavior of branches with different angles and sizes, another 8 orthotropic branches (B11-18) with an angle of 5° to 45° from vertical near the upper tree crown, were sampled in November 2011 (autumn), as all secondary xylem had already matured and growth strains were supposed to be stable. The mean length of these 8 branches was 176 (SD 29) cm and the mean diameter at 10 cm from the trunk was 2.6

14

(SD 0.3) cm. The plagiotropic branches sampled in November 2008 had some dry capsules on the tip; but only few on some of the orthotropic branches of 2011. Comparing with the heavy compound leaves, we consider the load of these papery capsules small. The spring-back strains (SBS) and longitudinal released growth strains (RGS) were measured during sampling, and the wood discs were collected for further examination of growth eccentricity and tension wood distribution. The bending tendency was evaluated with Huang's biomechanical model (Huang et al. 2010).

Released growth strain (RGS) measurement

RGS at the stem base and the half-height of the control and artificially inclined seedlings was measured seasonally (7/23, 10/20 in 2009 and 1/28, 4/21 in 2010) in the 2009-experiments and monthly (5/25, 6/25, 7/25) in the 2012-experiments. RGS on the plagiotropic branches was measured seasonally (August and November, 2008; February and May, 2009) and the orthotropic branches in November 2011. For each branch, strains were measured every 30 cm along the branch with the first site at 10 cm from the trunk (Fig. 2a). Knots were carefully avoided.

To measure RGS, the bark of the marked measuring site was removed. The strain gauge (FLA-5-11-5LT, Tokyo Sokki Kenkyujo Co., Ltd) was glued to the surface of secondary xylem using cyanoacrylate adhesive (Tokyo Sokki Kenkyujo Co., Ltd) and connected to a data logger (TD 102, Tokyo Sokki Kenkyujo Co., Ltd) (Figs. 1c and 2b). After the gauge being zeroed, the seedlings or branches were firstly cut off from the base and held straight to read spring-back strain (SBS; ε_{su} / ε_{sl}). Then, RGS (ε_{gu} / ε_{gl}) was measured after the cross-cutting at the positions 3 mm apart from the upper and the lower rims of the gauge (Fig. 2c) (Huang et al. 2010).

15

In order to realize the effect of defoliation, the three plagiotropic branches (ND1–ND3) sampled in February 2009 were naturally defoliated; the spring-back strain (ε_{1su} / ε_{1sl}) and growth stain (ε_{gudef} / ε_{gldef}) of three or four sites were measured. The branch B7 sampled in December 2008 was artificially defoliated. Before the branch was cut down, the defoliation spring-back strains (ε_{sudef} / ε_{sldef}) were measured after all leaves on the branch were removed.
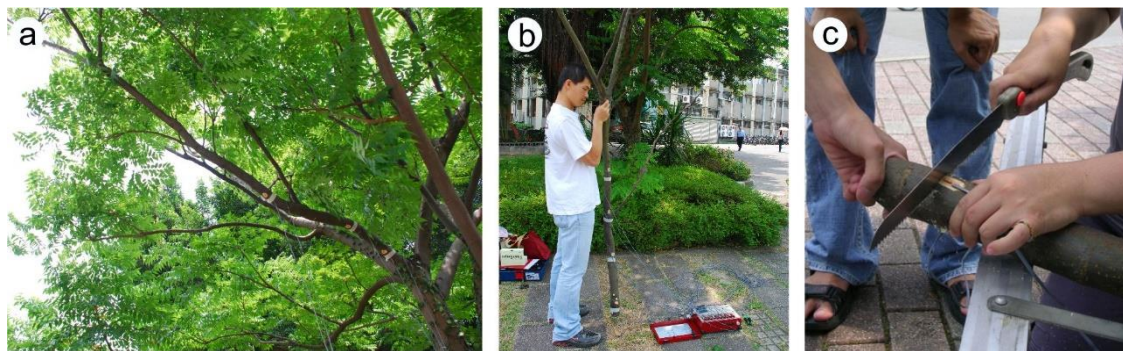
Figure 2. Sample collection of the *Koelreuteria henryi* branch.

a The plagiotropic branch B8 sampled in May 2009 with 3 measuring sites. **b** The branch was held vertical to record spring-back strain (SBS). **c** The released growth strain (RGS) was measured after the wood disc was cut

Wood anatomical structure and morphometry of the artificially inclined seedlings

Stem segments of 3 cm long with the marked pinholes were fixed and stored in FPGA (Formalin: Propionic acid: Glycerol: 95% Alcohol: distilled water = 1: 1: 3: 7: 8). By using sliding microtome (ERMA optical works, Ltd), 20 μm thick wood sections containing pinning-induced callus were collected and stained with 1% toluidine blue O in 1% sodium borax (TBO) or double stained with 0.5% safranin O and 0.1% alcian blue (in 0.3% acetic acid). Besides, for cellulose test some wood sections were histochemically

16

stained with zinc chloride-iodine. G-layers were stained purple-red with zinc chloride-iodine, purple with TBO, and light blue with alcian blue.

Whole stem sections were collected and photographed by using a digital camera (Sony DSC-T200). The wood diameters of the vertical and horizontal axis were measured with Image J and then the average radius (R) was calculated. The area of tension wood formed after inclination by each inclined seedling was also measured on the cross section using image J. The ratio of tension wood on the upper side (hereafter tension wood ratio) was calculated as tension wood area over whole wood area formed after inclination. Concerned the effective regions of the strain gauge measurement, we confined the whole wood area as 2 mm in width and between the pinning-induced callus and the recently matured wood (Fig. 1d). To measure the wood growth increment in the trunks, the upper and the lower sides of the trunk sections containing cambial marks and new formed wood tissue were photographed by Nikon D3 on Leica Diaplan Light Microscope. The variation of radius, i.e. the radial growth increments during the period of experiment including ΔR_a and ΔR_b for the A side and the B side of the control seedling; ΔR_u and ΔR_l for the upper side and the lower side of the inclined seedling were measured from the margin of the cambial mark to the cambial zone with Image J. The average growth increment ΔR was then calculated, ΔR is equal to $(\Delta R_a + \Delta R_b)/2$ for the control seedling and $(\Delta R_u + \Delta R_l)/2$ for the inclined seedling.

For studying the cambial activity and the cell wall ultrastructure, stem blocks were cut from 20 cm above the soil. The wood samples ($1 \times 1 \times 2$ mm^3) of the upper and the lower sides were fixed with 2.5% glutaraldehyde (in 0.1M phosphate buffer) and then followed by 1% osmium tetroxide (in 0.1M phosphate buffer), dehydrated with acetone series. For TEM, the samples were infiltrated and embedded in Spurr's resin (Spurr 1969) and cut by using an ultramicrotome (Ultracut E). Semi-thin sections (1μm) were stained

with TBO and photographed by Nikon D3 under Leica Diaplan Microscope. Ultra-thin sections were stained with a fresh mixture of 5% UA and 1% KMnO4 (1:3) and observed with Hitachi H-7650. For SEM, the fixed samples were further dehydrated by critical point drying method (Hitachi HCP-2) and coated with gold (Hitachi E101) and observed by FEI Inspect S. The MFA of fibers was measured from the SEM photographs using Image J.

Eccentricity calculation, radius and radial wood growth increment measurement of the branchwood

Eccentricity of the branchwood discs was calculated according to Japan Material Society (1982). On the surface of each wood disc, the vertical diameter (D_V), horizontal diameter (D_H), and the vertical distance from the pith to the lower edge (D_A) were measured with a caliper (Fig. 3). Eccentricity (Ec) is defined as eccentric distance (D_E, the vertical distance between the pith and the geometric center) over horizontal diameter:

$$Ec = D_E/D_H = (D_A - \frac{D_V}{2})/D_H$$

A positive sign indicates that the pith is above the geometric center, i.e., hypotrophic growth (promoted radial growth on the lower side); a negative sign means the reverse, i.e., epitrophic growth (promoted radial growth on the upper side).

The average radius of the wood disc (R) was calculated as ($D_V + D_H$)/4. And the radial growth increments during the last growing season, ΔR_u for the upper side and ΔR_l for the lower side, were also measured with a caliper (Fig. 3). The average growth increment (ΔR) equals ($\Delta R_u + \Delta R_l$)/2.

18
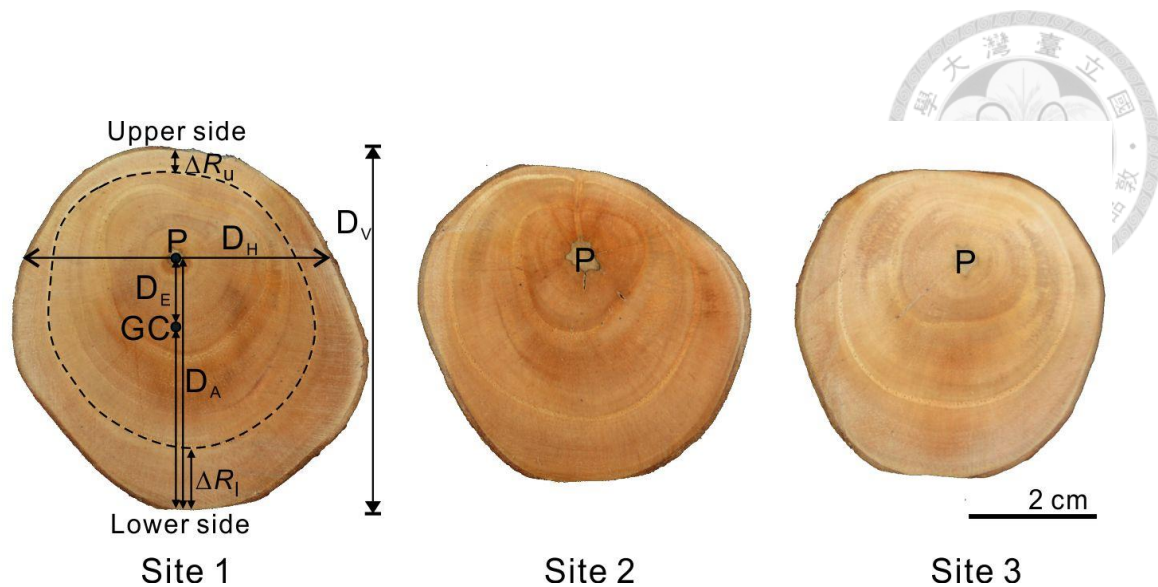
Figure 3. The 3 wood discs of the branch B5 showing the measurement of eccentricity and the hypotrophic growth on the lower side.

P pith, *GC* geometric center, D_H horizontal diameter, D_V vertical diameter, D_E the vertical distance between the pith and the geometric center, D_A the vertical distance from the pith to the lower edge, ΔR_u the radial growth increment on the upper side, ΔR_l the radial growth increment on the lower side

Tension wood distribution and branchwood structure

Wood discs obtained from the 3 plagiotropic and the 8 orthotropic branches sampled in autumn were examined for tension wood distribution. *K. henryi* contains living fibers and the massive starch grains in living fibers, making it difficult to use iodine-zinc chloride solution to detect G-fibers. Therefore, cross sections of wood discs of 20 μm were cut using sliding microtome (Reichert-Jung Hn 40) and doubly stained with 0.5% safranin O and 0.1% alcian blue (in 0.3% acetic acid). For wood discs that were too big for sliding microtome, they were sawn into several pieces first and then sectioned, doubly stained, and finally assembled. The whole sections of wood discs were photographed using Nikon D80. The outline of wood discs, annual rings and tension wood sectors were

19

traced using CorelDRAW X5 (Corel Corporation, 2010). For studying the anatomical features, the wood sections and macerated wood samples prepared by Schultze's methods (Johansen 1940) were observed and recorded by light microscope (Olympus CX41) and photographed by Cannon EOS 700D.
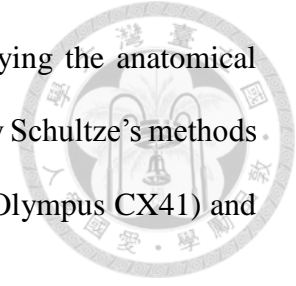
Prediction of the bending dynamics of trunks and branches

Huang's biomechanical model (Huang et al. 2010) was applied to predict the bending dynamics of the trunk and branches. The rate of change in curvature associated with growth increment is expressed as

$$\frac{\mathrm{d}C}{\mathrm{d}R} = \frac{\mathrm{d}C_\mathrm{s} + \mathrm{d}C_\mathrm{g}}{\mathrm{d}R} = \frac{4(\beta - \alpha)}{R^2} \qquad (1)$$

where $\mathrm{d}C_\mathrm{s}/\mathrm{d}R$ ($= 4\beta/R^2$) is the rate of change in curvature due to spring-back (self-weight) associated with growth increment, and $\mathrm{d}C_\mathrm{g}/\mathrm{d}R$ ($= -4\alpha/R^2$) is due to asymmetric growth strain; SBS parameter (β) associated with gravitational force is defined as half the difference of the SBS between the upper and the lower side: $\beta = (\varepsilon_\mathrm{su} - \varepsilon_\mathrm{sl})/2$; RGS parameter ($\alpha$) associated with gravitropic correction is defined as half the difference of the RGS between the upper and the lower side: $\alpha = (\varepsilon_\mathrm{gu} - \varepsilon_\mathrm{gl})/2$. When $\mathrm{d}C/\mathrm{d}R$ is positive, the branch tends to bend upward; when negative, the branch tends to bend downward. That is, the bending tendency can be predicted by simply examine the sign of $\beta - \alpha$, positive for upward bending and negative for downward bending. The bending tendency can also be predicted by the value of gravitropic performance ($P_G = \alpha/\beta$): greater than 1 for upward bending, smaller than 1 for downward bending (Fournier et al. 1994a).

20
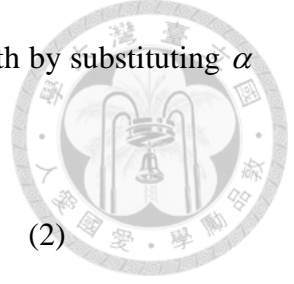
Equation (1) can be further rectified with eccentric radial growth by substituting α with α'

$$\alpha' = (\varepsilon_{gu}\frac{dR_u}{dR} - \varepsilon_{gl}\frac{dR_l}{dR})/2 \qquad (2)$$

where dR_u is the wood growth increment on the upper side, dR_l the lower side, and dR the average increment. The dR_u/dR and dR_l/dR were estimated with the measured $\Delta R_u/\Delta R$ and $\Delta R_l/\Delta R$, respectively. The corrected rate of change in curvature is expressed as dC'/dR.

$$\frac{dC'}{dR} = \frac{dC_s + dC'_g}{dR} = \frac{4(\beta - \alpha')}{R^2} \qquad (3)$$

Modified model for defoliating action of deciduous trees

During the defoliating season, β_1 is the half difference of spring-back strain between the upper and the lower side measured on the leafless branch, and α_1 is that of growth strain. With the spring-back strain during the defoliating process expressed as ε_{sudef} and ε_{sldef}, respectively, we obtain

$$\alpha_1 = \frac{(\varepsilon_{gudef} - \varepsilon_{gldef})}{2} = \frac{(\varepsilon_{gu} - \varepsilon_{sudef}) - (\varepsilon_{gl} - \varepsilon_{sldef})}{2} = \alpha - \beta_{def} \qquad (4)$$

$$\beta_1 = \frac{(\varepsilon_{su} - \varepsilon_{sudef}) - (\varepsilon_{sl} - \varepsilon_{sldef})}{2} = \beta - \beta_{def} \qquad (5)$$

$$\beta_1 - \alpha_1 = \beta - \alpha \qquad (6)$$

where $\beta_{def} = (\varepsilon_{sudef} - \varepsilon_{sldef})/2$ is the β during defoliating action, and ε_{gudef} and ε_{gldef} are, respectively, the measured growth strains on the upper side and the lower side of the branch after defoliation. It is clear that growth strain is the sum of measured growth

21

strain after defoliation and spring-back strain during defoliation. This means that growth strain is superimposed by the spring-back strain during defoliation. So that dC/dR can be expressed as

$$\frac{dC}{dR} = \frac{4(\beta - \alpha)}{R^2} = \frac{4(\beta_1 - \alpha_1)}{R^2} \qquad (7)$$

The rate of change in curvature of a defoliated branch associated with growth increment dC_1/dR and gravitropic performance P_{1G} can be expressed as

$$\frac{dC_1}{dR} = \frac{4(\beta_1 - \alpha_1 - \beta_{def})}{R^2} \qquad (8)$$

$$P_{1G} = \frac{\alpha}{\beta_1} = \frac{\alpha_1 + \beta_{def}}{\beta_1} \qquad (9)$$
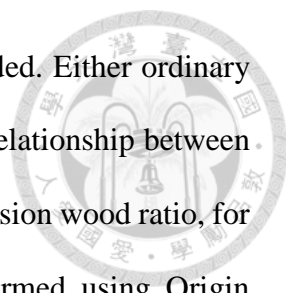
In the case of eccentric growth increment on the cross-section, a similar relation can be obtained as below:

$$\frac{dC\prime_1}{dR} = \frac{4(\beta_1 - \alpha\prime)}{R^2} \qquad (10)$$

$$P_{1G} = \frac{\alpha\prime}{\beta_1} \qquad (11)$$

Statistics

For the inclined seedlings, all data were tested for normality by Shapiro-Wilk test. When the data conformed to normal distribution, the means of RGSs of the upper and the lower sides were compared with paired t-test, for which t-value and p-value were provided. The means among different inclination durations (3, 6, 9 and 12 months) were compared with one-way ANOVA, for which F-value and p-value were provided. For heteroscedastic data or data deviated from normal distribution, Kruskal-Wallis rank sum

22

test was used instead, for which *chi*-square and *p*-value were provided. Either ordinary linear regression or polynomial regression was used to analyze the relationship between strain magnitude and inclination duration, and between RGSs and tension wood ratio, for which, r^2 and *p*-value were provided. Statistical tests were performed using Origin (OriginalLab, Northampton, MA) and R version 3.1.1 (the R Core Team, 2013). All statistical relationships were considered to be significant at $p<0.05$.

For the branches, all data were checked for normality by Shapiro-Wilk test. To compare between the plagiotropic and orthotropic branches, the means of parameters (ε_{gu}, ε_{gl}, β, and α) were compared with *t*-test or pooled *t*-test when the variances of the two samples are unequal. The means among seasons were compared with one-way ANOVA followed by Tukey's honestly significant multiple comparison if the difference is significant. The residual plots were examined for homoscedasticity; in the case of heterogeneous variance, we performed Kruskal-Wallis rank sum test followed by Dunn's test. The relationships between β and α, β and ε_{gu}, as well as β and ε_{gl} were described by ordinary linear regression and Pearson's correlation (r^2), for which *p*-value of the slope was provided. Statistical tests were performed using R software (R Core Team 2013). All statistical relationships were considered significant at $p < 0.05$.

Results

Study on the reorientation process of the artificially inclined seedlings of Koelreuteria henryi

Dynamics of the uprighting process of the inclined seedlings

In the 2009-experiment, we found that the uprighting process occurred mainly in the first 3 months after inclination in spring season. One week after tilting, five out of the 12 inclined seedlings sagged a little, while others showed only little change in orientation (Fig. 4a). Two weeks after tilting, all the 12 inclined seedlings curved upward. The proximal angle change after inclination was 2.7° (SD = 1.6°, n=12) in the 1st month, 2.7° (0.8°) in the 2nd month, and 2.1° (SD 1.0°) in the 3rd month; i.e., the total proximal angle change was 7.5° (SD = 2.52°, n=12) in the 1st season. Thereafter, the uprighting process was much slower: the proximal angle changed 1.5° (SD = 1.2°, n=9) in the 2nd season, 2.2° (1.1°, n=6) in the 3rd season, and 1.5° (SD = 0.9°, n=3) in the 4th season (Fig. 4a). At the end of this experiment, the average tilting angle for the last 3 seedlings was 19.9 (SD 3.7°). The apical region of the seedlings curved up soon after the inclination, they were straight and vertical after 6- to 8-weeks and mostly stayed vertical and only some of them showed overcorrection (Fig. 4).
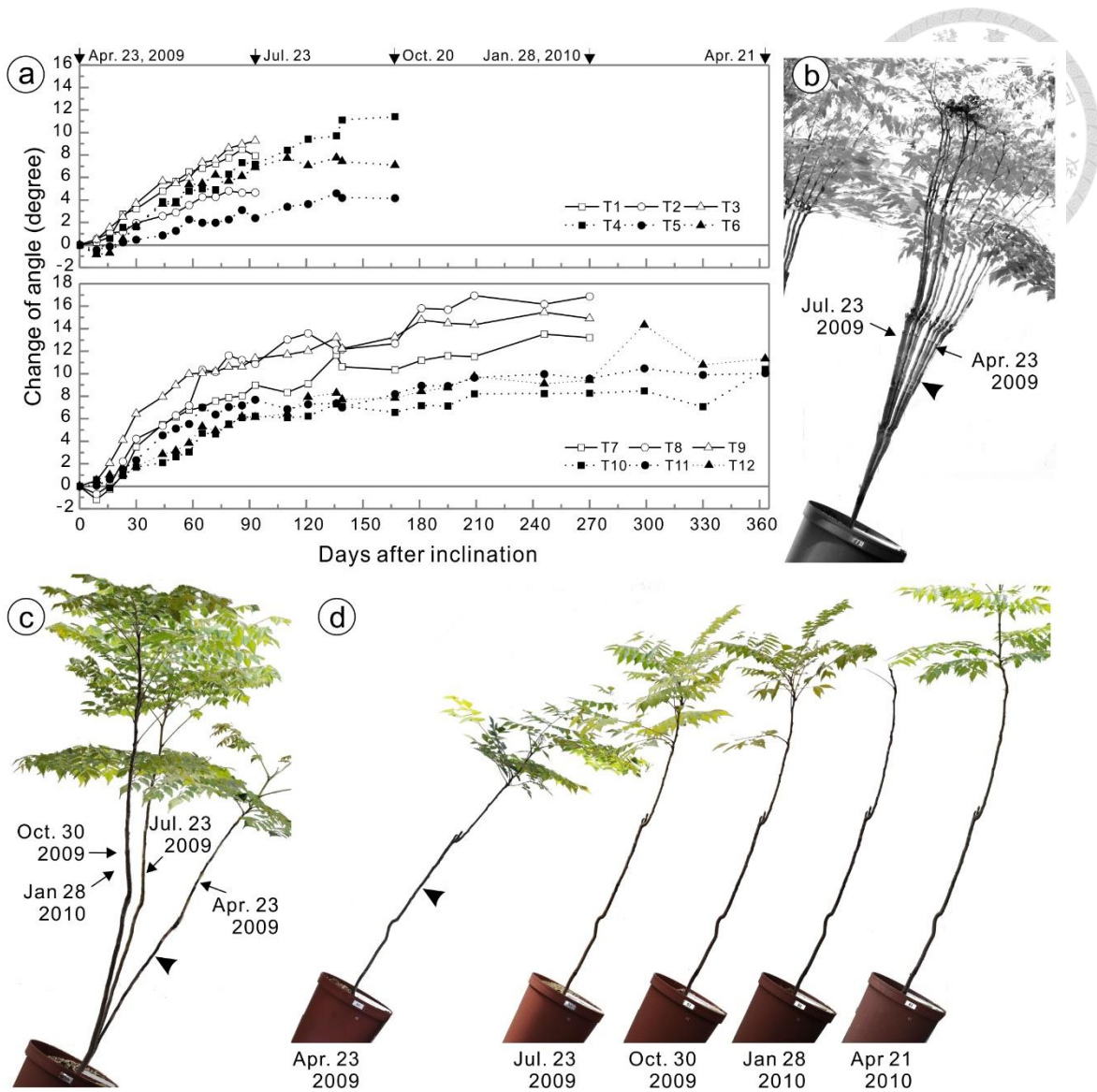
Figure 4. Dynamics of the uprighting process of the inclined seedlings.

a Changes of the proximal angle (positive for uprighting and negative for sagging) of the inclined seedlings in the 2009-experiments. **b** Tree shapes of the T3 seedling from April 23 to July 23, 2009. The proximal angle changed from 25.1 to 15.8° in these 3 months. **c** Seasonal tree shapes of the T9 seedling (April, July, October 2009 and January 2010). The tree shapes on the last two seasons were similar, however fewer leaves were observed on January 2010. **d** Seasonal photos of the T10 seedling (April, July, October 2009 and January, April 2010). Arrow heads point out the half-height of the trunks.

Released growth strain distribution

Since the stress is proportional to the strain within a proportional limit (Archer 1986), we estimated the pre-stress by measuring the RGSs of green wood. Figure 5a and b shows that the control seedlings exhibited either contractive (−) or extensive (+) strains on both sides of the trunk base and the half-height (Fig 5, Table 1). In the 2009-experiment, the RGSs measured on the A and B sides of the control seedlings showed no significant difference ($t = −0.343$, $p = 0.735$), indicating that in the green house there was no perspective effect. The average RGSs were small: $−120.21$ $\mu\varepsilon$ at the trunk base and $−76.67$ $\mu\varepsilon$ at the half-height, while strain values were more stable at the trunk base (SD $= 145.19$) than at the half-height (SD $= 232.48$) ($F = 0.379$, $p = 0.012$), because two stronger contractive values ($−610$ and $−652$ $\mu\varepsilon$) were measured at the half-height on the last sampling date. The RGSs of the trunk base of the control seedlings in the 2012-experiment fell into the range of those in the 2009-experiment (Fig. 5b).

In the 2009-experiment, the inclined seedlings exhibited only contractive strains on the upper sides (ε_{gu}: $−1690$ to $−64$ $\mu\varepsilon$), while on the lower side either contractive or extensive strains were measured at both the trunk base and the half-height (ε_{gl}: $−1276$ to $+495\mu\varepsilon$) (Fig. 5c, d, Table 1). The ε_{gu} and ε_{gl} showed no significant change during the whole experiment period (ε_{gu}: $\chi^2 = 3.43$, $p = 0.329$ for the trunk base, $\chi^2 = 2.897$, $p = 0.408$ for the half-height; ε_{gl}: $\chi^2 = 1.256$, $p = 0.740$ for the trunk base, $\chi^2 = 1.051$, $p = 0.789$ for the half-height), whereas the value of ε_{gu} was significantly smaller than ε_{gl} (paired $t = −2.653$, $p = 0.011$ for the trunk base, $t = −2.956$, $p = 0.007$ for the half-height). Similar results were observed in the 2012-experiment; however, the RGSs on the lower side are more extensive than those in the 2009-experiment (Fig. 5c, d). When the data of the two experiments were pooled, a negative relationship was found at the trunk base

26

between ε_{gl} and inclination duration ($r^2 = 0.29$, $p = 0.022$); the correlation coefficient is improved when a potential outlier was removed ($r^2 = 0.59$, $p < 0.01$)
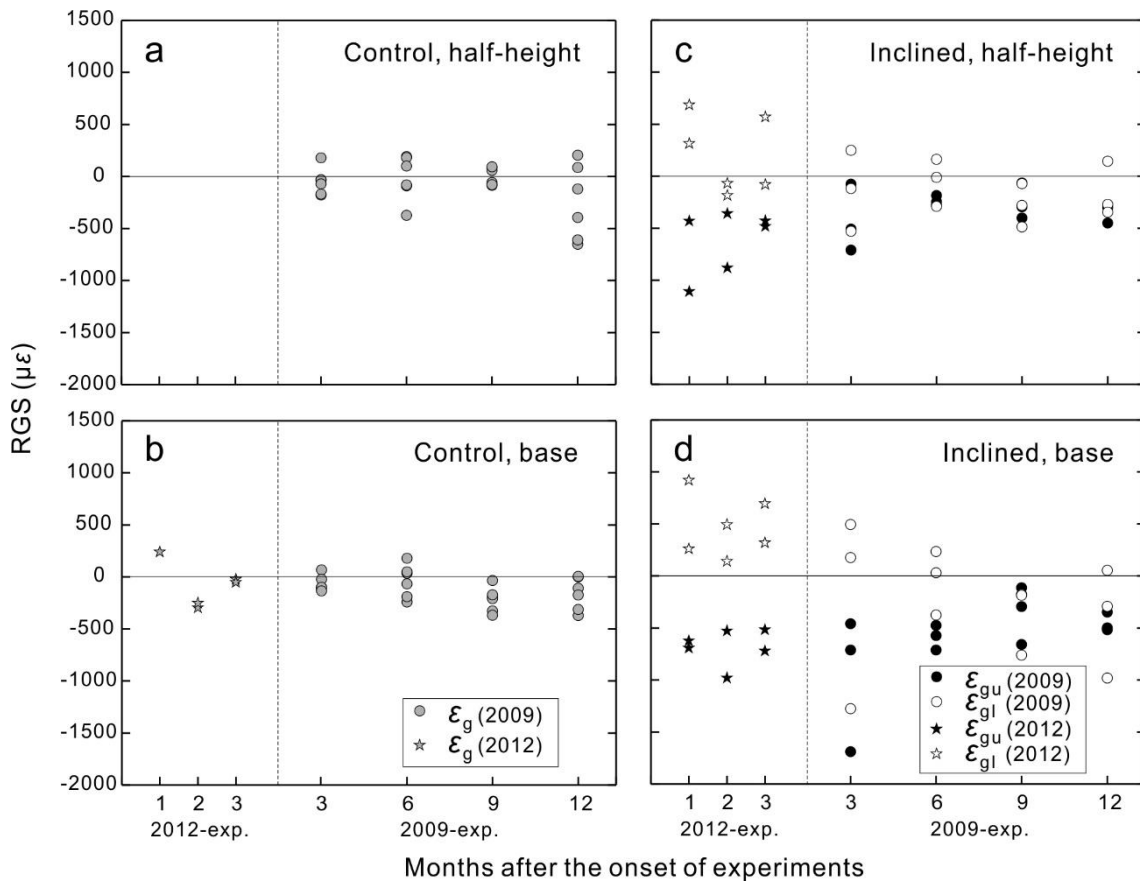
Figure 5. RGS distribution at the half-height (**a**, **c**) and the trunk base (**b**, **d**) of the control (**a**, **b**) and inclined (**c**, **d**) *Koelreuteria henryi* seedlings in the 2009- and 2012-experiment. ε_g RGS of both A side (ε_{ga})and B side (ε_{gb}) for the control seedlings, ε_{gu} *and* ε_{gl}, RGS for the upper and the lower side of inclined seedlings
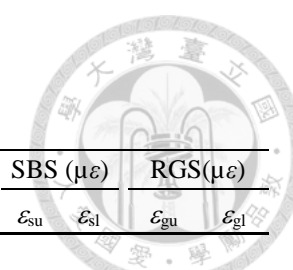
Table 1. Measured data of the control and the inclined seedlings of *Koelreuteria henryi*

Growth duration	Measuring site	R (mm)	ΔR_a (mm)	ΔR_b (mm)	ΔR (mm)	RGS(μɛ) ε_{ga}	ε_{gb}	Measuring site	R (mm)	ΔR_u (mm)	ΔR_l (mm)	ΔR (mm)	TW_{area} (mm²)	SBS (μɛ) ε_{su}	ε_{sl}	RGS(μɛ) ε_{gu}	ε_{gl}
						2009-experiment											
3 mo.	C1b	3.6	0.34	0.34	0.34	69	-22	T1b	4.02	1.36	0.38	0.87	8.4	-261	401	-712	177
	C1h	3.1	0.36	0.25	0.31	-32	-32	T1h	3.60	1.07	0.34	0.71	5.92	-95	130	-710	-528
	C2b	4.1	0.51	0.54	0.53	-108	-100	T2b	5.03	1.36	0.62	0.99	10.81	–	–	-1690	-1276
	C2h	3.7	0.37	0.61	0.49	180	-71	T2h	4.10	0.70	0.62	0.66	2.89	–	–	-507	-118
	C3b	4.6	0.68	0.55	0.62	-100	-133	T3b	4.17	1.00	0.21	0.61	9.71	–	–	-458	495
	C3h	3.8	0.63	0.46	0.55	-177	-169	T3h	3.46	0.71	0.13	0.42	2.54	–	–	-77	248
6 mo.	C4b	4.8	1.01	1.13	1.07	35	49	T4b	4.92	1.89	0.78	1.34	10.65	-165	130	-573	-375
	C4h	3.8	0.87	0.78	0.83	191	-81	T4h	3.96	1.19	0.71	0.95	4.71	-65	119	-273	-290
	C5b	5.0	1.18	1.06	1.12	-240	-66	T5b	6.15	2.16	1.29	1.73	6.6	-350	404	-476	235
	C5h	4.0	0.9	0.82	0.86	-372	181	T5h	4.09	1.29	1.07	1.18	4.52	-96	127	-186	-10
	C6b	5.1	1.35	1.76	1.56	-190	180	T6b	5.20	2.31	1.02	1.67	9.24	-240	237	-712	30
	C6h	4.3	1.59	1.24	1.42	-90	100	T6h	3.95	1.51	0.57	1.04	3.64	-116	173	-246	162
9 mo.	C7b	5.5	1.63	1.07	1.35	-35	-369	T7b	5.41	2.62	1.89	2.26	7.93	12	78	-295	-176
	C7h	4.4	1.19	0.72	0.96	85	-85	T7h	4.38	1.53	1.38	1.46	2.19	64	-36	-64	-72
	C8b	4.9	1.49	1.56	1.53	-191	-209	T8b	5.52	3.49	0.94	2.22	22.1	-48	108	-659	-760
	C8h	4.0	1.11	1.19	1.15	-58	-78	T8h	4.35	1.85	1.61	1.73	5.01	42	27	-294	-281
	C9b	4.6	0.93	1.36	1.15	-326	-171	T9b	5.09	2.37	1.23	1.80	9.07	-24	27	-114	-186
	C9h	4.0	0.96	1.02	0.99	59	93	T9h	4.04	1.60	1.37	1.49	3.94	60	-25	-400	-486
12 mo.	C10b	6.0	1.46	1.16	1.31	-108	-312	T10b	5.04	1.86	0.83	1.35	7.58	-140	-348	-348	55
	C10h	5.0	1.38	1.15	1.27	-394	-610	T10h	3.99	1.26	0.43	0.85	5.22	-46	-58	-278	144
	C11b	5.9	1.52	1.31	1.42	0	6	T11b	5.27	2.36	0.70	1.53	10.38	-18	176	-516	-980
	C11h	4.7	0.97	0.92	0.95	87	205	T11h	3.62	1.09	0.49	0.79	3.33	21	74	-450	-272
	C12b	7.2	3.48	2.86	3.17	-371	-173	T12b	6.63	3.01	1.33	2.17	17.26	-106	56	-498	-291
	C12h	6.1	2.52	1.83	2.18	-652	-120	T12h	4.96	1.86	1.49	1.68	7.57	132	-169	-301	-345

28

								2012-experiment									
1 mo.	C13b	4.29	0.15	0.15	0.15	--	240	T13b	4.41	0.31	0.20	0.26	–	-576	1004	-624	919
								T13h	–	–	–	–	–	-763	825	-1108	686
								T14b	3.81	1.00	0.32	0.66	–	-315	470	-693	260
								T14h	–	–	–	–	–	-371	475	-430	315
2 mo.	C14b	4.52	0.37	0.39	0.38	-297	-252	T15b	4.66	1.07	0.35	0.71	–	-273	422	-528	139
								T15h	–	–	–	–	–	-150	254	-360	-70
								T16b	4.82	1.13	0.42	0.78	–	-680	812	-980	492
								T16h	–	–	–	–	–	-527	583	-882	-184
3 mo.	C15b	3.6	1.08	1.15	1.12	-23	-52	T17b	4.92	1.42	0.74	1.08	–	-624	716	-721	318
								T17h	–	–	–	–	–	-182	363	-428	-81
								T18b	4.13	1.38	0.25	0.81	–	-340	681	-516	694
								T18h	–	–	–	–	–	-267	431	-481	570

C control seedling, *T* inclined seedling, *b* base, *h* half-height, *R* the average radius of wood calculated from the vertical and horizontal axis, ΔR_a and ΔR_b growth increment on two opposite sides of the stem in control seedlings, ΔR_u and ΔR_l: growth increment of the upper and the lower side of the stem in inclined seedlings, ΔR the average growth increment, *RGS* released growth strain, ε_{ga} and ε_{gb}: released growth strain on the A and the B side of the trunk in control seedlings, ε_{gu} and ε_{gl} released growth strain on the upper and the lower side of the trunk in inclined seedlings, *SBS* spring-back strain, ε_{su} and ε_{sl} spring-back strain on the upper and the lower side of the stem in inclined seedlings, *TW_{area}* total area of tension wood formed after inclination, − not measured

29

Eccentric growth and tension wood formation

Eccentric growth occurred in all inclined seedlings but not in the control seedlings (Fig. 6, Table 1, Appendix Ⅲ). The control seedlings present no eccentric growth at either the trunk base or the half-height on all the sampling dates (Fig. 6a, b). For the inclined seedlings, the amount of wood growth increment on the lower side (ΔR_l) of the trunk was similar with that of the control seedlings (ΔR_a and ΔR_b) (Fig. 6, Table 1). However, the wood growth increment was larger on the upper side (ΔR_u) than on the lower side (ΔR_l) (Fig. 6c, d, Table 1). The paired t-test revealed significant (<0.05) or at least marginally significant ($0.05 < p < 0.1$) results.

All fibers including G-fibers, opposite and normal wood fibers in *K. henryi* were all living fibers generally containing massive starch grains (Fig. 7). The histochemical results suggested that lignin was deposited in all the cell wall layers except for the G-layer and the double staining with safranin O and alcian blue gave an excellent contrast for the cell wall layers of G-fibers (Fig. 7c, f). Ultrastructure study revealed that the secondary wall of the fibers in normal wood and opposite wood consisted of S1+S2+S3 (Fig. 8a, c) while that of the G-fibers consisted of S1 and an additional G-layer (Fig. 8b, d). The microfribril angle of S2 layer in the normal wood fiber of *K. henryi* was about 25° (Fig. 8e), however the microfibrils in the G-layer were almost parallel to the axis of the G-fiber (Fig. 8f).

In the inclined *K. henryi* seedlings, a crescent tension wood zone containing G-fibers was observed on the upper side of the wood section (Fig. 9, Appendix Ⅲ). Included in the tension wood zone, a triangular callus induced by pinning was observed. The lower rim of the callus marked the position of cambial zone at the onset of pinning (Fig. 9a, d). The induced G-fibers were mostly observed on the outer side of the marked cambial zone, but a few layers of G-fibers were detected on the inner side (Fig. 9a, d). Two out of the 3 inclined seedlings were still producing G-fibers on the upper side of the trunk after 3-

30

months inclination when the cambium on the lower side appearing inactive (Fig. 10, Appendix IV). No developing G-fibers were observed 6 months after inclination. For the control seedlings, no G-fibers were observed in the wood tissues formed after the experiment except on the B side of the half-height in the C10 seedling.
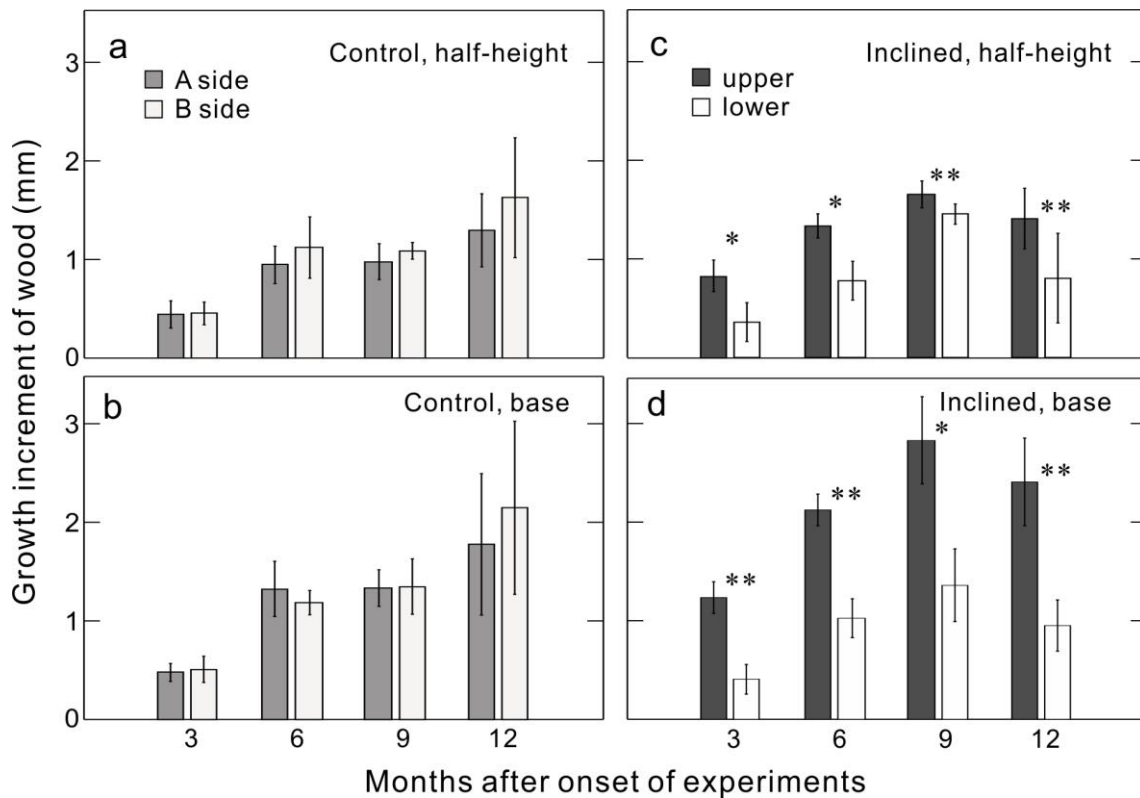
Figure 6. Radial wood growth increments at the half-height (**a**, **c**) and the trunk base (**b**, **d**) of the control (**a**, **b**) and the inclined (**c**, **d**) *Koelreuteria henryi* seedlings in the 2009-experiment.

The error bars represent standard errors. *$0.05 < p < 0.1$, **$p < 0.05$ (n=3)
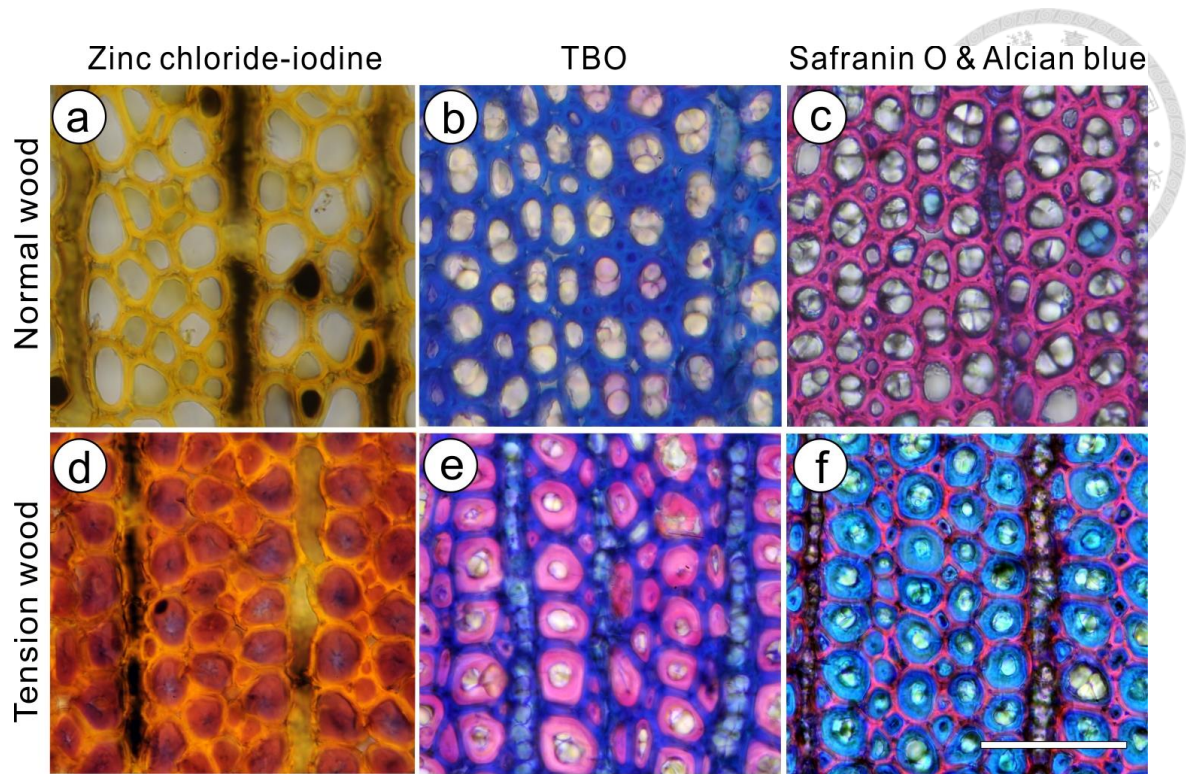
Figure 7. Histochemical stainings for normal wood (**a-c**) and tension wood (**d-f**). G-layers were stained purple-red with zinc chloride-iodine (**d**); purple with TBO (**e**); and light blue with alcian blue (**f**). *bar* 50μm
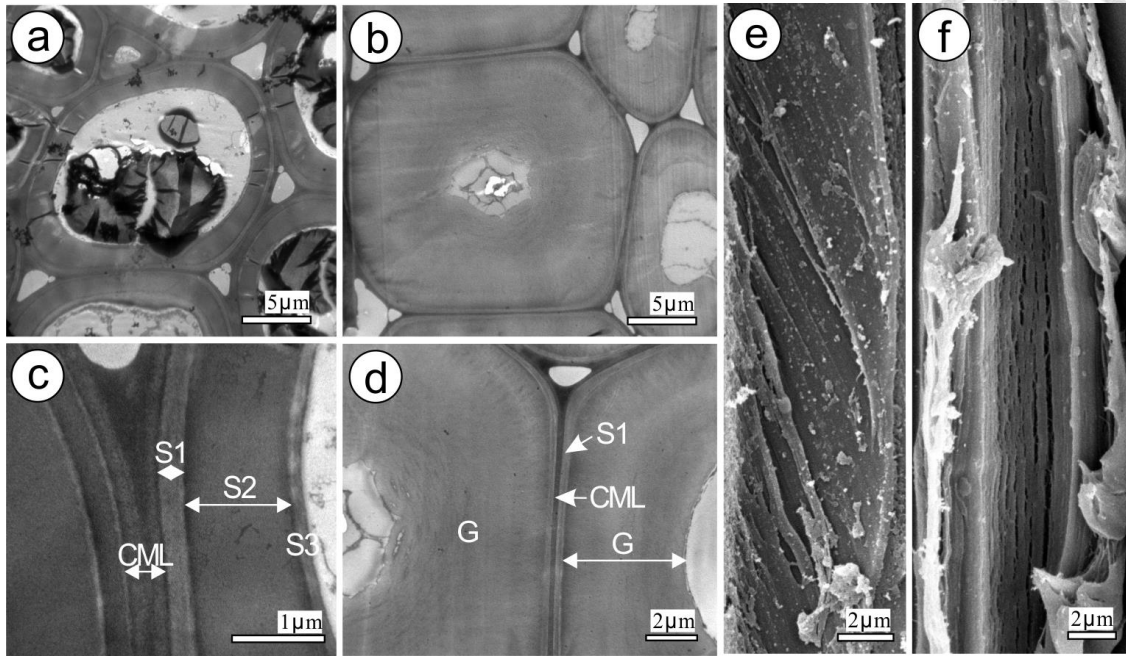
Figure 8. TEM (**a**-**d**) and SEM (**e**, **f**) photographs of opposite wood fibers (**a**, **c**, **e**) and G-fibers (**b**, **d**, **f**).

The secondary wall of the opposite wood fiber consisted of S1+S2+S3, while the secondary wall of the G-fiber was composed of S1+G. *S* secondary wall, *CML* compound middle lamella, *G* G-layer
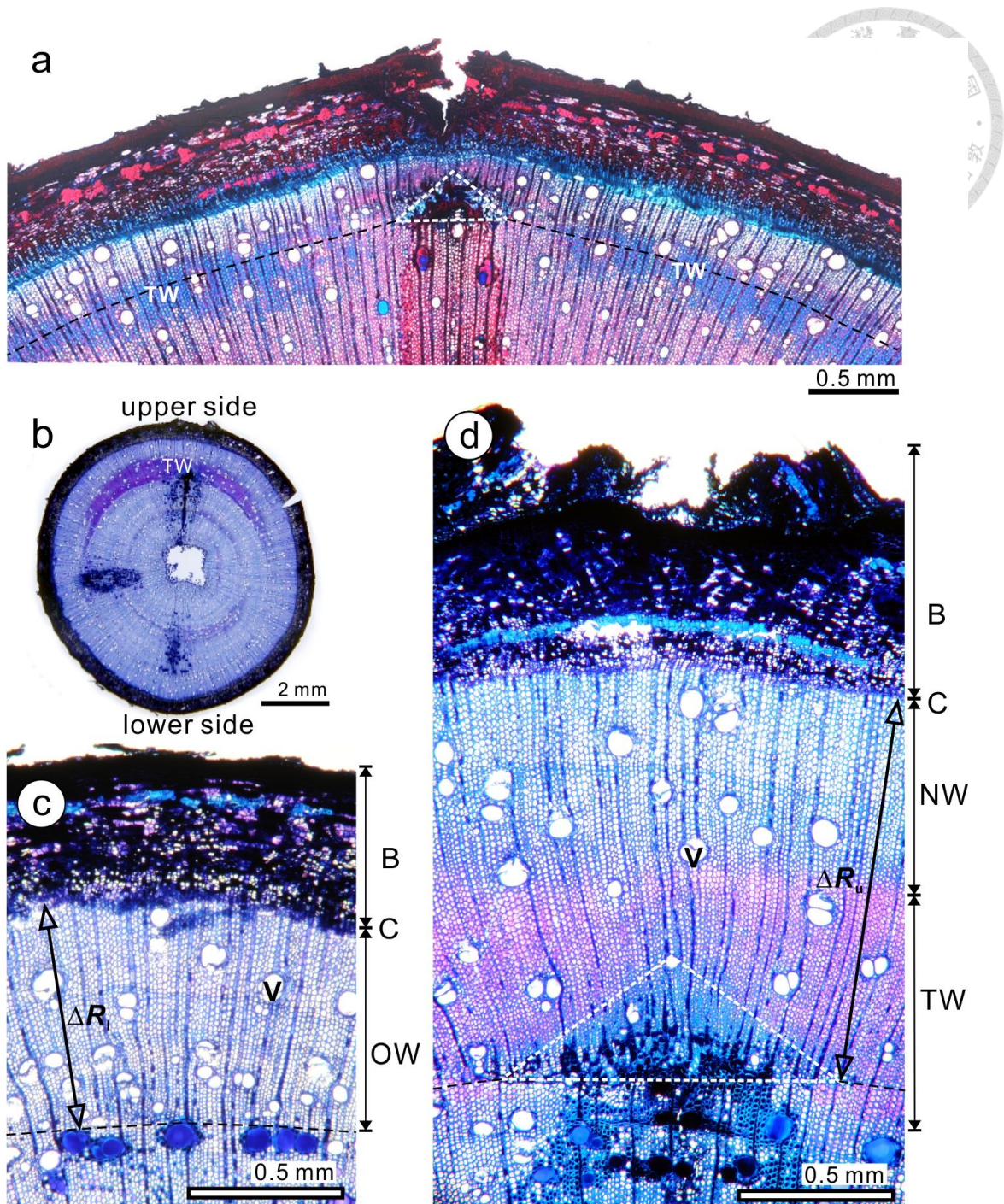
Figure 9. Light micrographs of cross sections of the trunk of inclined *Koelreuteria henryi* seedlings showing the tension wood formation.

a The upper side at the trunk base of the T13 seedling collected after one-month inclination and the section was stained with safranin O and alcian blue. **b-d** Whole trunk section (**b**), the lower side part (**c**), and the upper side part (**d**) at the half-height of the trunk of the T4 seedling collected after six-months inclination and the section was stained with TBO. The triangular wound tissues induced by pinning (outlined by white dotted

lines in **a**, **d**) directly marked the position of the vascular cambium at the onset of inclination (blacked dotted lines in **a**, **c**, **d**). Several layers of G-fibers were formed on the inner side of the marked cambial zone (**a**, **d**). Tension wood formed only on the upper side of the stem (**a**, **b**, **d**) but not in the lower side (**b**, **c**). *TW* tension wood, *B* bark, *C* cambium, *OW* opposite wood, *NW* normal wood, *V* vessel, *ΔR_l and ΔR_u* the wood growth increment on the lower and the upper side
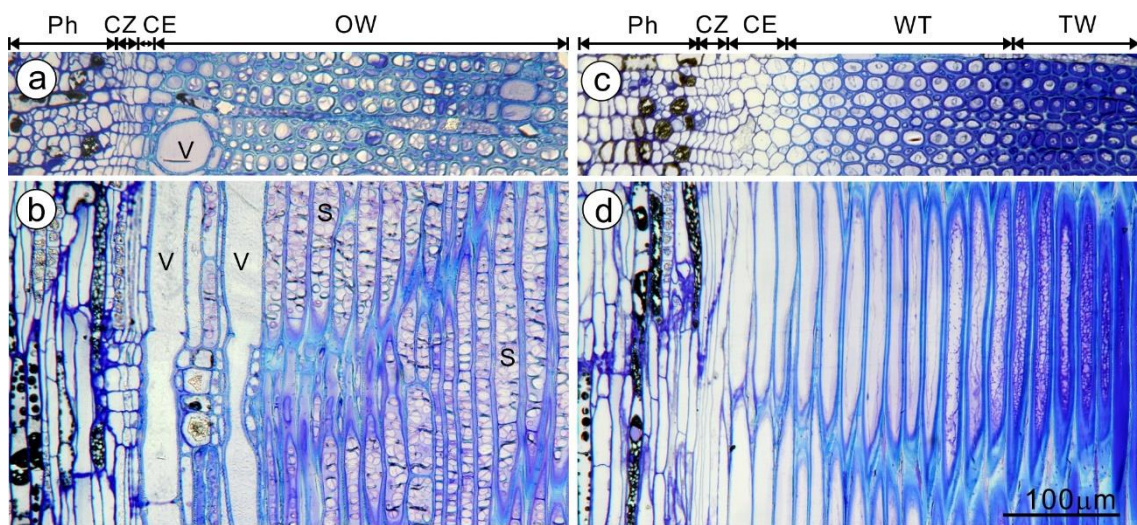
Figure 10. Light micrographs of cross (**a**, **c**) and radial longitudinal (**b**, **d**) plastic sections of the lower (**a**, **b**) and the upper side (**c**, **d**) of the trunk of the T3 seedling.

The cambial zone of the lower side is inactive and the opposite wood fibers were filled with starch grains (**a**, **b**). The cambial zone of the upper side was producing G-fibers. *Ph* phloem, *CZ* cambial zone, *CE* zone of cell enlargement, *WT* zone of cells under secondary wall thickening, *TW* tension wood with mature G-fibers, *OW* opposite wood, *V* vessel element, *S* starch grains

35
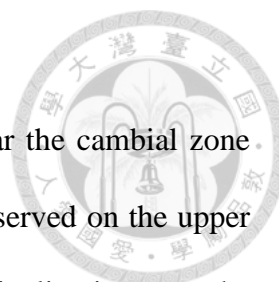
The relationship between RGSs and tension wood ratio

In the 2009-experiment, tension wood containing G-fibers near the cambial zone (Fig. 10) together with large, negative ε_{gu} values (Table. 1) were observed on the upper side of the inclined trunks 3 months after inclination. After 6-months inclination, near the cambial zone G-fibers were no longer found, and the magnitude of ε_{gu} was reduced but still larger than ε_{gl} (Table. 1). Figure 11 shows that the magnitude of RGSs on the upper side increased as the tension wood ratio increased ($r^2 = 0.46$; $p < 0.01$). The correlation coefficient could be higher if the outlier was removed ($r^2 = 0.54$; $p < 0.01$).
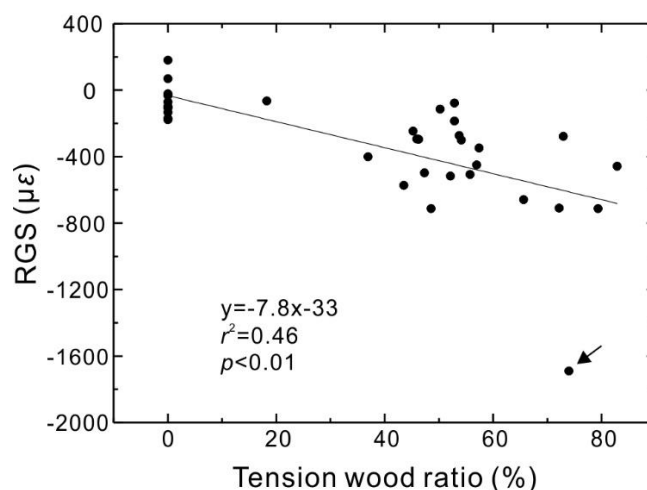
Figure 11. The relationship between tension wood ratio and RGSs.
The tension wood ratio was 0% in control seedlings. RGSs were taken from the data of both sides of the 3 control seedlings sampled at July 23 2009 and the data of the upper side (ε_{gu}) of all 12 inclined seedlings in the 2009-experiment. Arrow indicates a potential outlier

Prediction of bending dynamics

For analyzing the bending dynamics, we pooled the data from the inclined seedlings

36

of *K. henryi* in the 2009- and the 2012-experiments excluding those of the seedlings sampled 9 and 12 months after inclination. Because the inclined seedlings recovered to vertical mainly within 3 months and the seedlings gradually shed leaves since late October which may further complicate the interpretation of RGSs.

Table 2 presents the experimental data calculated according to Huang's model. Spring-back strain (SBS) parameter (β) and RGS parameter (α) indicate the direction and the magnitude of gravitational force and gravitropic correction, respectively. The negative β value of all inclined seedlings indicates that the weight of the inclined trunk generated a downward bending moment. On the contrary, the negative α value indicates that the bending moment generated by tension wood was to pull the trunk upward. The magnitude of α within 3 months after inclination was the largest and it was larger at the trunk base (-508 ± 180 $\mu\varepsilon$ (SD)) than at the half-height (-323 ± 256 $\mu\varepsilon$ (SD)) ($t = -1.77$, $p < 0.05$, n = 9). The magnitude of α gradually reduced to near 0 and it was sooner at the half-height of the trunks than at the base (Fig. 12).

The mean RGS parameter (α) and the mean of eccentrically corrected RGS parameter (α') for 9 inclined seedlings (3 in the 2009- and 6 in the 2012-experiment) examined within 3 months after tilting were -418 $\mu\varepsilon$ and -523 $\mu\varepsilon$, respectively. The promoted growth increment on the upper side of the inclined trunk increased the efficiency of correction by 25%. Downward bending tendency were predicted in 9 out of 14 measuring sites in 10 inclined seedlings. The eccentric correction changed the downward bending tendency to upward at 5 measuring sites (Table 2).

The rate of curvature change due to self-weight (dC_s/dR) and negative gravitropism (dC_g/dR) were also shown in Table 2. In the 2009-experiment, the average dC_s/dR was -58.38 m^{-2} for seedlings examined 3 months after inclination and -31.12 m^{-2} for 6

37

months. In the 2012-experiment, dC_s/dR is -115.6 m^{-2} for the seedlings examined within 3 months. All dC_s/dR were negative, indicating a downward bending moment.

In the 2009-experiment, the average dC_g/dR was 69.09 for the inclined seedlings sampled 3 months after inclination and 30.01 m^{-2} for 6 months. In the 2012-experiment, dC_g/dR is 117.65 m^{-2} within 3 months after inclination. All dC_g/dR were positive except 1 site at the half-height in the 2009-experiment, indicating an upward bending moment. Corrected by eccentric radial growth, the mean rates of curvature change due to gravitropism (dC'_g/dR) increased to 136.89 and 66.73 m^{-2} for the seedlings sampled 3 and 6 months after inclination in the 2009-experiment and 127.2 m^{-2} in the 2012-experiment. The correction efficiency increased 98.1%, 44.4% and 8.1%, respectively.

The mean net rate of curvature change (dC/dR) is 10.72 and -1.11 m^{-2} for seedlings examined 3 and 6 months after inclination in the 2009-experiment, and 2.05 m^{-2} in the 2012-experiment. After corrected with asymmetric growth increment, the mean value of dC'/dR increased to 78.51, 12.23, and 11.6 m^{-2}, respectively.
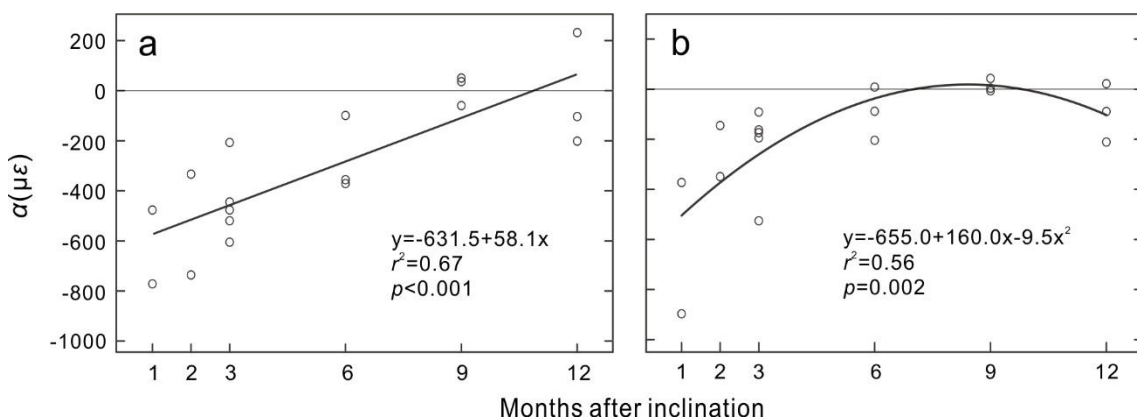
Figure 12. Relationship of growth strain parameter (α) and inclination duration at the trunk base (**a**) and at the half-height (**b**).

The magnitude of α was the largest in the first 3 months and gradually reduced to near 0
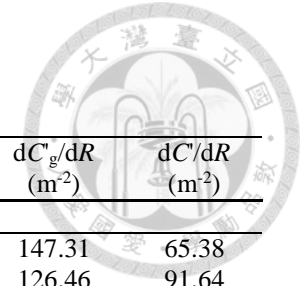
Table 2. Experimental data of the inclined seedlings of *Koelreuteria henryi* for prediction of bending dynamics

Growth duration	Seedling	β ($\mu\varepsilon$)	α ($\mu\varepsilon$)	α' ($\mu\varepsilon$)	$\beta\text{-}\alpha$ ($\mu\varepsilon$)	Bending tendency	$\beta\text{-}\alpha'$	Bending tendency	dC_s/dR (m^{-2})	dC_g/dR (m^{-2})	dC/dR (m^{-2})	dC'_g/dR (m^{-2})	dC'/dR (m^{-2})
						2009-experiment							
3 mo.	T1b	-331	-445	-595	114	UW	264	UW	-81.93	110.02	28.09	147.31	65.38
	T1h	-113	-91	-409	-22	DW	296	UW	-34.82	28.16	-6.65	126.46	91.64
	Mean	**-222**	**-268**	**-502**	**46**		**280**		**-58.38**	**69.09**	**10.72**	**136.89**	**78.51**
6 mo.	T4b	-148	-99	-295	-49	DW	147	UW	-24.42	16.39	-8.03	48.84	24.42
	T4h	-92	9	-63	-101	DW	-29	DW	-23.44	-2.17	-25.60	15.95	-7.49
	T5b	-377	-356	-385	-22	DW	8	UW	-39.87	37.60	-2.27	40.69	0.82
	T5h	-112	-88	-97	-24	DW	-14	DW	-26.63	21.02	-5.61	23.20	-3.43
	T6b	-239	-371	-502	133	UW	263	UW	-35.25	54.83	19.58	74.13	38.88
	T6h	-145	-204	-223	60	UW	78	UW	-37.09	52.37	15.27	57.24	20.15
	Mean	**-185.50**	**-184.83**	**-260.83**	**-0.50**		**75.50**		**-31.12**	**30.01**	**-1.11**	**43.34**	**12.23**
						2012-experiment							
1 mo.	T13b	-790	-772	-739	-19	DW	-51	DW	-162.41	158.61	-3.80	151.88	-10.53
	T14b	-393	-477	-589	84	UW	197	UW	-108.18	131.34	23.15	162.35	54.16
2 mo.	T15b	-348	-334	-431	-14	DW	84	UW	-64.09	61.51	-2.58	79.56	15.47
	T16b	-746	-736	-847	-10	DW	101	UW	-128.63	126.90	-1.72	146.03	17.40
3 mo.	T17b	-670	-520	-582	-151	DW	-88	DW	-110.78	85.90	-24.88	96.26	-14.52
	T18b	-511	-605	-543	95	UW	33	UW	-119.51	141.64	22.12	127.15	7.63
	Mean	**-576.33**	**-574.00**	**-621.83**	**-2.50**		**46.00**		**-115.60**	**117.65**	**2.05**	**127.21**	**11.60**

β spring-back strain parameter, α and α' asymmetric released growth strain parameters, *DW* downward bending, *UW* upward bending, *dCs/dR* rate of gravitational disturbance, *dCg/dR* and *dC'g/dR* rates of gravitropic correction, *dC/dR* and *dC'/dR* net rates of curvature change

Study on the distribution of growth strain and reaction wood of the branches

Strain distribution on branches of Koelreuteria henryi

The RGS on the upper side (ε_{gu}) and the lower side (ε_{gl}) for the examined 18 branches were listed in Table 1, and the scatterplot of the ε_{gu} and ε_{gl} was shown in Fig. 3. On the upper side, the 10 plagiotropic branches exhibited either contractive ($-$) or extensive ($+$) strains (ε_{gu}: -411 to 255 $\mu\varepsilon$ in May 2009; -732 to 212 $\mu\varepsilon$ in August 2008; and -2164 to 294 $\mu\varepsilon$ in November 2008 (Table 3, Figs. 13, 14a). The trend of the magnitude of ε_{gu} increased from spring to autumn was observed without statistical significance ($\chi^2 = 3.29$, $p = 0.19$) (Fig. 4a). However, the orthotropic branches exhibited almost all contractive strains on the upper side (ε_{gu}: -630 to 195 $\mu\varepsilon$ in November 2011) (Table 3, Figs. 13, 14a). Comparing the ε_{gu} value between the orthotropic and the plagiotropic branches collected in autumn, no significant difference was found ($t = -1.38$, $p = 0.205$) (Fig. 14a).

On the lower side, the plagiotropic branches also exhibited either contractive or extensive strains (ε_{gl}: from -624 to 427 $\mu\varepsilon$ in May 2009, -472 to 370 $\mu\varepsilon$ in August 2008, and -1023 to 305 $\mu\varepsilon$ in November 2008) (Table 3, Figs. 13, 14b) and no significant difference of the ε_{gl} values was found among seasons ($F = 1.81$, $p = 0.182$). However, the orthotropic branches exhibited mostly contractive strains on the lower side (ε_{gl}: from -922 to 141 $\mu\varepsilon$ in November 2011) (Table 3, Figs. 13, 14b). There was also no difference between the ε_{gl} values on the plagiotropic and the orthotropic branches collected in autumn ($t = 0.09$, $p = 0.926$).

The measured longitudinal SBS on the upper side (ε_{su}) and the lower side (ε_{sl}) of all examined branches were listed in Table 3. For all sampled branches, the ε_{su} values were almost all contractive ($-1,408$ to -161 $\mu\varepsilon$) for the plagiotropic branches, and either contractive or extensive (-517 to 98 $\mu\varepsilon$) for the orthotropic branches. However, the ε_{sl}

40

values were almost all extensive and ranged from −37 to 1,440 με for the plagiotropic

branches (ε_{su}) and ranged from −107 to 892 με for the orthotropic branches.
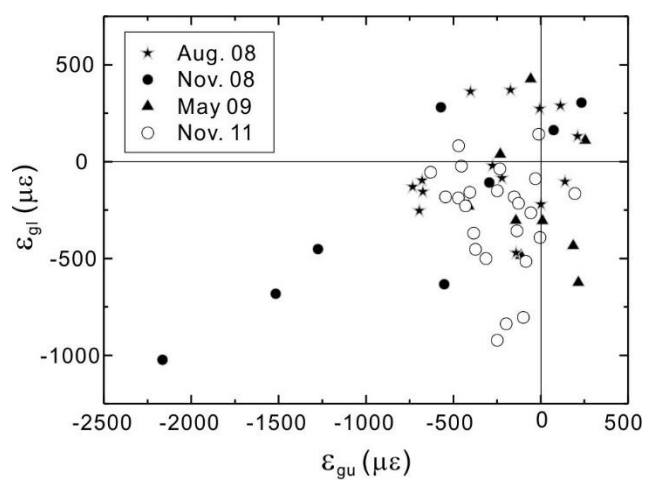
Figure 13. Scatterplot of the RGS on the upper (ε_{gu}) and the lower side (ε_{gl}) of the plagiotropic branches (closed symbols) and the orthotropic branches (open symbols). Correlation between ε_{gu} and ε_{gl} was only found on the plagiotropic branches sampled in Nov. 2008 ($r^2 = 0.746$, $p < 0.01$)
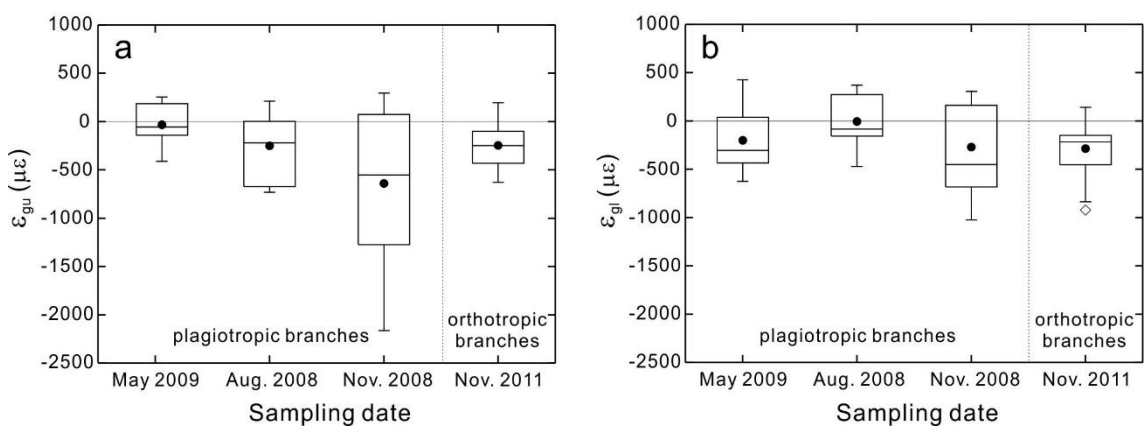
Figure 14. Seasonal RGS distribution on the upper side (ε_{gu}) (**a**) and on the lower side (ε_{gl}) (**b**) of the plagiotropic and the orthotropic branches.

The sampling date was listed in the order of seasons

41

Table 3. Eccentricity, spring-back strains (SBS), and released growth strains (RGS) on the branches of *Koelreuteria henryi*

Branch type	Sampling date	Branch No.	site	L (cm)	R (cm)	Ec	ΔR_u	ΔR_l	ΔR	$\Delta R_u/\Delta R$	$\Delta R_l/\Delta R$	SBS (με) ε_{su}	ε_{sl}	RGS (με) ε_{gu}	ε_{gl}
Plagiotropic	Aug. 2008 Summer	B1	1	10	2.85	0.15	2.77	16.15	9.46	0.29	1.71	-1303	688	-402	361
			2	37	2.73	0.15	3.40	7.14	5.27	0.65	1.35	-1034	1377	-695	-254
			3	68	2.19	0.12	2.86	4.73	3.79	0.75	1.25	-515	1099	-221	-85
			4	97	2.27	0.12	2.67	5.59	4.13	0.65	1.35	-486	1320	139	-104
		B2	1	10	1.98	0.23	2.44	6.58	4.51	0.54	1.46	-565	1028	113	288
			2	40	1.76	0.19	1.71	7.44	4.57	0.37	1.63	-900	450	212	130
			3	69	1.73	0.13	2.83	7.91	5.37	0.53	1.47	-355	459	--	48
		B3	1	10	2.36	0.44	1.16	3.89	2.53	0.46	1.54	-1269	463	-5	273
			2	39	2.46	0.4	3.55	5.62	4.59	0.77	1.23	-459	179	-140	-472
			3	69	2.43	0.11	3.03	4.90	3.97	0.76	1.24	-512	602	-173	370
			4	99	2.08	0.22	3.01	4.40	3.70	0.81	1.19	-1004	600	-275	-22
			5	128	1.92	0.13	2.00	5.01	3.50	0.57	1.43	-724	-37	-732	-130
		B4	1	10	2.94	0.22	1.82	5.56	3.69	0.49	1.51	-568	784	-678	-98
			2	42	2.65	0.11	1.18	3.41	2.30	0.52	1.48	-806	546	1	-221
			3	70	2.28	0.14	1.28	3.31	2.29	0.56	1.44	-1112	1440	--	--
			4	100	2	0.17	0.96	3.84	2.40	0.4	1.6	-1408	1434	-674	-156
		Mean										**-814**	**777**	**-252**	**-5**
		SD										**340**	**458**	**335**	**246**
	Nov. 2008 Autumn	B5	1	10	2.69	0.16	3.90	9.28	6.59	0.59	1.41	-676	--	294	--
			2	42	2.33	0.22	2.12	9.59	5.85	0.36	1.64	-638	730	-553	-633
			3	92	2.29	0.26	1.55	10.77	6.16	0.25	1.75	-560	463	-295	-108
		B6	1	10	2.38	0.11	5.08	5.40	5.24	0.97	1.03	-887	774	73	162
			2	33	2.11	0.01	5.54	4.25	4.89	1.13	0.87	-692	950	234	305
			3	58	2.05	0.04	5.04	5.04	5.04	1	1	-728	656	-571	281
		B7	1	10	1.93	0.1	4.32	5.09	4.71	0.92	1.08	-571	870	-1516	-682
			2	40	1.88	0.11	4.20	4.29	4.24	0.99	1.01	-551	596	-2164	-1023
			3	69	1.76	0.1	4.57	4.78	4.68	0.98	1.02	-239	645	-1275	-451
		Mean										**-616**	**711**	**-641**	**-269**
		SD										**176**	**155**	**849**	**500**
	May 2009 Spring	B8	1	12	2.81	0.14	2.36	5.11	3.74	0.63	1.37	-958	645	-142	-304
			2	44	2.68	-0.07	6.12	3.72	4.92	1.24	0.76	-161	658	186	-434
			3	77	2.37	0.07	4.72	3.60	4.16	1.13	0.87	-834	1074	11	-306
		B9	1	10	2.83	0.15	5.96	9.36	7.66	0.78	1.22	-672	488	255	109
			2	40	2.7	0.17	3.48	8.47	5.97	0.58	1.42	-381	622	-411	-230
			3	91	2.23	0.11	3.82	3.67	3.75	1.02	0.98	-574	897	215	-624

42

		B10	1	10	3.2	0.15	4.02	8.56	6.29	0.64	1.36	-478	168	-112	-485
			2	60	2.6	0.15	2.08	6.17	4.12	0.5	1.5	-560	981	-231	38
			3	90	2.5	0.17	3.54	6.70	5.12	0.69	1.31	-205	1020	-57	427
		Mean										**-536**	**728**	**-32**	**-201**
		SD										**266**	**294**	**222**	**332**
orthotropic	Nov 2011	B11	1	10	1.01	0.1	3.19	2.59	2.89	1.10	0.90	-142	218	-470	81
			2	40	0.97	0.02	2.5	2.93	2.72	0.92	1.08	-8	353	-152	-182
			3	70	0.88	0.01	3.28	3.36	3.32	0.99	1.01	44	47	-471	-188
		B12	1	10	1.43	0.14	2.5	6.64	4.57	0.55	1.45	-393	892	-197	-837
			2	40	1.39	0.03	3.71	5.6	4.66	0.80	1.20	-517	535	-374	-453
			3	70	1.3	0.02	3.36	6.72	5.04	0.67	1.33	-298	700	-249	-150
		B13	1	10	1.41	0.14	4.91	5.09	5.00	0.98	1.02	-91	258	-12	141
			2	40	1.29	0.03	4.22	4.66	4.44	0.95	1.05	-94	257	-431	-229
			3	72	1.24	0.02	5.26	4.57	4.91	1.07	0.93	-11	17	-406	-159
		B14	1	10	1.24	0.12	4.4	5.09	4.74	0.93	1.07	-295	463	-314	-501
			2	40	1.15	0.03	3.71	5.69	4.70	0.79	1.21	-260	457	-630	-55
			3	70	1.01	0.01	4.57	5.95	5.26	0.87	1.13	-61	288	-234	-38
		B15	1	12	1.27	0.11	3.97	3.88	3.92	1.01	0.99	-149	260	-85	-515
			2	40	1.18	0.03	5.09	3.45	4.27	1.19	0.81	-58	152	-249	-922
			3	70	1.07	0.02	5.09	5.17	5.13	0.99	1.01	98	-107	-100	-805
		B16	1	10	1.48	0.15	3.02	7.07	5.04	0.60	1.40	-450	519	195	-165
			2	43	1.26	0.03	2.16	5.26	3.71	0.58	1.42	-308	477	-57	-265
			3	71	1.24	0.02	2.16	6.29	4.22	0.51	1.49	-364	434	-4	-392
		B17	1	10	1.36	0.14	6.03	7.16	6.59	0.92	1.08	-268	210	-545	-182
			2	40	1.31	0.03	4.74	7.33	6.03	0.79	1.21	-203	241	-384	-370
			3	70	1.23	0.02	3.71	7.16	5.43	0.68	1.32	-58	216	-136	-358
		B18	1	10	1.19	0.12	7.07	12.5	9.78	0.72	1.28	-163	189	-30	-88
			2	39	1.11	0.03	7.07	9.31	8.19	0.86	1.14	-271	179	-454	-23
			3	60	1.03	0.02	7.24	8.62	7.93	0.91	1.09	-25	82	-127	-216
		Mean										**-181**	**306**	**-247**	**-286**
		SD										**162**	**224**	**204**	**276**

R, the average radius of wood calculated from the vertical and horizontal axis, Ec eccentricity: positive for hypotrophic and negative for epitrophic growth, ΔR_u and ΔR_l radial growth increment on the upper and lower sides of the branch, ΔR average increment, ε_{su} and ε_{sl} SBS of the upper and lower sides, ε_{gu} and ε_{gl} RGS of the upper and lower sides of the branch

43

Growth eccentricity and tension wood distribution of K. henryi branches

Annual rings were observed on the cross section of *K. henryi* branches (Fig. 3). Almost all branchwood discs showed hypotrophic eccentricity, i.e., radial growth promotion occurs on the lower side (Table 3, Fig. 15). The pattern of eccentricity along the plagiotropic branches varies individually; however, a decreasing trend was consistently found in orthotropic branches (Fig. 15).

Figure 16a showed a macerated normal wood fiber with MFA of $32°$. Tension wood of *K. henryi* is characterized by G-fibers with the S2 and S3 layers replaced by a special G-layer which consists of highly crystalline cellulose fibrils that are almost parallel to the fiber axis (Fig. 16b). In the wood sections of the studied branches, G-layers were stained blue (alcian blue) and secondary wall red (safranin O) (Fig 16c-e). For the plagiotropic branches, no specific pattern of tension wood distribution was observed; tension wood arcs were found on the upper, the lower side, and also both flanks of the wood sections (Fig. 17). At different measuring sites along the same branch, the distribution of tension wood was not consistent as well (Fig. 17). For the orthotropic branches, similar result was found except for the branches B17 and B18, on which none or only trace amount of tension wood was observed on their wood sections (Fig. 18).
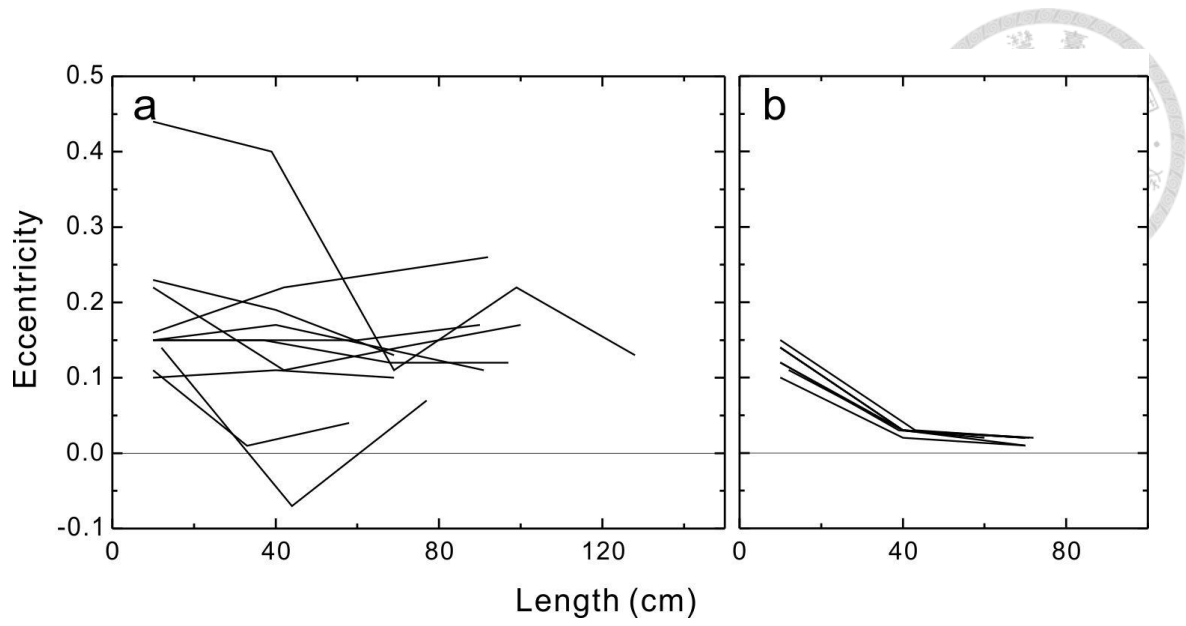
Figure 15. Pith eccentricity on the wood discs of the measuring sites of the plagiotropic branches (**a**) and the orthotropic branches (**b**).

Positive values for hypotrophic eccentricity and negative for epitrophic eccentricity
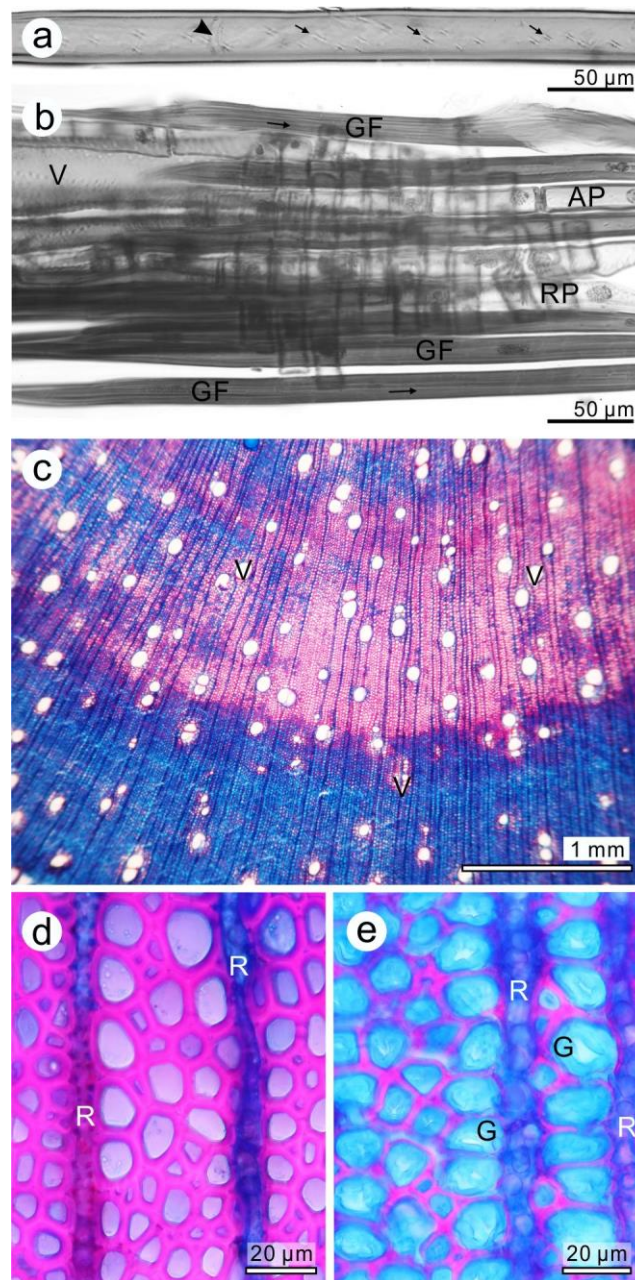
Figure 16. Anatomical features of the branchwood of *Koelreuteria henryi*.

a. A macerated normal wood fiber showing a septate (arrow head) and pits (arrows); the pit angle, indicating MFA, is about 32°. **b** A piece of macerated tension wood samples containing G-fibers; the microfibril in the G-layer is almost parallel to the axis of the G-fiber (arrows). **c** Wood sections stained with safranin O and alcian blue showing normal wood in red and tension wood in blue. **d** The normal wood fibers contain lignified secondary wall color in red. **e** The G-fibers in tension wood contain non-lignified G-layers (stained blue) inside the thinner lignified secondary wall (red). *V* vessel, *R* ray, *G* G-layer, *GF* G-fibers, *AP* axial parenchyma, *RP* ray parenchyma

46
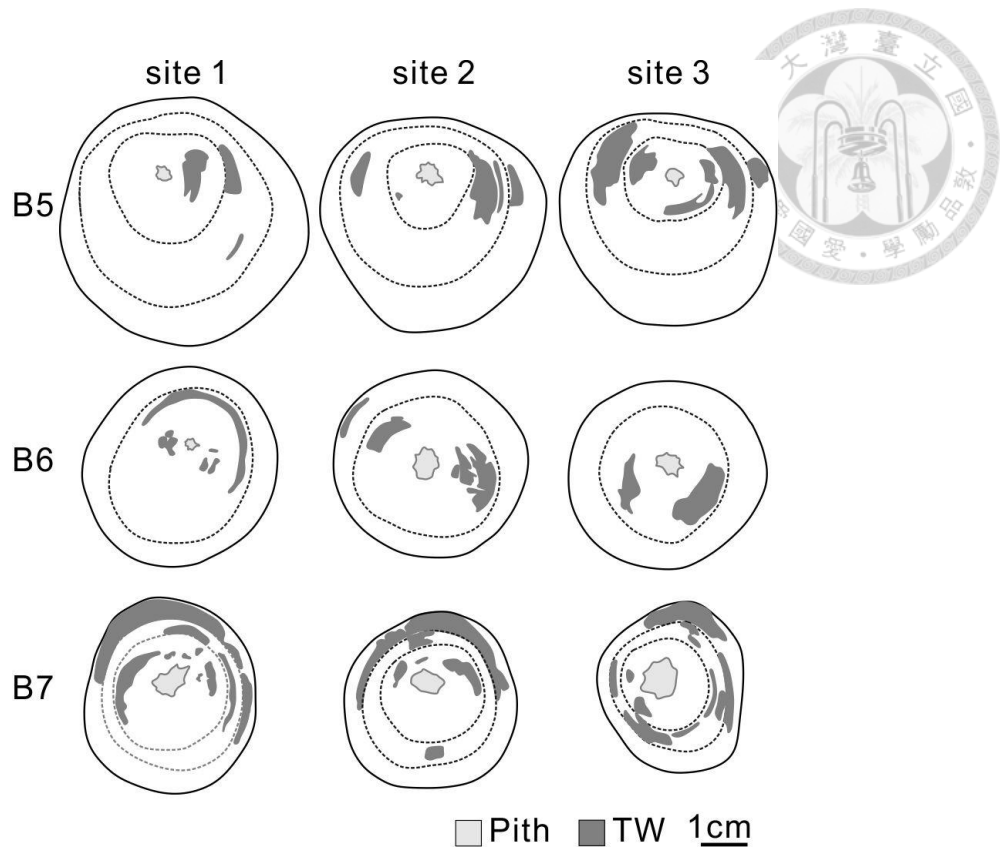
Figure 17. Distribution of tension wood on the wood sections at the 3 measuring sites of every plagiotropic branch sampled in Nov. 2008
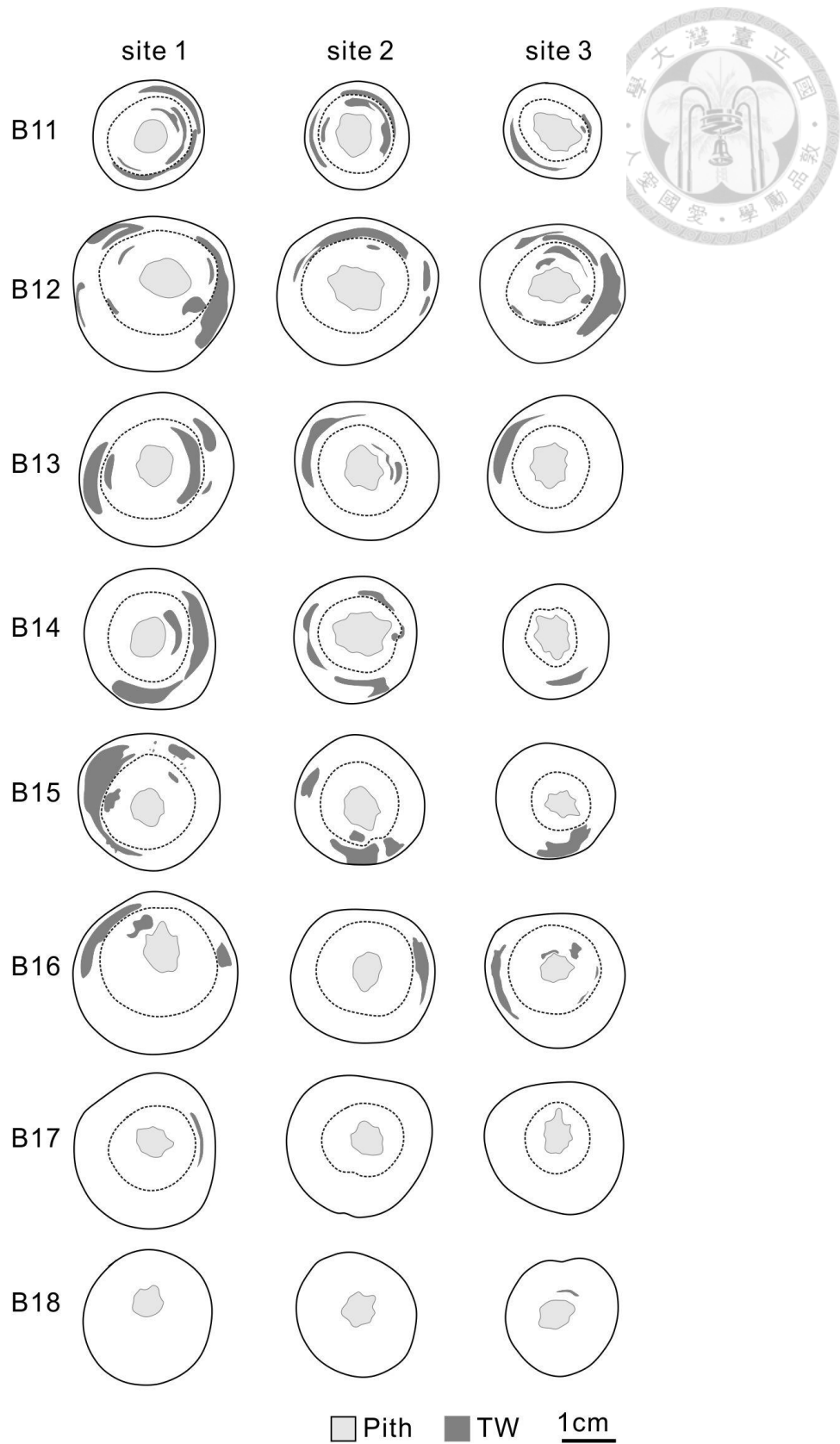
Figure 18. Distribution of tension wood on the wood sections at the 3 measuring sites of the orthotropic branches B11-18 sampled in Nov. 2011

48

Prediction of the bending tendency of K. henryi branches
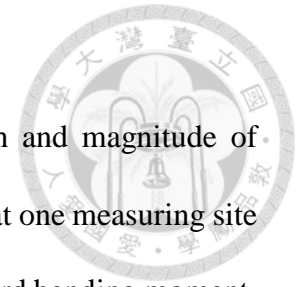
In Huang's model, SBS parameter (β) indicates the direction and magnitude of gravitational force. All branches exhibited negative β values except at one measuring site (Table 4), meaning that the weight of the branch generated a downward bending moment. For the plagiotropic branches, the mean values of β were −632 (SD 202) in May 2009; −789 (297) $\mu\varepsilon$ in August 2008, and −660 (140) $\mu\varepsilon$ in November 2008; and for the orthotropic branches it was −244 (183) $\mu\varepsilon$ in November 2011. Within the plagiotropic branches, no significant difference was found among different seasons, ($F = 1.41$, $p = 0.262$, Fig. 19a). Nevertheless, for the branches sampled in autumn, the magnitude of β value was larger in the plagiotropic branches than in the orthotropic branches ($t = −5.87$, $p < 0.001$, Fig. 19a).

RGS parameter (α) representing the direction and magnitude of gravitropic correction was found either negative or positive in the branches of *K. henryi* (Table 4). The negative value indicates that the moment generated by the wood is to pull the branch upward, while the positive one implies a downward bending moment. For the plagiotropic branches, the averaged α values were 85 (SD 214) $\mu\varepsilon$ in May 2009, −122 (SD 177) $\mu\varepsilon$ in August 2008, and −245 (SD 234) $\mu\varepsilon$ in November 2008; and they were significantly different among seasons ($F = 5.82$, $p < 0.01$, Fig. 19b). In summer and autumn the α values were mostly negative; however, positive α values occurred in 6 out of the 9 measuring sites in spring (Table 4). For the orthotropic branches, negative and positive α values occurred quite evenly (Table 4), and the mean value was 20 (185) $\mu\varepsilon$ in November 2011. It was different from that of the plagiotropic branches sampled in in November 2008 ($t = −3.29$, $p < 0.01$).

49

The correlation between β and α, β and ε_{gu}, as well as β and ε_{gl} were tested to understand how the growth stress is related to the self-weight of the branch, and no significant correlation was found on either the plagiotropic or the orthotropic branches (Fig. 20).

We predict the bending tendency by examining the sign of $\beta - \alpha$ and α/β. The results revealed that all the examined plagiotropic branches tended to bend downward. Most orthotropic branches also showed downward bending tendency with several measuring sites exhibiting upward bending tendency (Table 4).

Figure 19. Seasonal SBS parameter (β) (**a**) and RGS parameter (α) (**b**) of the plagiotropic and orthotropic branches of *Koelreuteria henryi*. The sampling date was listed in the order of seasons

Table 4. SBS parameters (β) and RGS parameters (α), bending tendency, and the rate of curvature change of *Koelreuteria henryi* branches

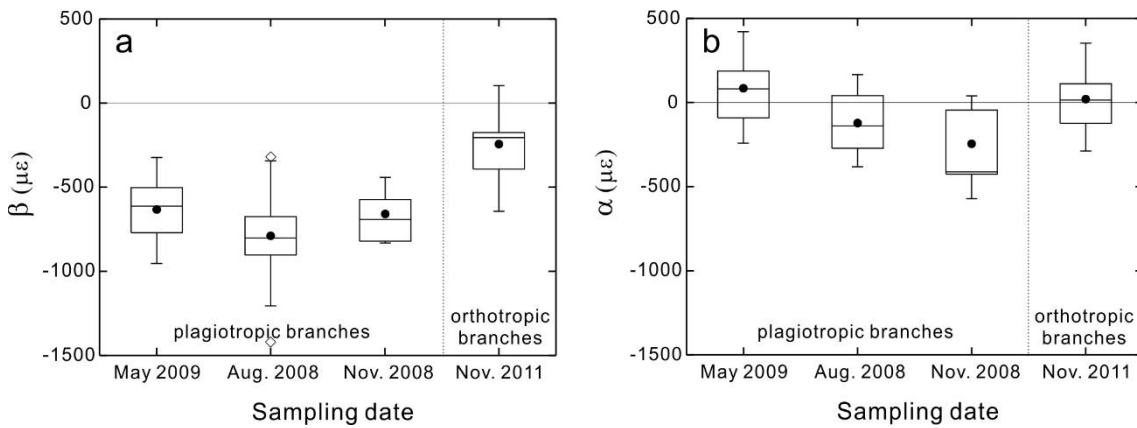| Branch type	Sampling date	Branch no.	site	L (cm)	β	α	α'	β-α	α/β	Bending tendency	β-α'	Bending tendency	dC_s/dR (m⁻²)	dC_g/dR (m⁻²)	dC/dR (m⁻²)	dC_g'/dR (m⁻²)	dC'/dR (m⁻²)
plagiotropic	Aug. 2008 Summer	B1	1	10	-996	-382	-367	-614	0.38	DW	-628	DW	-4.9	1.88	-3.02	1.81	-3.09
			2	37.2	-1206	-221	-52	-985	0.18	DW	-1153	DW	-6.48	1.19	-5.3	0.28	-6.2
			3	67.7	-807	-68	-30	-739	0.08	DW	-777	DW	-6.72	0.57	-6.15	0.25	-6.46
			4	96.9	-903	122	115	-1025	-0.14	DW	-1018	DW	-6.99	-0.94	-7.94	-0.89	-7.89
		B2	1	10	-797	-88	-180	-709	0.11	DW	-617	DW	-8.13	0.89	-7.23	1.83	-6.29
			2	39.5	-675	41	-66	-716	-0.06	DW	-609	DW	-8.72	-0.53	-9.25	0.85	-7.86
		B3	1	10	-866	-139	-211	-727	0.16	DW	-655	DW	-6.25	1	-5.24	1.53	-4.72
			2	39.4	-319	166	235	-485	-0.52	DW	-554	DW	-2.12	-1.1	-3.22	-1.56	-3.68
			3	69.3	-557	-272	-295	-286	0.49	DW	-262	DW	-3.77	1.84	-1.93	1.99	-1.77
			4	99.1	-802	-127	-99	-676	0.16	DW	-703	DW	-7.45	1.18	-6.28	0.92	-6.53
			5	128.1	-344	-301	-116	-43	0.88	DW	-227	DW	-3.72	3.26	-0.46	1.26	-2.46
		B4	1	10	-676	-290	-93	-386	0.43	DW	-583	DW	-3.14	1.35	-1.79	0.43	-2.71
			2	42	-676	111	164	-787	-0.16	DW	-840	DW	-3.84	-0.63	-4.47	-0.93	-4.78
			4	99.6	-1421	-259	-9	-1162	0.18	DW	-1412	DW	-14.21	2.59	-11.62	0.09	-14.12
		Mean			**-789**	**-122**	**-72**	**-667**			**-717**		**-6.17**	**0.90**	**-5.28**	**0.56**	**-5.61**
		SD			**297**	**177**	**167**	**298**			**317**		**3.06**	**1.32**	**3.10**	**1.11**	**3.16**
	Nov. 2008 Autumn	B5	2	42	-684	40	418	-724	-0.06	DW	-1102	DW	-5.04	-0.29	-5.33	-3.08	-8.12
			3	92	-512	-94	57	-418	0.18	DW	-569	DW	-3.89	0.71	-3.18	-0.44	-4.33
		B6	1	10	-831	-45	-48	-786	0.05	DW	-782	DW	-5.85	0.31	-5.54	0.34	-5.52
			2	32.9	-821	-36	0	-786	0.04	DW	-821	DW	-7.39	0.32	-7.07	0	-7.39
			3	57.8	-692	-426	-426	-266	0.62	DW	-266	DW	-6.6	4.06	-2.54	4.06	-2.54
		B7	1	10	-721	-417	-328	-304	0.58	DW	-393	DW	-7.71	4.46	-3.25	3.5	-4.2
			2	39.5	-574	-571	-554	-3	0.99	DW	-20	DW	-6.47	6.44	-0.03	6.25	-0.22
			3	68.7	-442	-412	-392	-30	0.93	DW	-50	DW	-5.74	5.35	-0.39	5.09	-0.64
		Mean			**-660**	**-245**	**-159**	**-415**			**-500**		**-6.09**	**2.67**	**-3.42**	**1.97**	**-4.12**
		SD			**140**	**234**	**322**	**321**			**387**		**1.24**	**2.68**	**2.48**	**3.22**	**2.89**
	May 2009 Spring	B8	1	12	-802	81	163	-883	-0.10	DW	-965	DW	-4.06	-0.41	-4.47	-0.83	-4.89
			2	44	-410	310	280	-720	-0.76	DW	-689	DW	-2.27	-1.72	-4	-1.55	-3.83
			3	77	-954	159	139	-1113	-0.17	DW	-1093	DW	-6.77	-1.12	-7.89	-0.98	-7.75
		B9	1	10	-580	73	33	-653	-0.13	DW	-613	DW	-2.89	-0.36	-3.26	-0.16	-3.06
			2	39.5	-502	-91	43	-411	0.18	DW	-545	DW	-2.75	0.5	-2.26	-0.24	-2.99
			3	90.5	-736	420	415	-1155	-0.57	DW	-1151	DW	-5.94	-3.39	-9.33	-3.35	-9.29
		B10	1	10	-323	187	294	-510	-0.58	DW	-617	DW	-1.26	-0.73	-1.99	-1.15	-2.41
			2	60	-771	-135	-87	-636	0.18	DW	-684	DW	-4.57	0.8	-3.77	0.51	-4.06
			3	90	-613	-242	-299	-371	0.39	DW	-313	DW	-3.91	1.54	-2.36	1.91	-2
		Mean			**-632**	**85**	**109**	**-717**			**-741**		**-3.82**	**-0.54**	**-4.37**	**-0.65**	**-4.48**
		SD			**202**	**214**	**217**	**284**			**274**		**1.76**	**1.46**	**2.57**	**1.45**	**2.48**

51

									β				dC_s/dR	dC_g/dR	dC/dR	dC'_g/dR	dC'/dR
orthotropic	Nov 2011 Autumn	B11	1	10	-180	-276	-296	96	**1.53**	UW	116	UW	-7.06	10.8	3.74	11.6	4.54
			2	40	-181	15	28	-196	-0.08	DW	-209	DW	-7.71	-0.64	-8.35	-1.21	-8.92
			3	70	-2	-142	-137	140	**71.00**	UW	136	UW	-0.08	7.31	7.23	7.09	7.01
		B12	1	10	-643	320	554	-963	-0.50	DW	-1197	DW	-12.52	-6.24	-18.76	-10.8	-23.33
			2	40	-526	40	124	-566	-0.08	DW	-650	DW	-10.85	-0.81	-11.67	-2.55	-13.4
			3	70	-499	-50	17	-450	0.10	DW	-516	DW	-11.9	1.18	-10.72	-0.41	-12.31
		B13	1	10	-175	-77	-78	-98	0.44	DW	-97	DW	-3.51	1.54	-1.97	1.56	-1.95
			2	40	-176	-101	-85	-75	0.57	DW	-91	DW	-4.23	2.44	-1.8	2.05	-2.18
			3	72	-14	-124	-143	110	**8.86**	UW	129	UW	-0.37	3.23	2.86	3.74	3.38
		B14	1	10	-379	94	123	-473	-0.25	DW	-502	DW	-9.82	-2.42	-12.24	-3.19	-13.01
			2	40	-359	-288	-215	-71	0.80	DW	-143	DW	-10.94	8.77	-2.17	6.57	-4.37
			3	70	-175	-98	-80	-77	0.56	DW	-94	DW	-6.81	3.82	-2.98	3.13	-3.68
		B15	1	12	-205	215	212	-420	-1.05	DW	-416	DW	-5.11	-5.37	-10.49	-5.29	-10.4
			2	40	-105	337	224	-442	-3.21	DW	-329	DW	-3	-9.63	-12.63	-6.41	-9.41
			3	70	103	353	356	-250	3.43	DW	-254	DW	3.61	-12.43	-8.82	-12.57	-8.95
		B16	1	10	-485	180	174	-665	-0.37	DW	-658	DW	-8.88	-3.3	-12.18	-3.19	-12.07
			2	43	-393	104	171	-497	-0.26	DW	-564	DW	-9.85	-2.61	-12.46	-4.3	-14.15
			3	71	-399	194	291	-593	-0.49	DW	-690	DW	-10.38	-5.05	-15.43	-7.57	-17.95
		B17	1	10	-239	-182	-151	-58	0.76	DW	-88	DW	-5.19	3.94	-1.25	3.27	-1.92
			2	40	-222	-7	74	-215	0.03	DW	-296	DW	-5.21	0.16	-5.05	-1.73	-6.95
			3	70	-137	111	189	-248	-0.81	DW	-326	DW	-3.65	-2.96	-6.61	-5.05	-8.7
		B18	1	10	-176	29	45	-205	-0.16	DW	-221	DW	-4.95	-0.82	-5.77	-1.28	-6.23
			2	39	-225	-216	-183	-10	0.96	DW	-42	DW	-7.27	6.96	-0.31	5.91	-1.36
			3	60	-54	45	59	-98	-0.83	DW	-113	DW	-2.03	-1.69	-3.71	-2.25	-4.28
		Mean			**-244**	**20**	**53**	**-264**			**-296**		**-6.15**	**-0.16**	**-6.31**	**-0.95**	**-7.11**
		SD			183	185	201	276			312		4.12	5.60	6.49	5.77	7.12

β, spring-back strain parameter, *α and α'* asymmetric RGS parameter, *DW* downward bending, *UW* upward bending; *dC_s/dR* rate of curvature change due to self-weight; *dC_g/dR* and *dC'_g/dR* rate of curvature change due to gravitropic correction, *dC/dR and dC'/dR* net rate of curvature change. *SD*
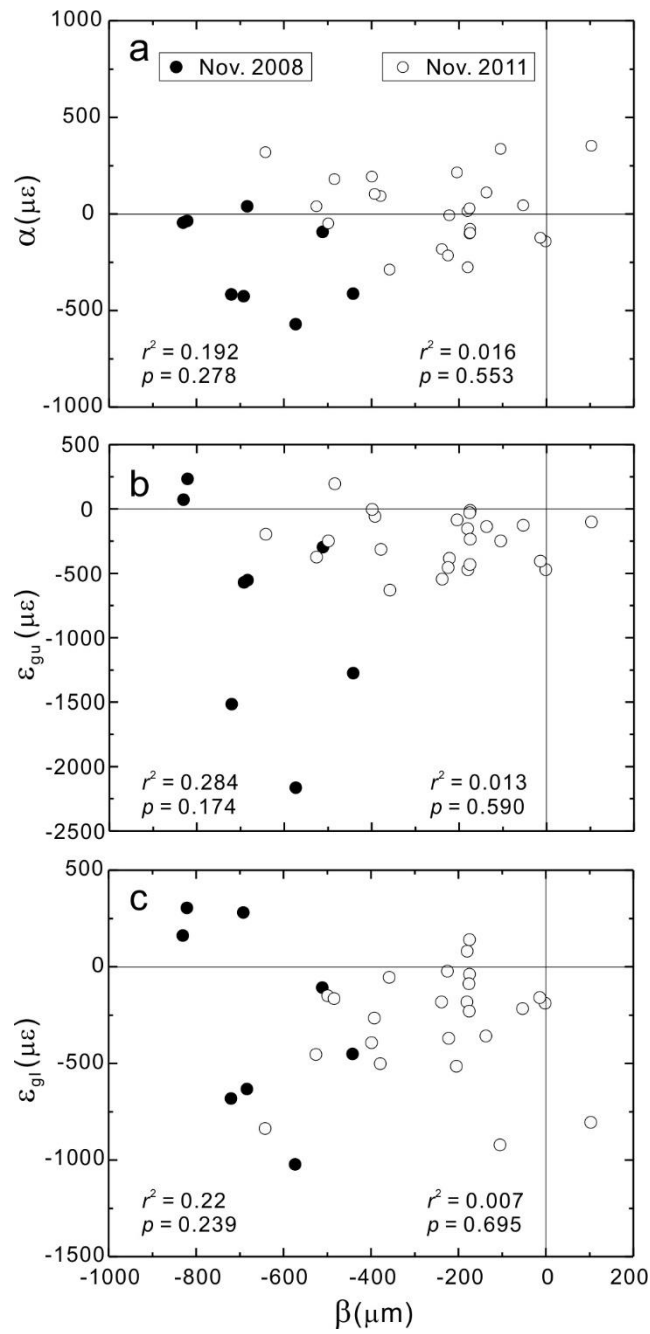
52

Figure 20. Relationships between β and α (**a**), β and ε_{gu} (**b**), and β and ε_{gl} (**c**) for the plagiotropic branches collected in Nov. 2008 (closed symbols) and the orthotropic branches in Nov. 2011 (open symbols)

53

Rates of curvature change

By applying Huang's model, we are able to further evaluate the rates of curvature change caused by self-weight (dC_s/dR) and gravitropic correction (dC_g/dR) and the consequent net rate of gravitropic response (dC/dR) which are submitted to a size effect. The values for each measuring site and the mean values for each sampling dates were listed in Table 4; and the values along the branch in the plagiotropic and orthotropic branches sampled in autumn were shown on Fig. 21.

Among all the sampled branches, the mean values of dCs/dR were all negative, meaning downward bending and the magnitude was the smallest in the plagiotropic branches of May 2009 (Table 4). The sign of the mean values of dCg/dR were different, meaning different bending movement due to gravitropic correction: upward bending for the plagiotropic branches of August and November; downward bending for the plagiotropic branches of May and the orthotropic branches of August. Finally, the mean values of dC/dR were all negative (Table 4). These results suggest that the plagiotropic branches tended to bend downward; and most orthotropic branches also tend to bend downward but with some measuring sites tended to bend upward (Fig. 21).
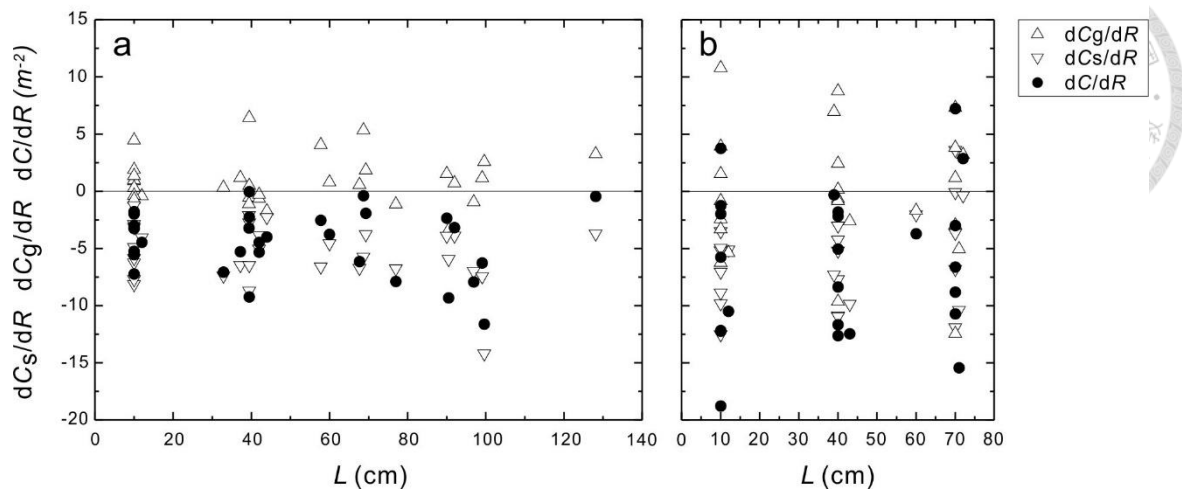
54

Figure 21. The relationship between dC_s/dR, dC_g/dR, dC/dR and the distance from the measuring sites to the trunk for the plagiotropic branches (**a**) and the orthotropic branches (**b**).

dC$_s$/dR rates of curvature change due to self-weight, *dC$_g$/dR* rates of curvature change due to gravitropic correction, *dC/dR* net rate of curvature change. Positive value for upward bending tendency and negative for downward

The effect of eccentric growth increment on bending tendency of the branches

Assuming that the cambial zone enters dormancy after defoliation and the annual wood production reaches its maximum, we evaluated the effect of growth eccentricity on α and the rate of curvature change due to growth, dC_g/dR, using the data of the plagiotropic and orthotropic branches collected in autumn. After being corrected with eccentric growth, the mean α increased from -245 (SD 234) $\mu\varepsilon$ to α' -159 (322) $\mu\varepsilon$, mean dC_g/dR from 2.67 (2.68) m^{-2} to dC_g'/dR 1.97 (3.22) m^{-2} for the plagiotropic branches. For the orthotropic branches, the mean α changed from 20 (185) $\mu\varepsilon$ to α' 53 (201) $\mu\varepsilon$, mean dC_g/dR from -0.16 (5.6) m^{-2} to dC_g'/dR -0.95 (5.77) m^{-2} (Table 4).

55

Effects of defoliation on the gravitropic response

Measured strain data of naturally and artificially defoliated branches of *K. henryi* Dummer. were shown in Table 5. Our analysis has shown that growth strain is the sum of measured growth strain after defoliation and spring-back strain during defoliation. As shown in Table 6, the mean α_1 of the naturally defoliated branches are positive due to overlay of spring-back strain. In full-leaf condition, the tendency is for downward bending with the mean $P_G = 0.84$, whereas after defoliation the tendency becomes upward bending (the mean $P_{1G} = 1.58$) due to weight loss. Therefore, the weight of leaves plays an important role in gravitational disturbance. The curvature change can be calculated by using measured strain and spring-back strain after defoliation. The values of dC/dR are all negative indicating downward bending tendency. After defoliation dC_1/dR becomes positive indicating upward bending tendency. The spring-back strain during artificial defoliation of a branch ($\beta_{def} = -270$) and that after defoliation ($\beta_1 = -309$) have the same order of magnitude, indicating that the bending moment of leaf and that of branchwood are roughly equal.
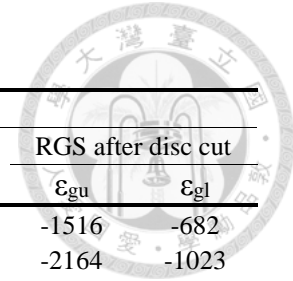
Table 5. Measured strain data of the natural and artificial defoliation branches of *Koelreuteria henryi*

Branch	Site	L(cm)	R(m)	Natural defoliation strain (με)				Artificial defoliation strain (με)					
				SBS after branch cut		RGS after disc cut		SBS after leaves removed		SBS after branch cut		RGS after disc cut	
				ε_{1su}	ε_{1sl}	ε_{gudef}	ε_{gldef}	ε_{sudef}	ε_{sldef}	ε_{su}	ε_{su}	ε_{gu}	ε_{gl}
B7	1	10	0.019					-251	403	-571	870	-1516	-682
	2	40	0.019					-233	307	-551	596	-2164	-1023
	3	69	0.018					-73	351	-239	645	-1275	-451
	4	99	0.016					-184	361	-339	551	-991	-453
	Mean							-185	356	-425	666	-1487	-652
	SD							80	39	162	142	500	270
ND1	1	10	0.024	-111	215	384	-1155						
	2	45	0.020	-28	152	-55	-1256						
	3	75	0.017	-93	138	422	-1895						
	Mean			-77	168	250	-1435						
	SD			44	41	265	401						
ND2	1	10	0.022	-224	304	-91	-437						
	2	50	0.019	-236	222	175	-271						
	3	80	0.017	-96	245	104	-733						
	Mean			-185	257	63	-480						
	SD			78	42	138	234						
ND3	1	10	0.024	-223	446	-85	-1404						
	2	40	0.021	-223	149	191	-101						
	3	70	0.019	-133	196	154	-527						
	4	110	0.016	-413	340	-563	-647						
	Mean			-248	283	-76	-670						
	SD			118	136	347	543						
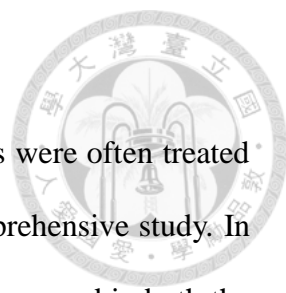
AD artificially defoliated branch, *ND* naturally defoliated branch, ε_{1su} and ε_{1sl} SBS on the upper side and the lower side after the naturally defoliated branch was cut, ε_{gudef} and ε_{gldef}, RGS on the upper side and the lower side after the wood disc of naturally defoliated branch was cut, ε_{sudef} and ε_{sldef} SBS on the upper side and the lower side after the leaves were artificially removed, ε_{su} and ε_{su} SBS on the upper side and the lower side after the branch was cut, ε_{gu} and ε_{gl} RGS on the upper side and the lower side after the wood disc was cut

Table 6. Experimental data of *Koelreuteria henryi* used for calculating the curvature change of branches

Branch	α (µε)	α_1(µε)	β_{def}(µε)	β (µε)	β_1(µε)	dC/dR (m^{-2})	dC_1/dR (m^{-2})	P_G	P_{1G}
B7	-417	-90	-327	-721	-394	-3.25	0.25	0.58	1.06
	-571	-301	-270	-574	-304	-0.03	3.01	0.99	1.88
	-412	-200	-212	-442	-230	-0.39	2.36	0.93	1.79
Mean	**-467**	**-197**	**-270**	**-579**	**-309**	**-1.22**	**1.88**	**0.84**	**1.58**
SD	**90**	**105**	**58**	**139**	**82**	**1.76**	**1.44**	**0.22**	**0.45**
ND1		770			-163	-6.37			
		601			-90	-6.99			
		1159			-116	-18.61			
Mean		**843**			**-123**	**-10.66**			
SD		**286**			**37**	**6.89**			
ND2		173			-264	-3.52			
		223			-229	-4.90			
		419			-171	-7.72			
Mean		**272**			**-221**	**-5.38**			
SD		**130**			**47**	**2.14**			
ND3		660			-335	-6.69			
		146			-186	-2.90			
		341			-165	-5.73			
		42			-377	-6.44			
Mean		**297**			**-265**	**-5.44**			
SD		**271**			**106**	**1.74**			

Asymmetric growth strain parameter of defoliated branch (α_1), spring-back strain parameter during defoliating action (β_{def}) and after defoliation (β_1), net rate of curvature change after defoliation (dC_1/dR), and gravitropic performance of full-leaf branch (P_G) and defoliated branch (P_{1G}). The values of each branch are averages computed from 3 to 4 measuring sites
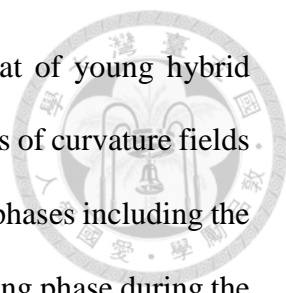
58

Discussion

The stem mechanical properties and related anatomical features were often treated in separate scopes of researches; only few integrated them in a comprehensive study. In this study, we attempt to understand the biomechanical role of tension wood in both the trunk and the branches of *Koelreuteria henryi* in maintaining the tree architecture. Firstly, we documented the trunk mechanical properties of *K. henryi*. We investigated the bending tendency of the inclined trunk of the seedlings, focusing on both physical behavior and anatomical changes during the uprighting process of *K. henryi*. And then we further examined the bending tendency and its relationships with growth eccentricity and tension wood in orthotropic and plagiotropic branches. We proposed that the branches of different angles or locations may have different bending tendency and the consequent physiological functions are distinguished from the trunk.

Dynamics of the up-righting process of the inclined trunk of Koelreuteria henryi seedlings

The reorientation of an inclined tree is based on asymmetric growth of the new axis created by the terminal bud at the primary growth level and of the pre-existing trunk at the secondary growth level (Thibaut et al. 2001). During the righting process the trunk curves continuously upward. Before reaching the vertical line, a counter autotropic curving initiated from the tip to keep the distal part of the trunk straight (Moulia et al. 2006).

Koelreuteria henryi is a tropical deciduous tree with a growth season from March to December. By a whole year's observation (Fig. 4), we found the reorientation process of the inclined seedlings takes place mainly in the first 3 months after tilting. The gravitropic
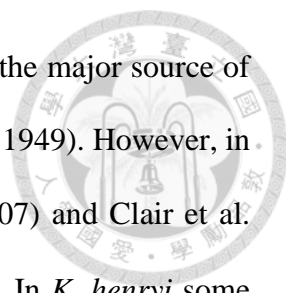
response of the tested inclined *K. henryi* seedlings is similar to that of young hybrid *Populus* studied by Coutand et al. (2007). By analyzing the kinematics of curvature fields and tension wood distribution along the trunk, they recognized three phases including the latent phase, the upward gravitropic phase, and the autotropic decurving phase during the righting process. These phases were also recognized in *Pinus pinaster* by Sierra-De-Grado et al. (2008) and in 8 tropical angiosperm species by Alméras et al. (2009).

Spatial and temporal RGS distribution on the trunk of the inclined Koelreuteria henryi seedlings

The intrinsic moving force generated by the wood structure of a tilted trunk is the cumulative effect of the stresses on the upper and the lower sides (Clair et al. 2006a; Huang et al. 2010). In general, typical RGS values for trunks range from −150 to −1000 $\mu\varepsilon$ for normal wood, from −1,000 to −4,000 $\mu\varepsilon$ for tension wood (Alméras et al. 2005; Clair et al. 2006a, c; Fournier et al. 1994b; Jullien et al. 2013; Kuo-Huang et al. 2007; Ruelle et al. 2007a). In seedlings, the magnitude of RGSs of tension wood is smaller (−600 to −1600 $\mu\varepsilon$) (Coutand et al. 2007; 2014). Our results with *K. henryi* showed even lower RGSs in tension wood (−661.39 ± 351.10 $\mu\varepsilon$ (SD)). Considering the seedling sizes in this study were smaller than those in the experiments of Coutand et al. (2014), our results support the trend that the smaller trees exhibit smaller levels of RGSs (Coutand et al. 2014). For *K. henryi* seedlings around 1 m in height, a relative small amount of tensile stress may be enough to pull the trunk back to an equilibrium position, or the opposite wood may also contribute to the uprighting process.
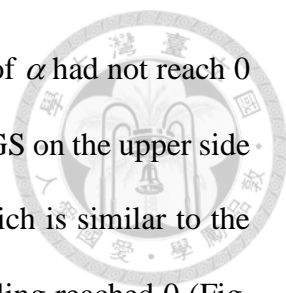
In 21 angiosperm species been studied by Clair et al. (2006c), the RGS on the upper side were 1.9 to 23.9 times of those on the lower side. The tensile stress on the upper side

60

rather than the stress occurred on the lower side is considered to be the major source of upward bending moment (Clair et al. 2006c; Fang et al. 2008; Onaka 1949). However, in the opposite wood of angiosperm trees, both Kuo-Huang et al. (2007) and Clair et al. (2006a) observed some light compressive strains (+100 ~ +200 $\mu\varepsilon$). In *K. henryi* some stronger, positive compressive strains were also found. Furthermore, we noticed that the ability of a tree trunk to bend upward, expressed by RGS parameter (α), decreased during the uprighting process. This reduction of α is due to the decrease of RGSs on the lower side (ε_{gl}) (Fig. 12). We therefore propose that in seedlings of *K. henryi,* the tensile stress on the upper side and the compressive stress on the lower side work intimately to reorient the tilted trunks.

A spatial variation of RGS was found in the inclined seedlings of *Liriodendron tulipifera* and *Prunus spachiana*, the RGSs decreased with the tree height in both fixed and free parts of the trunks (Yoshida et al. 2000a). Our experiment showed the same trend (Fig. 5), suggesting that the trunk base plays a key role in trunk reorientation. These results further explain the largest curvature found in the trunk base of poplar after 40 days of tilting (Coutand et al. 2007). The magnitude of α gradually reduced to near 0 and was sooner at the half-height of the trunks than at the base (Fig. 12).

Coutand et al. (2014) investigated the spatial and temporal variation in residual longitudinal maturation strains (rlms) weekly during the gravitropic response of young hybrid poplar. They found that at 100 cm from the stem base, the rlms reached the maximum at 35 days after tilting and then decreased. The differential of rlms between the upper and the lower side changed from negative to positive at 47 days after tilting which indicating the beginning of the autotropic phase. In our study the RGS was measured monthly and at the stem we found that the magnitude of RGS on the upper side was larger

61

than the lower side and lasted for 6 months (Fig. 5d); and the value of α had not reach 0 in six month (Fig. 12a). However, at the half-height the maximum RGS on the upper side was largest in 1 month after tilting and then decreased (Fig. 5c) which is similar to the observation of Coutand et al. (2014); and the value of α in one seedling reached 0 (Fig. 12b) indicating the beginning of the autotropic phase. These results suggest that the spatial and temporal variation in growth strain or stress are important in the study of gravitropic response.

Strain distribution on the branches of Koelreuteria henryi
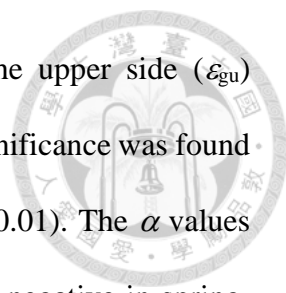
In angiosperms, the contractive strains on the upper side play an important role to pull the tilted tree trunk to the upright position (Clair et al. 2006c; Wilson and Archer 1977). Besides, extensive strains (compressive stress) found on the lower side of some species also help to bend upward (Clair et al. 2006a; Kuo-Huang et al. 2007). However, the diversified RGS distribution on the branches may reflect the individual biomechanical requirement of each branch depending on the environmental factors including gravitational stimuli and non-gravitational factors such as the architectural position of the branch, wind, and even sunlight (Fisher 1985; Matsuzaki et al. 2006; Matsuzaki et al. 2007). Researches concerning strain distribution of angiosperm branches are relatively rare. Tsai et al. (2012) compared the longitudinal RGS between the branches of 11 species and the tilted trunks of 37 species. Their results showed that the RGS on the upper side (ε_{gu}) of both the tilted trunks and the branches was contractive; nevertheless, the RGS on the lower side (ε_{gl}) was contractive on most tilted trunks and was extensive on most branches. Wang et al. (2009) observed various patterns of RGS on the branches of *Viburnum odoratissimum* var. *awabuki*: weak contractive or extensive strains on the

62

upper side and contractive on the lower side, contractive strains on the upper side and extensive strains on the lower side, and contractive strains on both sides.

In *K. henryi*, the artificially tilted trunks showed contractive strain on the upper side and either contractive or extensive on the lower side. On the other hand, the strain distribution of branches is complicated: for orthotropic branches the strain distribution is similar to that of the upright angiosperm trunks, but for plagiotropic branches either contractive or extensive strains was found on both sides, including an unusual pattern: extensive strains on both sides (Table 3). This pattern was discussed in gymnosperm pertaining to branch morphology (Huang et al. 2010), but to our knowledge, has not been described in the literature regarding angiosperm branches. We are currently not sure if this pattern is common or not, because the number of branches reported previously is still limited. Thus, accumulation of data of angiosperm branches from various species is required to estimate the proportion of every strain patterns within a species or a forest stand, and further to associate them with morphological or physiological functionality, as an angiosperm analogous study to the gymnosperm one (Huang et al. 2010).

Seasonal change of growth strain and RGS parameter on the branches of Koelreuteria henryi

The seasonal change of growth strain in upright trunks of Japanese cedar was studied by Okuyama et al. (1981). The average growth strains were $-200\ \mu\varepsilon$ in early June (early wood), reached a plateau at $-400\ \mu\varepsilon$ from late August (late wood) to next March before the spring flush occurred; they concluded that the growth stress stopped increasing when latewood formation had been finished, and the stress was thus accumulated in the trunk. The seasonal change of reaction strains has not been studied in branches. In the surveyed
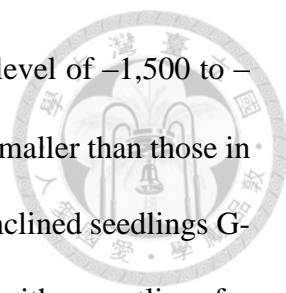
plagiotropic branches of *K. henryi*, the mean growth strain on the upper side (ε_{gu})

decreased from May to November (Fig. 14a) despite no statistical significance was found

($p = 0.19$). The RGS parameter (α) showed seasonal changes ($p < 0.01$). The α values

were mostly negative in summer and autumn, but either positive or negative in spring,

probably because the wood cells in spring did not proceed to cell wall maturation and

thus were not able to exert growth stress. Interestingly, positive α, which was rarely

published (but see Wang et al 2009), was observed in half of the measuring sites in the

orthotropic branches of *K. henryi* examined in autumn, suggesting the maturation stress

within orthotropic branches did not bend upward or downward in a uniform manner.

Strain and tension wood ratio in the inclined trunk of Koelreuteria henryi seedlings

Zinc chloride-iodine (Herzberg reagent) is commonly used to histochemically stain

G-fibers in tension wood (Doğu and Grabner 2010; Grzeskowiak et al. 1996; Tsai et al.

2012). However, this dye stains also the starch a blackish color, seriously disturbing the

measurement of tension wood zones. Both G-fibers and normal wood fibers of *K. henryi*

are living fibers generally filled with starch grains. We therefore used zinc chloride-iodine

to verify the presence of G-fibers, while resorting to the TBO staining in the delimitation

and measurement of tension wood zones.

In *K. henryi*, the tension wood ratio is highly correlated to the RGSs (Fig. 11), which

agrees the previous studies (Fang et al. 2008; Okuyama et al. 1994; Washusen et al.

2003b). In 11-year-old *Eucalyptus globulus*, Washusen et al. (2003a) found that G-fibers

presented in the investigated 3 populations at a level of -1200 $\mu\varepsilon$. In the non-conductive

tissues of a leaning 15 year-old poplar tree, Fang et al. (2008) found no G-fibers under a

growth strain level of −600 to −800 με, but 100% G-fibers above a level of −1,500 to −1,900 με. In this study, the seedlings of *K. henryi* were younger and smaller than those in the previous studies. In all RGS measuring site on the upper side of inclined seedlings G-fibers were detected where the RGSs ranged from −64 to −712 με (with an outlier of −1690) (Fig. 11), which is smaller than the threshold listed above. We therefore propose that smaller trees produces tension wood with smaller growth strains. This hypothesis certainly needs to be verified with bigger dataset including more species and large span of seedling size.

Tension wood distribution and its role in branch bending

Typical tension wood with G-fibers, commonly found in the upper side of leaning tree trunks of angiosperm, are proposed to generate tensile stress to compensate for the effect of self-weight or to recover stems to upright position (Bastien et al. 2014; Onaka 1949; Scurfield 1973). This phenomenon was also confirmed in inclined seedlings of *K. henryi*. The literature concerning the distribution of G-fibers in branches are limited. Fisher and Stevenson (1981) surveyed branches from 122 angiosperms and found G-fibers in 56 species. Among them, most species (44/56) produce G-fibers on the upper side of branches. However, there are numbers of exceptions. For example, G-fibers was observed on the lower side of branches in *Endospermum malaccense*, *Hevea brasiliensis*, and *Terminalia catappa*; on both upper and lower sides in *Salix fragilis* (Robards 1965), *Cinnamomun iners*, *Endospermum malaccense*, *Hevea brasiliensis*, *Maesopsis emini*, *T. catappa* and *Trema* sp. (Fisher and Stevenson 1981), or even as a complete ring *Sassafras officinale* (Kučera and Philipson 1977b), *Cassia polyphylla*, *Haematoxylum campechianum*, *Inga pastern*, and *Piscidia piscipula* (Fisher and Stevenson 1981). The

tension wood of *K. henryi* can be found in the upper, lower sides and/or left, right flanks of branches. The scattered patterns of G-fibers could imply dynamic adjustments of branch orientation due to factors besides negative gravitropism.
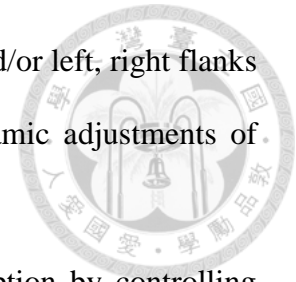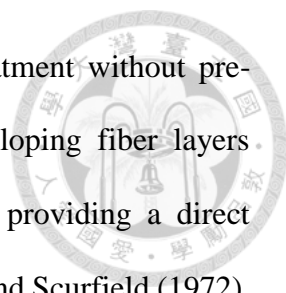
Trees tend to maximize their effective area for light interception by controlling branch angle (Fisher and Honda 1979). The tension wood formed on the lower side of branch could pull the branch downward (Fisher and Stevenson 1981), helping to create space in the tree crown for new twigs. The direction of illumination was shown to change stem orientation of *Quercus* species, by inducing tension wood (Matsuzaki et al. 2006, 2007). The lateral tension wood found in *K. henryi* might function in micro-adjusting horizontal distances between branches according to the light microenvironment in the tree crown.

The onset and formation of G-fibers

We verify the origin of G-fibers with pinning method. Pinning method, first introduced by Wolter (1968), marks the position of cambial zone at the time of pinning. This method is employed to monitor seasonal dynamics of cambial activity or wood formation for many tree species (Gričar et al. 2007; Mäkinen et al. 2008; Ohashi et al. 2001; Schmitt et al. 2004).
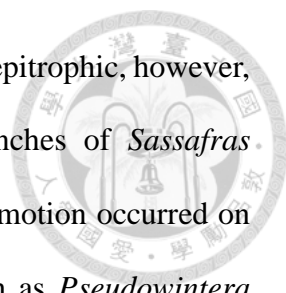
Concerning the research of reaction wood formation, Mukogawa et al. (2003) marked the vascular cambium with a knife instead of a pin to observe the eccentric growth of leaning trees in a macroscopic view. To study the phototropic and negative gravitropic bending, Matsuzaki et al. (2007) used pinning method to mark the radial direction and measured possible torsion of the main stem. We first employed the mothed to study the onset of artificially induced tension wood, and found it particularly useful in

discriminating the origin of G-fibers induced by the inclining treatment without pre-experimental noise. Our results clearly showed that several developing fiber layers preceded pinning wound were turned into G-fibers (Fig. 9a, d), providing a direct evidence to support the proposal of Jourez and Avella-Shaw (2003) and Scurfield (1972). At the onset of tilting, the differentiating xylary fiber cells in different stages may react to gravitational stimulus and add a G-layer in the innermost cell wall. Thus, the cell wall may consist of layers P+S1+S2 +G, P+S1+G, or even P+S1+S2+S3+G. The quick transformation from developing cells to G-fibers allows the plant to promptly recover to an equilibrium position. The formation of tension wood may result to the large contractive growth strain on the upper side (ε_{gu}) (Fig. 5), and finally bend the inclined seedlings to upright position. In our results, this recovering process lasted 3 months (Figs. 4, 5, Table 1). After the equilibrium has reached, the cells within vascular cambial region would then resume normal wood production.

The role of eccentric growth increment in gravitropic correction

Bending dynamics of a leaning trunk or a tilting branch depends on the mutual interaction of gravitational disturbance, phototropic response, and consequently the gravitropic correction (Alméras et al. 2005; Huang et al. 2010). Besides asymmetric growth strain and heterogeneous distribution of tension wood, the efficiency of gravitropic correction is also affected by eccentric growth increment. In the leaning trunk of a conifer, the additional radial growth is mostly found on the lower side, or hypotrophic. Despite some exceptions, the great majority of conifer branches are also hypotrophic with less pronounced eccentric growth than in trunks. Broadleaved trees are often epitrophic, i.e., additional growth on the upper side of leaning trunks, the branches of angiosperms

67

were more complicated (Timell 1986b). They were once regarded as epitrophic, however, a growing number of contradictions were published. In the branches of *Sassafras officinale*, tension wood formed on the upper side while growth promotion occurred on the lower side (White 1962). In species free of tension wood such as *Pseudowintera colorata* (Kuĉera and Philipson 1978) and *Viburnum odoratissimum* (Wang et al. 2009), growth increment was observed on the lower side. In a survey of 8 angiosperm species with or without G-fibers, (Tsai et al. (2012) found that the eccentricities are most positive (hypotrophic) in the branch base and generally decreased from basal to distal parts.

The eccentric growth in leaning trunks was found to increase the efficiency of reorientation by 31% for angiosperms and 26% for gymnosperms (Alméras et al. 2005). In this study, we found a 25% increase in efficiency of correction in the inclined trunk of *K. henryi* seedlings and the reaction wood is associated with promoted growth increment. Formation of tension wood and eccentric radial growth were proposed to be driven by different mechanisms without functional relationship (Duncker and Spiecker 2008; Timell 1986b); however, the co-occurrence of reaction wood and promoted growth increment at the same side in tree trunks is considered an ''economic'' solution to facilitate the reorientation process (Alméras et al. 2005).

Concerning the branches, eccentric growth increases efficiency of reorientation by 12.5% in *Chamaecyparis formosensis* (gymnosperm) (Huang et al. 2010) and as in the trunk, the promoted radial growth was found on the same side of reaction wood. Unlike the epitrophic growth eccentricity in the trunk, the branches of *K. henryi* show hypotrophic growth eccentricity which decreases the efficiency of upward bending for the plagiotropic branches (α changed from -245 $\mu\varepsilon$ to α' -159 $\mu\varepsilon$) and increases the efficiency of downward bending (α changed from 20 $\mu\varepsilon$ to α' 53 $\mu\varepsilon$) for the orthotropic branches. Besides, the promoted eccentric growth is not associated with the formation of

68

tension wood. The hypotrophic eccentric growth in branches functioned in obstructing upward movement and even facilitates downward movement, probably because the dissociation between tension wood and eccentric growth.
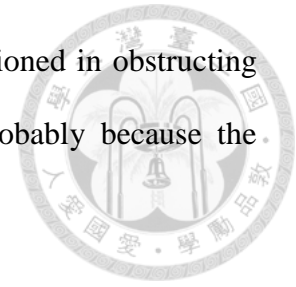
Interrelation between gravitational force and gravitropic correction

There are positive relationships between α and β in branches of *Chamaecyparis formosensis* (Huang et al. 2010), *Viburnum odoratissimum var. awabuki* (Wang et al. 2009), and 8 broadleaf tree species (Tsai et al. 2012), implying that the production of reaction maturation stress was probably controlled by branch weight. To be precise, the control of branch weight increased the generation of extensive strain on the lower side (ε_{gl}) of the *C. formosensis* (gymnosperm) branches (Huang et al. 2010), but in the 8 angiosperm species the contractive strain on the upper side (ε_{gu}) was induced (Tsai et al. 2012). However, the correlation between α and β was not statistically significant in both plagiotropic and orthotropic of *K. henryi*, indicating complicated factors other than gravitation involved in biomechanical behavior in branches of *K. henryi* (Fig. 20).

Functional differences between the branches and tree trunks

As reported in several angiosperm species (Tsai et al. 2012), most examined branches of *K. henryi* showed downward bending tendency, in contrast to the upward tendency in the leaning trunks. These results demonstrated the distinct functions of branches and trunks within a single species. Furthermore, instead of downward tendency in the plagiotropic branches, there are still 3 measuring sites showing upward tendency in the orthotropic ones. We propose a zonation pattern existing in a tree crown: the lower

69

zone contains sagging plagiotropic branches leading to larger space for young twigs; the upper zone contains a mixture of upward or downward bending branches to fine-tune for better light condition.
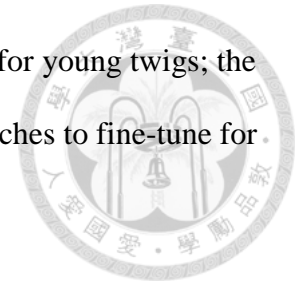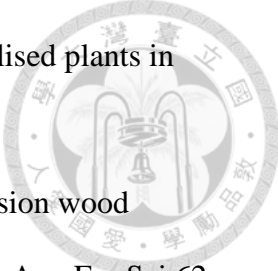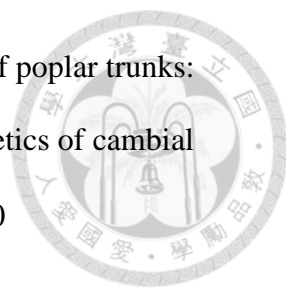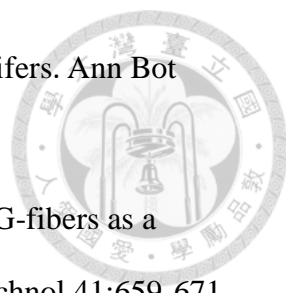
Conclusion

Our studies exemplify the different role of tree trunks and branches in maintaining tree mechanical equilibrium and maximizing light interception. We confirmed that at the time of inclination both the developing fibers and the vascular cambium on the upper side of the inclined *K. henryi* trunk are able to perceive the signal of mechanical change and produce G-fibers that generate a strong contractile strain to pull the trunk upright until the equilibrium is reached. The trunk base plays a key role in trunk uprighting and the associated eccentric growth increment on the upper side increases the efficiency of gravitropic correction. However, the varied distribution of tension wood on the branches implies that the bending of branches including upward, downward or lateral direction is possibly controlled by both gravitropism and phototropism to maximize light interception. In contrast to trunks, the dissociation between tension wood and eccentric growth in branches functions in obstructing upward movement and even facilitates downward movement.

References

Alméras T, Derycke M, Jaouen G, Beauchene J, Fournier M (2009) Functional diversity in gravitropic reaction among tropical seedlings in relation to ecological and developmental traits. J Exp Bot 60:4397-4410 doi:10.1093/jxb/erp276

Alméras T, Fournier M (2009) Biomechanical design and long-term stability of trees: Morphological and wood traits involved in the balance between weight increase and the gravitropic reaction. J Theor Biol 256:370-381

Alméras T, Thibaut A, Gril J (2005) Effect of circumferential heterogeneity of wood maturation strain, modulus of elasticity and radial growth on the regulation of stem orientation in trees. Trees 19:457-467 doi:10.1007/s00468-005-0407-6

Araki N, Fujita M, Saiki H, Harada H (1983) Transition of fiber wall structure from normal wood to tension wood in certain species having gelatinous fibers of S1+G and S1+S2+S3+G types. J Jap Wood Res Soc 29:491-499

Archer RR (1986) Growth stresses and strains in tress. Springer-Verlag, Berlin

Baba K, Park YW, Kaku T, Kaida R, Takeuchi M, Yoshida M, Hosoo Y, Ojio Y, Okuyama T, Taniguchi T, Ohmiya Y, Kondo T, Shani Z, Shoseyov O, Awano T, Serada S, Norioka N, Norioka S, Hayashi T (2009) Xyloglucan for generating tensile stress to bend tree stem. Mol Plant 2(5):893-903

Bamber RK (1987) The Origin of Growth Stresses: A Rebuttal. IAWA 8:80-84

Bamber RK (2001) A general theory for the origin of growth stresses in reaction wood: How trees stay upright. IAWA 22:205-212

Bastien R, Douady S, Moulia B . (2014) A unifying modeling of plant shoot gravitropism with an explicit account of the effects of growth. Front Plant Sci 5: 136

Batianoff, G.N. & Butler, D.W. (2002) Assessment of invasive naturalised plants in south-east Queensland. Plant Prot Q 17: 27-34.

Badia AM, Mothe F, Constant T, Nepveu G (2005) Assessment of tension wood detection based on shiny appearance for three poplar cultivars. Ann For Sci 62 62:43-49

Bowling AJ, Vaughn KC (2008) Immunocytochemical characterization of tension wood: Gelatinous fibers contain more than just cellulose. Am J Bot 95:655-663. doi:10.3732/ajb.2007368

Boyd JD (1972) Tree growth stresses—Part V: Evidence of an origin in differentiation and lignification. Wood Sci Technol 6:251-262

Boyd JD (1973) Compression wood force generation and functional mechanics. NZ JI For Sci 3:240-258

Clair B, Alméras T, Pilate G, Jullien D, Sugiyama J, Riekel C (2011) Maturation stress generation in poplar tension wood studied by synchrotron radiation microdiffraction. Plant Physiol 155(1):562-570

Clair B, Alméras T, Sugiyama J (2006a) Compression stress in opposite wood of angiosperms: observations in chestnut, mani and poplar. Ann For Sci 63:507-510 doi:10.1051/forest:2006032

Clair B, Alméras T, Yamamoto H, Okuyama T, Sugiyama J (2006b) Mechanical behavior of cellulose microfibrils in tension wood, in relation with maturation stress generation. Biophys J 91(3):1128-1135

Clair B, Ruelle J, Beauchêne J, Prévost MF, Fournier M (2006c) Tension wood and opposite wood in 21 tropical rain forest species 1. Occurrence and efficiency of the G-layer. IAWA 27:329-338

Clarke SH (1939) Stresses and strains in growing timber. Forestry 13:68-79

Coutand C, Fournier M, Moulia B (2007) The gravitropic response of poplar trunks: Key roles of prestressed wood regulation and the relative kinetics of cambial growth versus wood maturation. Plant Physiol 144:1166-1180 doi:10.1104/pp.106.088153

Coutand C, Pot G, Badel E (2014) Mechanosensing is involved in the regulation of autostress levels in tension wood. Trees 28:687-697 doi:10.1007/s00468-014-0981-6

Dassot M, Fournier M, Ningre F, Constant T (2012) Effect of tree size and competition on tension wood production over time in beech plantations and assessing relative gravitropic response with a biomechanical model. Am J Bot 99:1427-1435. doi:10.3732/ajb.1200086

Dinwoodie JM (1966) Growth Stresses in Timber—A Review of Literature. Forestry 39:162-170

Doğu AD, Grabner M (2010) A staining method for determining severity of tension wood. Turk J Agric For 34(5):381-392

Donaldson L (2008) Microfibril angle: measurement, variation and relationships - a review. IAWA 29(4):345-386

Du S, Yamamoto F (2003) Ethylene evolution changes in the stems of *Metasequoia glyptostroboides* and *Aesculus turbinata* seedlings in relation to gravity-induced reaction wood formation. Trees 17:522-528. doi:10.1007/s00468-003-0275-x

Du S, Yamamoto F (2007) An overview of the biology of reaction wood formation. J Integr Plant Biol 49:131-143

Duncker P, Spiecker H (2008) Cross-sectional compression wood distribution and its relation to eccentric radial growth in *Picea abies* [L.] Karst. Dendrochronologia 26(3):195-202

Ewart AJ, Mason-Jones AJ (1906) The formation of red wood in conifers. Ann Bot 20:201-204

Fang CH, Clair B, Gril J, Alméras T (2007) Transverse shrinkage in G-fibers as a function of cell wall layering and growth strain. Wood Sci Technol 41:659-671

Fang CH, Clair B, Gril J, Liu SQ (2008) Growth stresses are highly controlled by the amount of G-layer in poplar tension wood. IAWA 29(3):237-246

Fisher JB (1985) Induction of reaction wood in *Terminalia* (Combretaceae): roles of gravity and stress. Ann Bot 55:237-248

Fisher JB, Honda H (1979) Branch geometry and effective leaf area: A study of *Terminalia*-branching pattern. 1. Theoretical trees. Am J Bot 66:633-644

Fisher JB, Stevenson JW (1981) Occurrence of reaction wood in branches of dicotyledons and Its role in tree architecture. Bot Gaz 142:82-95

Florida Exotic Pest Plant Council (2015) Florida Exotic Pest Plant Council's 2015 List of Invasive Plant Species. http://www.fleppc.org/. accessed 24 June 2016

Fournier M, Bordonne PA, Guitard D, Okuyama T (1990) Growth stress patterns in tree stems. Wood Sci Technol 24:131-142

Fournier M, Bailleres H, Chanson B (1994a) Tree biomechanics: growth, cumulative prestresses, and reorientations. Biomimetics 2:229-251

Fournier M, Chanson B, Thibaut B, Guitard D (1994b) Measurements of residual growth strains at the stem surface. Observations on different species. Ann For Sci 51(3):249-266

Funada R, Kubo T, Fushitani M (1990) Earlywood and latewood formation in *Pinus densiflora* trees with different amounts of crown. IAWA 11:281-288

Funada R, Miura T, Shimizu Y, Kinase T, Nakaba S, Kubo T, Sano Y (2008)
Gibberellin-induced formation of tension wood in angiosperm trees. Planta
227:1409-1414. doi:10.1007/s00425-008-0712-6

Gardiner B, Barnett J, Saranpää P, Gril J (2014) The biology of reaction wood.
Springer-Verlag Berlin Heidelberg.

Goswami L, Dunlop JWC, Jungnikl K, Eder M, Gierlinger N, Coutand C, Jeronimidis
G, Fratzl P, Burgert I. (2008) Stress generation in the tension wood of poplar is
based on the lateral swelling power of the G-layer. Plant J 56:531-538.

Gričar J, Zupančič M, Čufar K, Oven P (2007) Wood formation in Norway spruce
(*Picea abies*) studied by pinning and intact tissue sampling method. Wood Res
52(2):1-9

Grzeskowiak V, Sassus F, Fournier M (1996) Macroscopic staining, longitudinal
shrinkage and growth strains of tension wood of poplar (*Populus* x
euramericana cv I.214). Ann Sci For 53(6):1083-1097

Heinrich I, Banks J (2002) Using the pinning method to track intra-seasonal growth in
Toona ciliata (Australian Red Cedar) - Christmas Greetings from Australia!
IAWA 23:458-458

Hellgren JM, Olofsson K, Sundberg B (2004) Patterns of auxin distribution during
gravitational induction of reaction wood in poplar and pine. Plant Physiol
135:212-220

Höster HR, Liese W (1966) On the occurrence of reaction tissue in roots and branches
of dictyledons. Holzforschung 20:80-90

Huang YS, Hung LF, Kuo-Huang LL (2010) Biomechanical modeling of gravitropic
response of branches: roles of asymmetric periphery growth strain versus self-
weight bending effect. Trees 24:1151-1161 doi:10.1007/s00468-010-0491-0

Jacobs MR 1945 The growth stresses of woody stems. Commonwealth Forestry Bureau, Australia, Bull 28.

Japan Material Society (1982) Dictionary of wood industry. In: Committee of Woody Material Department (ed) Wood Industry Publishers, Kyoto, p 573 (In Japanese)

Johansen DA (1940) Plant microtechnique. McGraw-Hill Book Company, Inc., New York, USA

Jourez B, Avella-Shaw T (2003) Effet de la durée d'application d'un stimulus gravitationnel sur la formation de bois de tension et de bois opposé dans de jeunes pousses de peuplier (*Populus euramericana* cv 'Ghoy'). Ann For Sci 60:31-41

Jourez B, Riboux A, Leclercq A (2001) Comparison of basic density and longitudinal shrinkage in tension wood and opposite wood in young stems of Populus euramericana cv. Ghoy when subjected to a gravitational stimulus. Can J For Res 31:1676-1683
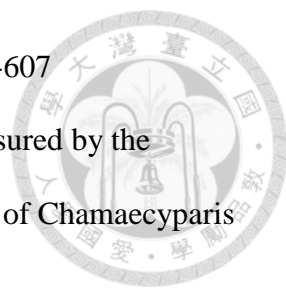
Jullien D, Widmann R, Loup C, Thibaut B (2013) Relationship between tree morphology and growth stress in mature European beech stands. Ann For Sci 70(2):133-142

Kubler, H. 1987. Growth stresses in trees and related wood properties. For Abstr 48:131-189.

Kučera LJ, Philipson WR (1977a) Growth eccentricity and reaction anatomy in branchwood of *Drimys winteri* and five native New Zealand trees. New Zeal J Bot 15:517-524

Kučera LJ, Philipson WR (1977b) Occurrence of reaction wood in some primitive dicotyledonous species. New Zeal J Bot 15:649-654

Kučera LJ, Philipson WR (1978) Growth eccentricity and reaction anatomy in

branchwood of *Pseudowintera colorata*. Am J Bot 65(6):601-607

Kuroda K, Kiyono Y (1997) Seasonal rhythms of xylem growth measured by the wounding method and with a band-dendrometer: An instance of Chamaecyparis obtusa. IAWA 18:291-299

Kuo-Huang LL, Chen SS, Huang YS, Chen SJ, Hsieh YI (2007) Growth strains and related wood structures in the leaning trunks and branches of *Trochodendron aralioides* - A vessel-less dicotyledon. IAWA 28:211-222

Mäkinen H, Nöjd P, Saranpää P (2003) Seasonal changes in stem radius and production of new tracheids in Norway spruce. Tree Physiol 23:959-968

Mäkinen H, Seo JW, Nöjd P, Schmitt U, Jalkanen R (2008) Seasonal dynamics of wood formation: a comparison between pinning, microcoring and dendrometer measurements. Eur J For Res 127(3):235-245

Matsuzaki J, Masumori M, Tange T (2006) Stem phototropism of trees: A possible significant factor in determining stem inclination on forest slopes. Ann Bot 98:573-581 doi:10.1093/aob/mcl127

Matsuzaki J, Masumori M, Tange T (2007) Phototropic bending of non-elongating and radially growing woody stems results from asymmetrical xylem formation. Plant Cell Environ 30:646-653 doi:10.1111/j.1365-3040.2007.01656.x

Mellerowicz EJ, Gorshkova TA (2012) Tensional stress generation in gelatinous fibres: a review and possible mechanism based on cell-wall structure and composition. J Exp Bot 63(2):551-565

Mellerowicz EJ, Immerzeel P, Hayashi T (2008) Xyloglucan: The molecular muscle of trees. Ann Bot 102(5):659-665

Moulia B, Coutand C, Lenne C (2006) Posture control and skeletal mechanical acclimation in terrestrial plants: Implications for mechanical modeling of plant

architecture. Am J Bot 93(10):1477-1489

Münch, E. 1938. Statics and dynamics of the cell wall's spiral structure, especially in compression wood and tension wood. Flora 32, 357-424.

Mukogawa Y, Nobuchi T, Sahri MJ (2003) Tension wood anatomy in artificially induced leaning stems of some tropical trees. Forest Res 75:27-33

Nicholson JE (1971) A rapid method for estimating longitudinal growth stresses in logs. Wood Sci Technol 5:40-48

Nishikubo N, Takahashi J, Roos AA, Derba-Maceluch M, Piens K, Brumer H, Teeri TT, Stalbrand H, Mellerowicz EJ (2011) Xyloglucan *endo*-transglycosylase-mediated xyloglucan rearrangements in developing wood of hybrid aspen. Plant Physiol 155(1):399-413

Nix LE, Brown CL (1987) Cellular kinetics of compression wood formation in slash pine Wood Fiber Sci 19:126-134

Nocetti M, Romagnoli M (2008) Seasonal cambial activity of spruce (Picea abies Karst.) with indented rings in the Paneveggio forest (Trento, Italy). Acta Biol Cracoviensia Ser Bot 50:27-34

Norberg PH, Meier H (1966) Physical and chemical properties of the gelatinous layer in tension wood fibres of aspen (*Populus tremula* L.). Holzforschung 20:174-178

Nugroho, WD, Nakaba, S, Yamagishi Y, Begum S, Marsoem SN, Ko JH, Funada R (2013). Gibberellin mediates the development of gelatinous fibres in the tension wood of inclined *Acacia mangium* seedlings. Ann Bot 112: 1321-1329. doi:10.1093/aob/mct198

Nugroho WD, Yamagishi Y, Nakaba S, Fukuhara S, Begum S, Marsoem SN, Funada R. (2012) Gibberellin is required for the formation of tension wood and stem gravitropism in *Acacia mangium* seedlings. Ann Bot 110: 887-895. doi:Doi

10.1093/Aob/Mcs148

Ohashi Y, Sahri MH, Yoshizawa N, Itoh T (2001) Annual rhythm of xylem growth in
    rubberwood (*Hevea brasiliensis*) trees grown in Malaysia. Holzforschung
    55(2):151-154

Okuyama T, Sasaki Y, Kikata Y, Kawai N (1981) The seasonal change in growth stress
    in the tree trunk. J Jpn Wood Res Soc 27:350-355

Okuyama T, Yamamoto H, Yoshida M, Hattori Y, Archer RR (1994) Growth stresses in
    tension wood - role of microfibrils and lignification. Ann Sci For 51(3):291-300

Onaka F (1949) Studies on compression- and tension-wood. Mokuzai Gakkaishi 1:1-88

Patel JD, Menon ARS, Reghu CP (1984) Growth eccentricity in the branchwood of
    Kigella pinnata (JACQ.) DC. IAWA 5:81-84

Pilate G et al. (2004) Lignification and tension wood. C R Biol 327:889-901.
    doi:10.1016/j.crvi.2004.07.006

Robards AW (1965) Tension wood and eccentric growth in Crack willow (*Salix fragilis,*
    L.). Ann Bot 29:419-431

Ruelle J, Beauchêne J, Yamamoto H, Thibaut B (2011) Variations in physical and
    mechanical properties between tension and opposite wood from three tropical
    rainforest species. Wood Sci Technol 45(2):339-357

Ruelle J, Clair B, Beauchêne J, Prévost MF, Fournier M (2006) Tension wood and
    opposite wood in 21 tropical rain forest species 2. Comparison of some
    anatomical and ultrastructural criteria. IAWA 27:341-376

Ruelle J, Yamamoto H, Thibaut B (2007a) Growth stresses and cellulose structural
    parameters in tension and normal wood from three tropical rainforest
    angiosperms species. Bioresources 2:235-251

Ruelle J, Yoshida M, Clair B, Thibaut B (2007b) Peculiar tension wood structure in

Laetia procera (Poepp.) Eichl. (Flacourtiaceae). Trees 21:345-355 doi:10.1007/s00468-007-0128-0
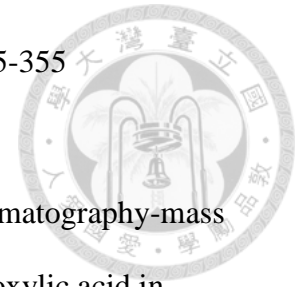
Savidge RA, Mutumba GM, Heald JK, Wareing PF (1983) Gas chromatography-mass spectros-copy identification of 1-aminocyclopropane-1-carboxylic acid in compression wood vascular cambium of *Pinus contorta* Dougl. Plant Physiol 71:434-436

Schmitt U, Jalkanen R, Eckstein D (2004) Cambium dynamics of *Pinus sylvestris* and *Betula* spp. in the northern boreal forest in Finland Silva Fenn 38(2):167-178

Schmitz N, Robert EMR, Verheyden A, Kairo JG, Beeckman H, Koedam N (2008) A patchy growth via successive and simultaneous cambia: Key to success of the most widespread mangrove species Avicennia marina? Ann Bot 101:49-58. doi:10.1093/aob/mcm280

Scurfield G, Wardrop AB (1963) The nature of reaction wood. VII. Lignification in reaction wood. Aust J Bot 11:107-116

Scurfield G (1972) Histochemistry of reaction wood cell walls in two species of *Eucalyptus* and in *Tristania conferta* R. BR. Aust J Bot 20:9-26

Scurfield G (1973) Reaction wood: its structure and function: lignification may generate the force active in restoring the trunks of leaning trees to the vertical. Science 179:647-655

Seo JW, Eckstein D, Schmitt U (2007) The pinning method: From pinning to data preparation. Dendrochronologia 25:79-86. doi::10.1016/j.dendro.2007.04.001

Sierra-De-Grado R, Pando V, Martinez-Zurimendi P, Penalvo A, Bascones E, Moulia B (2008) Biomechanical differences in the stem straightening process among *Pinus pinaster* provenances. A new approach for early selection of stem straightness. Tree Physiol 28(6):835-846

Sinnott EW (1952) Reaction wood and the regulation of tree Form. Am J Bot 39:69-78

Spurr A (1969) A low-viscosity epoxy resin embedding medium for electron

    microscopy. J Ultrastruct Res 26:31-43

The R Core Team. (2013). R : A Language and Environment for Statistical Computing

Thibaut B, Grila J, Fournier M (2001) Mechanics of wood and trees: some new

    highlights for an old story. C R Acad Sci Paris Série II b 329(9):701-716

Timell TE (1986a) Compression wood in Gymnosperms vol I. Springer-Verlag, Berlin

Timell TE (1986b) Compression wood in Gymnosperms vol II. Springer-Verlag, Berlin

Tsai CC, Hung LF, Chien CT, Chen SJ, Huang YS, Kuo-Huang LL (2012)
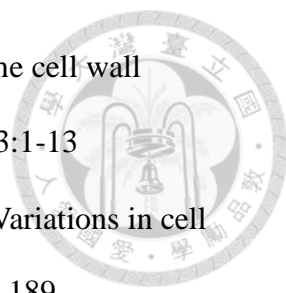
    Biomechanical features of eccentric cambial growth and reaction wood

    formation in broadleaf tree branches. Trees 26:1585-1595 doi:DOI

    10.1007/s00468-012-0733-4
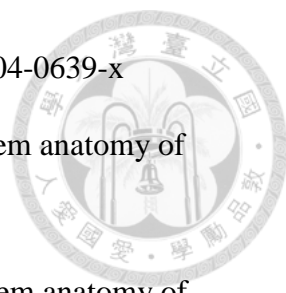
Veenin T, Nobuchi T, Fujita2 M, Siripatanadilok S (2006) Seasonal characteristics of

    wood formation in the elite genetic – Based *Eucalyptus camaldulensis* Dehnh.

    Kasetsart J (Nat Sci) 40:83-90

Wang Y, Gril J, Clair B, Minato K, Sugiyama J (2010) Wood properties and chemical

    composition of the eccentric growth branch of *Viburnum odoratissimum* var.

    awabuki. Trees 24:541-549 doi:10.1007/s00468-010-0425-x

Wang Y, Gril J, Sugiyama J (2009) Variation in xylem formation of *Viburnum*

    odoratissimum var. *awabuki*: growth strain and related anatomical features of

    branches exhibiting unusual eccentric growth. Tree Physiol 29:707-713

    doi:10.1093/treephys/tpp007

Wardrop AB, Dadswell HE (1948) The nature of reaction wood. I. The structure and

    properties of tension wood fibres. Aust J Sci Res 1:1-16

Wardrop AB, Dadswell HE (1950) The nature of reaction wood II. The cell wall

organization of compression wood tracheids. Aust J Biol Sci 3:1-13

Wardrop AB, Dadswell HE (1955) The nature of reaction wood. IV. Variations in cell

wall organization of tension wood fibres. Aust J Bot 3(2):177-189

Washusen R, Ilic J, Waugh G (2003a) The relationship between longitudinal growth

strain and the occurrence of gelatinous fibers in 10 and 11-year-old *Eucalyptus

globulus* Labill. Holz Roh Werkst 61:299-303 doi:10.1007/s00107-003-0388-3

Washusen R, Ilic J, Waugh G (2003b) The relationship between longitudinal growth

strain, tree form and tension wood at the stem periphery of ten- to eleven-year-

old *Eucalyptus globulus* Labill. Holzforschung 57:308-316

White DJB (1962) Tension wood in a branch of sassafras. J I Wood Sci 10:74-80

Wilson BF, Archer RR (1977) Reaction wood - induction and mechanical action. Annu

Rev Plant Phys 28:23-43

Wilson BF, Archer RR (1979) Tree design: some biological solutions to mechanical

problems. BioScience 29:293-298

Wilson BF, Ching-Te C, Zaerr JB (1989) Distribution of endogenous indole-3-acetic

acid and compression wood formation in reoriented branches of Douglas fir.

Plant Physiol 91:338-344

Wolter KE (1968) A new method for marking xylem growth. For Sci 14(1):102-104

Yamaguchi K, Shimaji K, Itoh T (1983) Simultaneous inhibition and induction of

compression wood formation by morphactin in artificially inclined stems of

Japanese larch (Larix leptolepis Gordon). Wood Sci Technol 17:81-89

Yamamoto H, Abe K, Arakawa Y, Okuyama T, Gril J (2005) Role of the gelatinous layer

(G-layer) on the origin of the physical properties of the tension wood of *Acer

sieboldianum. J Wood Sci 51:222-233 doi:10.1007/s10086-004-0639-x

Yamamoto F, Angeles G, Kozlowski TT (1987) Effect of ethrel on stem anatomy of *Ulmus-americana* seedlings. IAWA 8:3-10

Yamamoto F, Kozlowski TT (1987) Effect of ethrel on growth and stem anatomy of *Pinus-halepensis* seedlings. IAWA 8:11-20

Yang J-L, Waugh G (2001) Growth stress, its measurement and effects. Aust For 64:127-135

Yoshida M, Nakamura T, Yamamoto H, Okuyama T (1999) Negative gravitropism and growth stress in GA(3)-treated branches of *Prunus spachiana* Kitamura f. spachiana cv. Plenarosea. J Wood Sci 45:368-372

Yoshida M, Ohta H, Yamamoto H, Okuyama T (2002) Tensile growth stress and lignin distribution in the cell walls of yellow poplar, *Liriodendron tulipifera* Linn. Trees 16:457-464 doi:10.1007/s00468-002-0186-2

Yoshida M, Okuda T, Okuyama T (2000a) Tension wood and growth stress induced by artificial inclination in *Liriodendron tulipifera* Linn. and *Prunus spachiana* Kitamura f. ascendens Kitamura. Ann For Sci 57:739-746

Yoshida M, Yamamoto H, Okuyama T (2000b) Estimating the equilibrium position by measuring growth stress in weeping branches of *Prunus spachiana* Kitamura f. spachiana cv. *Plenarosea*. J wood Sci 46:59-62

Yoshimura K, Hayshi S, Itoh T (1981) Studies on the improvement of the pinning method for marking xylem growth I. Minute examination of pin marks in taeda pine and other species. Wood Res 67:1-16

Yoshizawa N, Satoh M, Yokota S, Idei T (1993a) Formation and structure of reaction wood in *Buxus microphylla* var. *insularis* Nakai. Wood Sci Technol 27:1-10

Yoshizawa N, Watanabe N, Yokota S, Idei T (1993b) Distribution of guaiacyl and syringyl lignins in normal and compression wood of *Buxus microphylla* var. *insularis* Nakai. IAWA 14(2):139-151

Appendix Ⅰ. Height and diameter growth of the studied seedlings

Plant materials and measurement

The height growth and the diameter growth of the studied upright and artificially inclined seedlings were monitored during the experiment. The tree height, the vertical diameter (D_V; the distance between the upper and the lower side) and the horizontal diameter (D_H; the diameter perpendicular to the vertical diameter) (Fig. A1) of the stem at the base (10 cm above soil) and the half-high of each seedling were measured monthly.
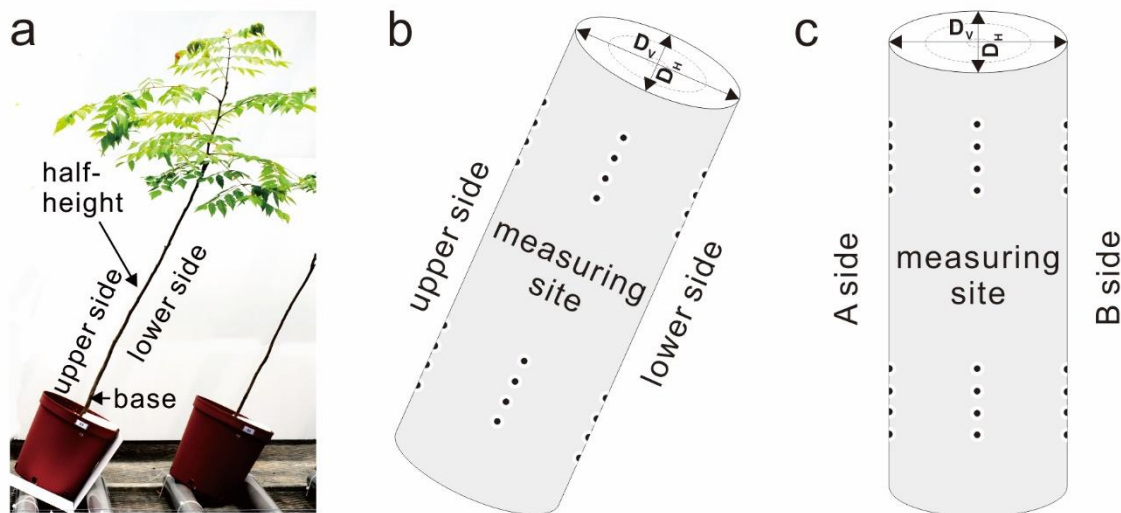
Figure A 1. Diameter measurement.

a Picture of an inclined seedling showing the location of measurement sites (the stem base and the half-height) and the position of the upper side and the lower side. **b** Illustration of a wood segment showing the upper side and the lower side of the inclined seedling; and its vertical diameter (D_V) and horizontal diameter (D_H). **c** The corresponding A side, B side, D_V, and D_H of the control seedling.

Results

All the control and inclined seedlings kept growing for the first three months (April 20 ~ July 23, 2009) (Fig. A2). After the first sampling (July 23, 2009), the remaining seedlings except T10~T12 kept height growing until late September 2009 (Fig. A2). Since then almost no height growth was observed for all the seedlings until late January 2010. Then the left 6 seedlings (C10~T12 and T10~T12) grew rapidly in height (Fig. A2).
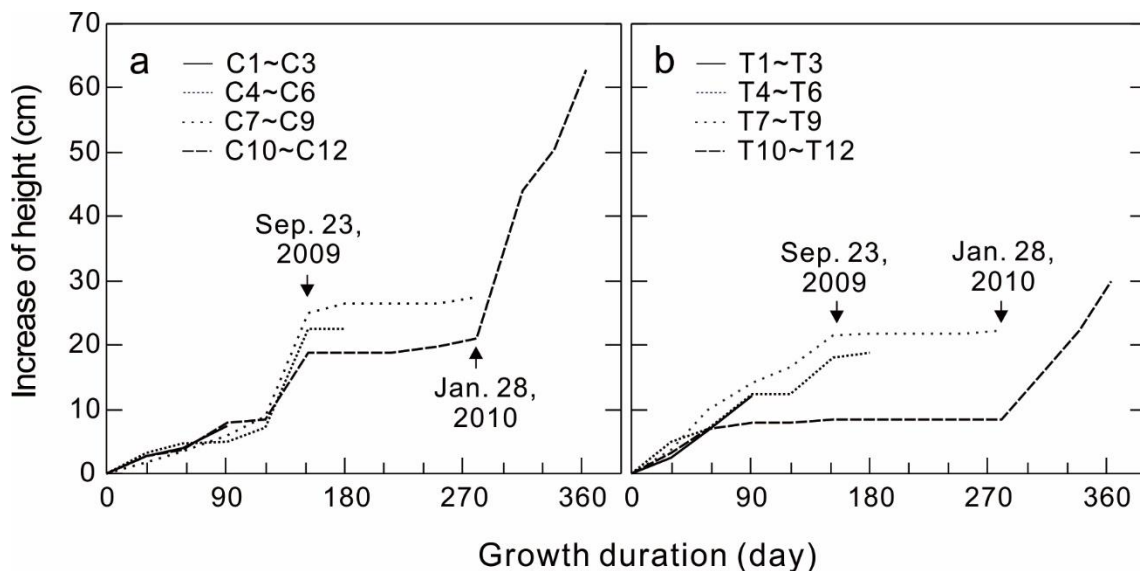
Figure A 2. The height growth of the control (**a**) and the inclined (**b**) seedlings.

The increase of the vertical and the horizontal diameter of the control seedlings was almost equal for the whole year (Fig. A3a-d). However, for the inclined seedlings, the increase of the vertical diameter at the stem base appeared larger than the horizontal diameter for at least six months after inclination (Fig. A3e, g). The same phenomenon was observed at the half-height of the inclined seedlings T10~T12 (Fig. A3h), but not for T7~T9 (Fig. A3f).

87
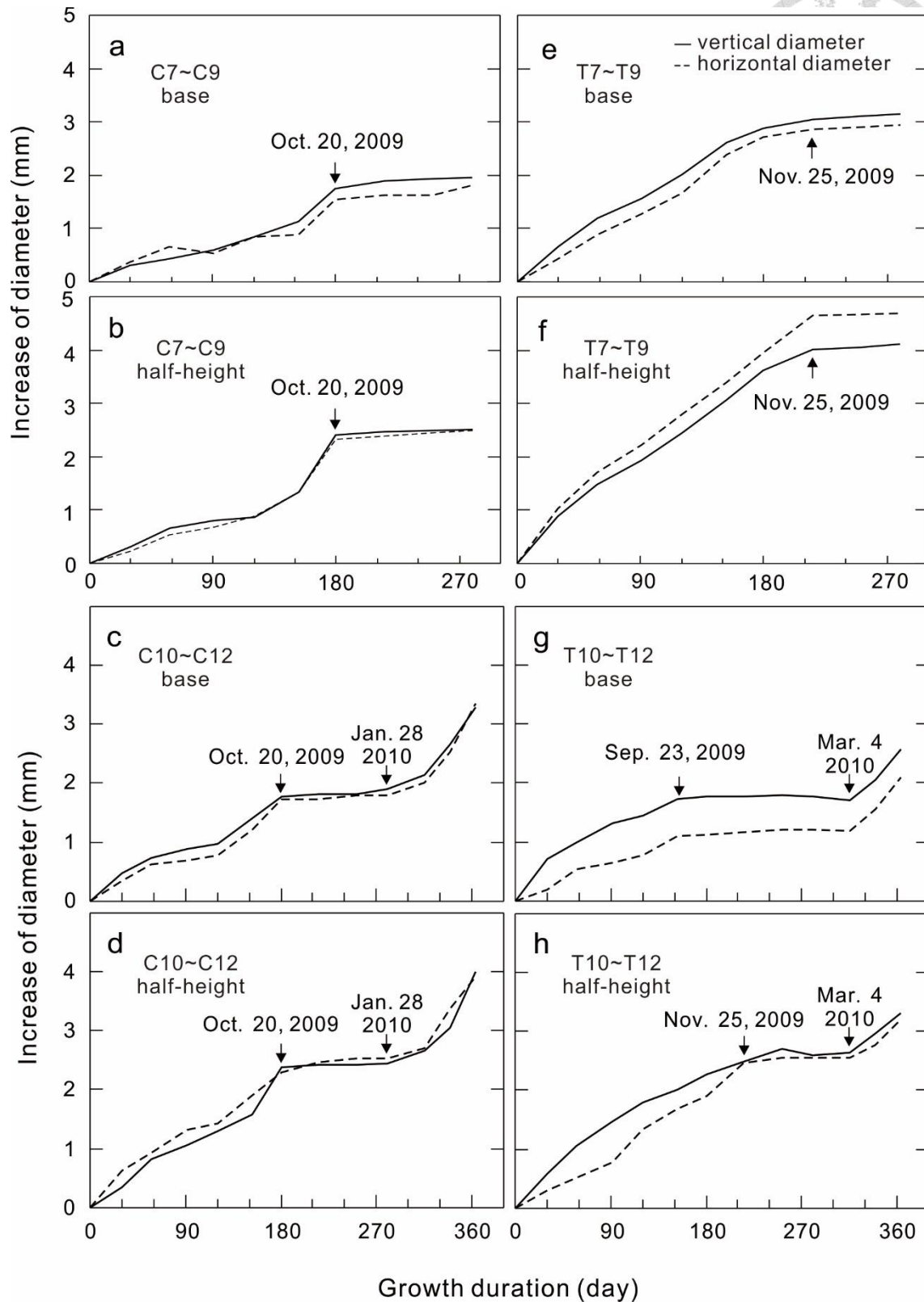
Figure A 3. Diameter growth (the vertical and the horizontal diameter) of the control seedlings C7~C12 and the inclined seedlings T7~T12.

Appendix Ⅱ. Practice of the pinning method and interpretation of the pinning result

Plants and practice of pinning method

The studied control and artificially inclined *K. henryi* seedlings were pinned at both the stem base and the half-height at the beginning of the experiment. Four pinning holes in a row were made on the upper (A side), the lower (B side), and the lateral sides of the inclined (control) trunk, respectively (Fig. A4a and b). The position of each pinning hole was first marked with white-out. Using a pair of pliers, an insect needle (0.4 mm in diameter) was inserted through the bark into the xylem (Fig. A4c) and then removed. The pinned seedlings were felled after the designed inclination duration. Stem segments of 3 cm long with the marked pinholes were fixed and stored in FPGA (Formalin: Propionic acid: Glycerol: 95% Alcohol: distilled water = 1: 1: 3: 7: 8).

By using sliding microtome (ERMA optical works, Ltd), serial wood sections (20 μm thick) containing pinning-induced callus were collected and stained with 1% toluidine blue O in 1% sodium borax (TBO) or double stained with 0.5% safranin O and 0.1% alcian blue (in 0.3% acetic acid). Whole stem sections were photographed by using a digital camera (Sony DSC-T200) and the wood sections by Nikon D3 on Leica Diaplan Light Microscope. The measurement was made by using Image J and plotted by SigmaPlot.
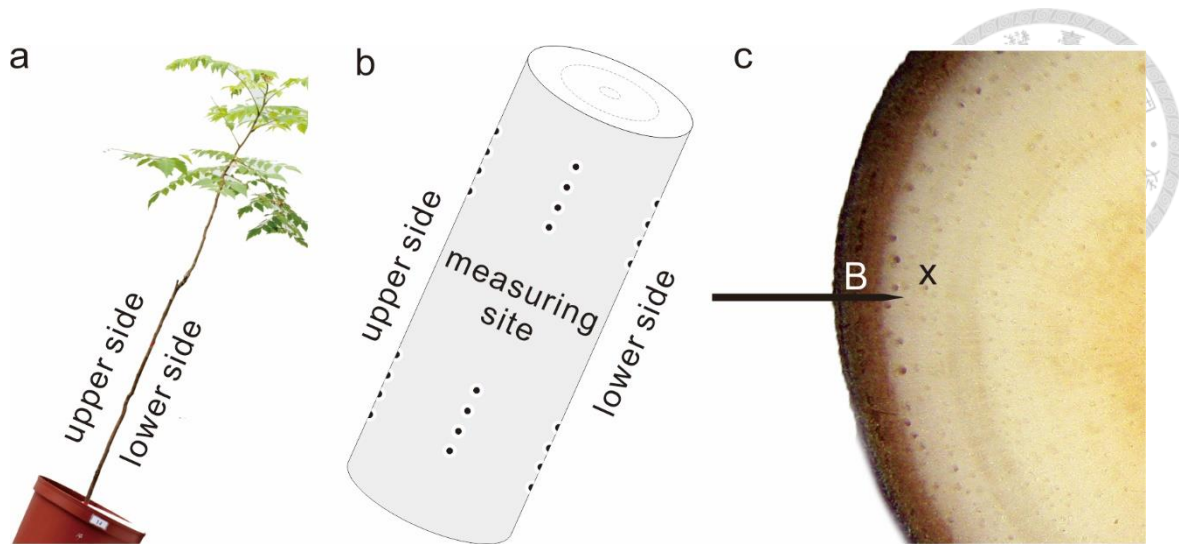
Figure A 4. The experimental design and the practical procedure of pinning method.
a The artificially inclined 2-year-old seedling of *Koelreuteria henryi* Dummer. **b** the pinning method was applied above and below the strain measuring site on the upper, the lower, and the lateral sides; mark with white-out before pinning. **c** a 0.4 mm insect pin is inserted through the bark to the xylem
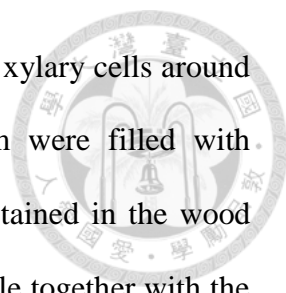
Sample preparation

The interpretation of the pinning result

Macroscopically, a stained wound area appears around the pin hole on the surface view of the cross-cut stem and the tension wood area was shown as a light colored crescent zone (Fig. A5a). Wood sectioning and staining makes these characteristics more obvious and clear (Fig. A5b). The stained area on the section of a pinhole could be subdivided to two subareas, a dense triangular and a loose rectangular or irregular area (Fig. A5). The triangular wound mark occurs as an isosceles triangle on each of the serial sections of a pin hole. The height is the maximum in the pin hole center and decreases gradually from the center to the edge (Fig. A6).

When the pin was inserted through the cambial zone into the youngest xylem, all the living cells around the pinhole were affected. The cells on the path of the pin insertion

90

were destroyed and left a gap after the pin was removed. The young xylary cells around the pinhole seemed to physiological affected and some of them were filled with substances that colored brown in the fresh cut wood surface and stained in the wood section. Callus cells formed by the cambial initials around the pinhole together with the cell debris in the gap formed the triangular mark (Figs. A7a, b, A8a). For the wood sections with a triangular mark, the position of the cambial zone at the time of pinning thus could be determined by the base of the isosceles triangular wound tissue (Figs. A6, A7a, b, A8a). However, for the sections which are far away from the pinhole center, on the edge of the pinhole, the position of the cambial zone could be recognized by the upper edge of the stained affected xylary tissue (Figs. A6, A7c, d).

With the position of the cambial zone at the time of pinning determined, the radial growth increment during the experimental period could be measured from the images of wood sections (Fig. A9). In sections which are near the edge of the pinhole the radial growth increment was measured from the center of the wound to the current cambium; and in sections which are close to the pinhole, the growth increment is the average of the measurements from both wound edges. For eliminating the methodological and artificial errors, we measured the radial growth increment in each of the serial sections of the same pinhole with three repetitions, the result showed that the radial growth increment is uniform in the three repetitions (Fig. A10).
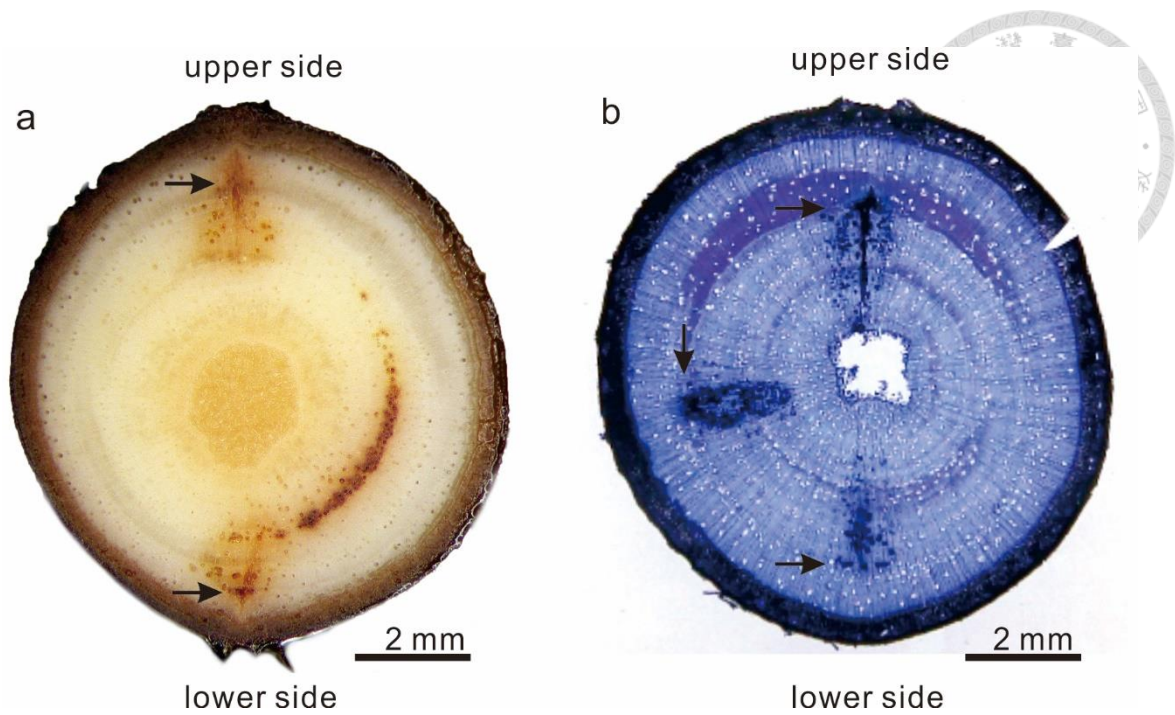
Figure A 5. Pinning marks in the cross sections of the inclined *K. henryi* stems.

a Two cambium marks (arrows) on the surface view of the razor blade-cut wood segment, the seedling was inclined on 04/23/2009, pinned on 05/23, and sampled on 07/23. **b** Three cambium marks (arrows) on the wood section made by a sliding microtome and stained with TBO, the seedling was inclined and pinned on 04/23/2009 and sampled on 10/20/2009.
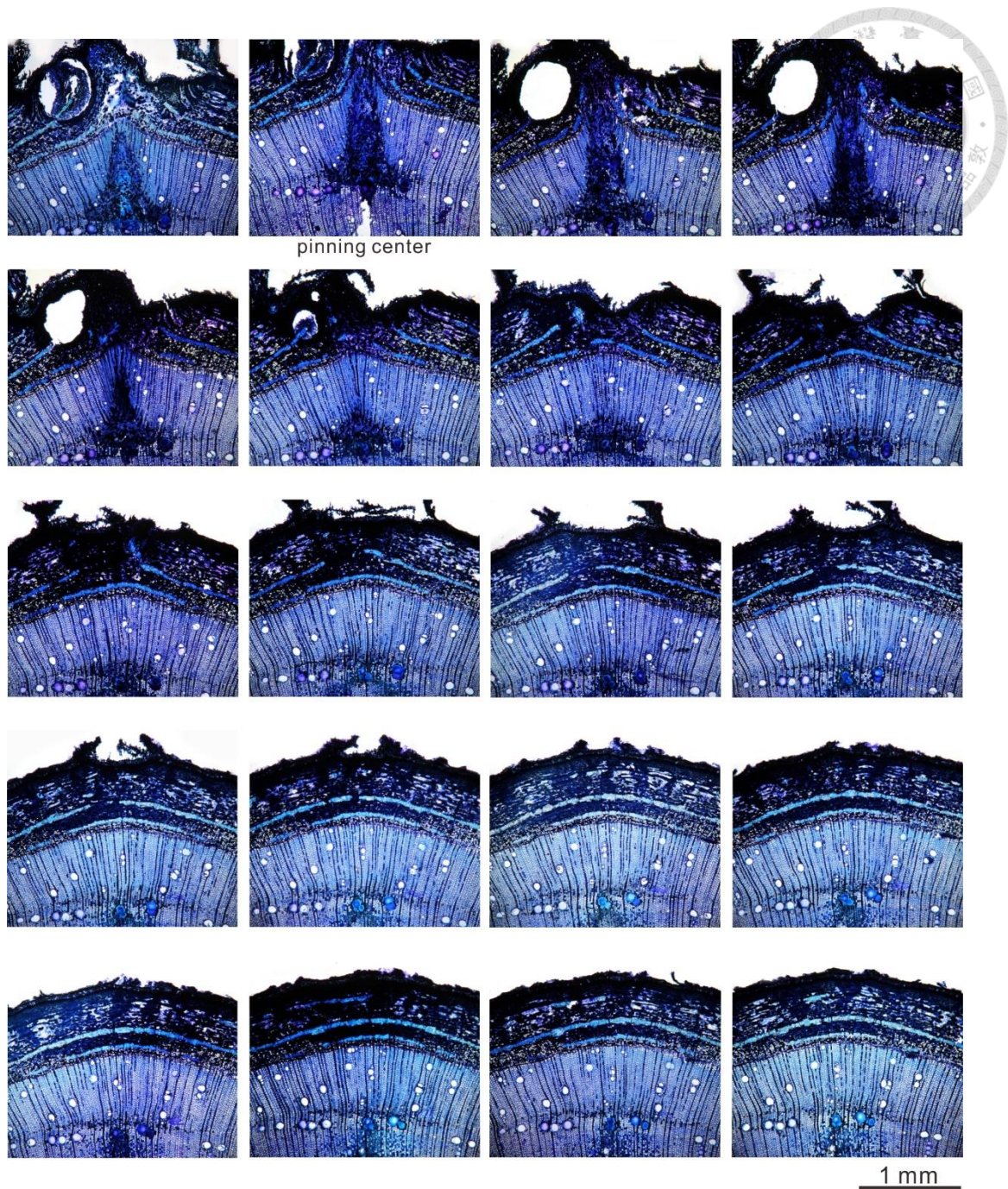
Figure A 6. Selected serial sections of a pinning mark in the normal wood from the pinning center to the edge.

The pinning was applied in an upright seedling on 4/23/2009 and sampled on 7/23. The section is 20 μm thick and the two adjacent sections are 100 μm apart. The wound area is a triangle in the center and the area decreases gradually to the edge.

93
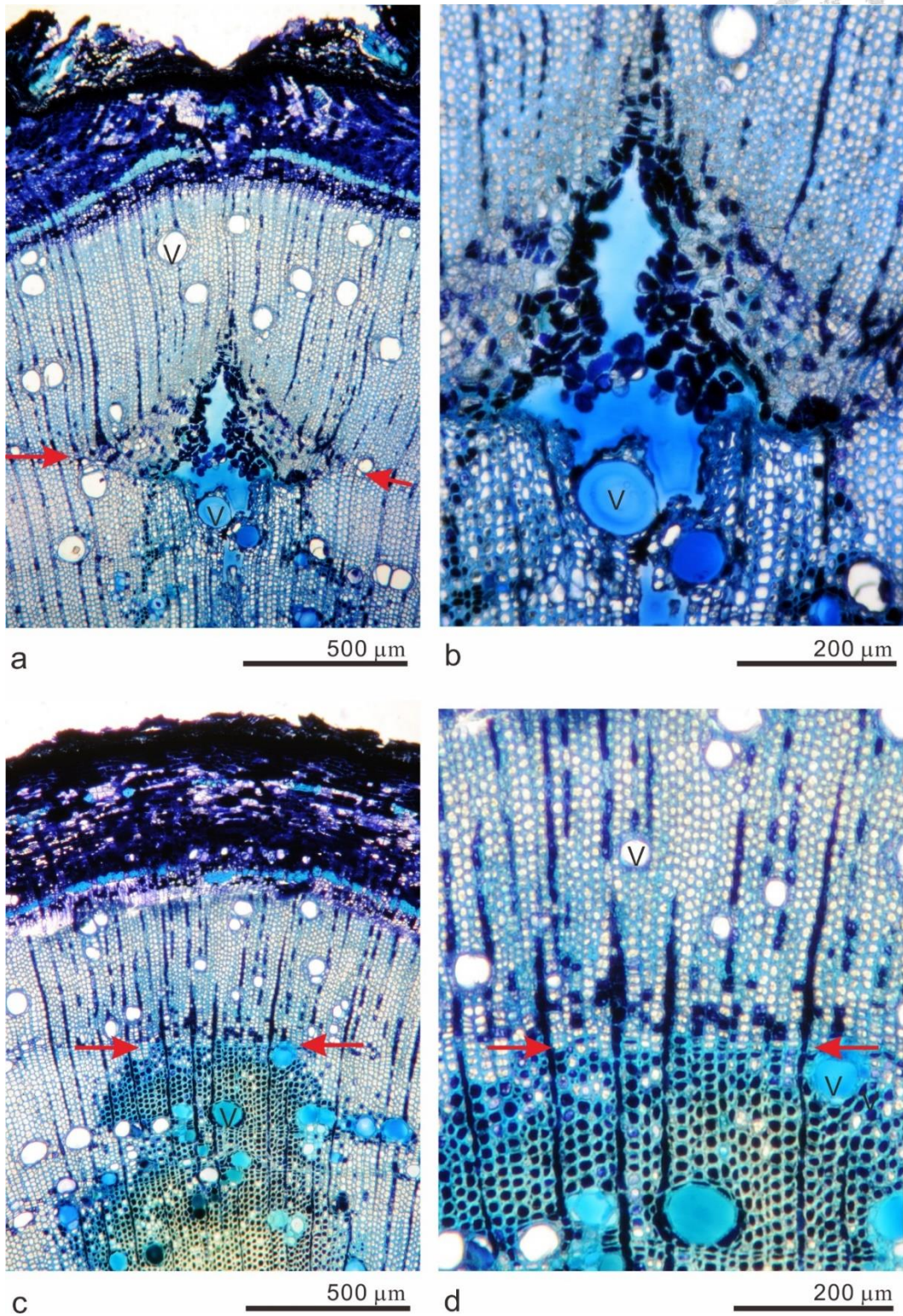
Figure A 7. Cross sections of a pin mark in the normal wood showing the wound tissue in the center (**a**, **b**) and at the edge of a pinhole (**c**, **d**).

V, vessel element. The arrows point to the position of the vascular cambium at the time of pinning

94
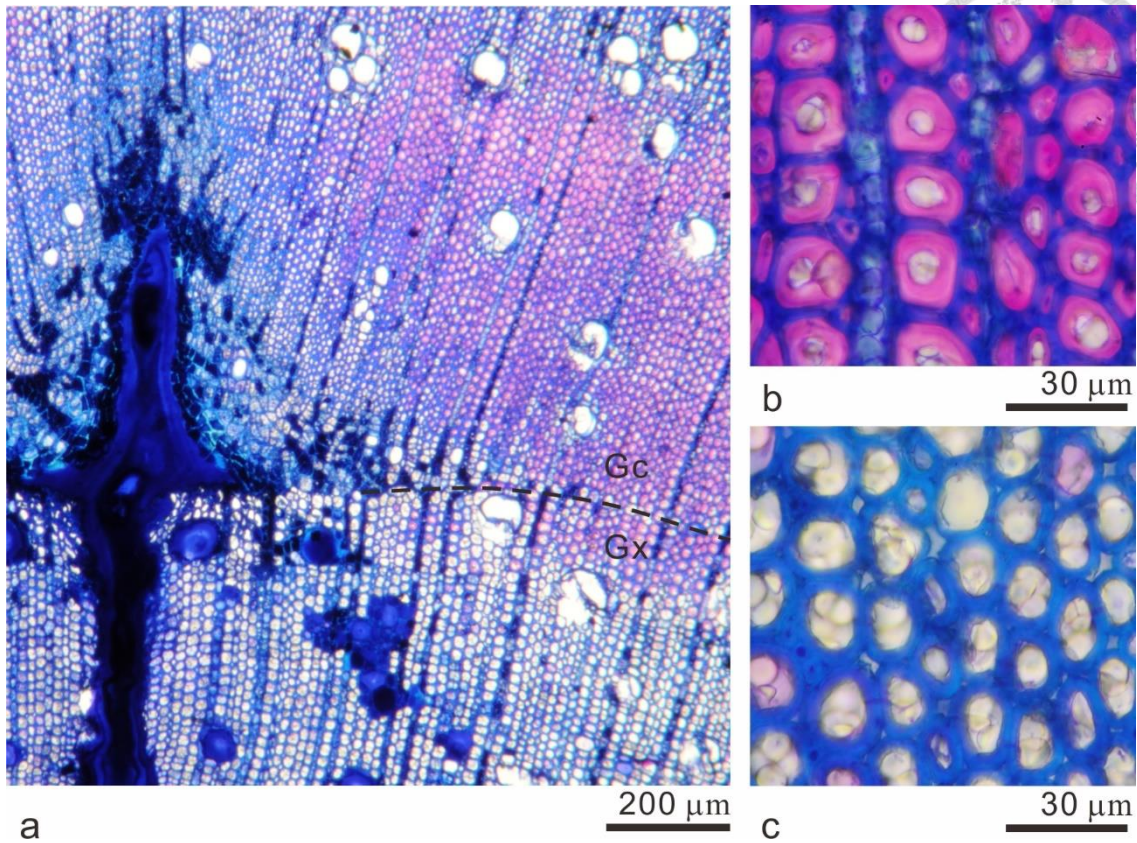
Figure A 8. Cross sections of a pinning mark in the tension wood.

a. With the cambium mark we can define the origin of the G-fibers. Most G-fibers are produce by the cambium after pinning (*Gc*) and some are developed from the developing xylary cells at the time of pinning (*Gx*). **b** G fibers. **c** normal wood fibers
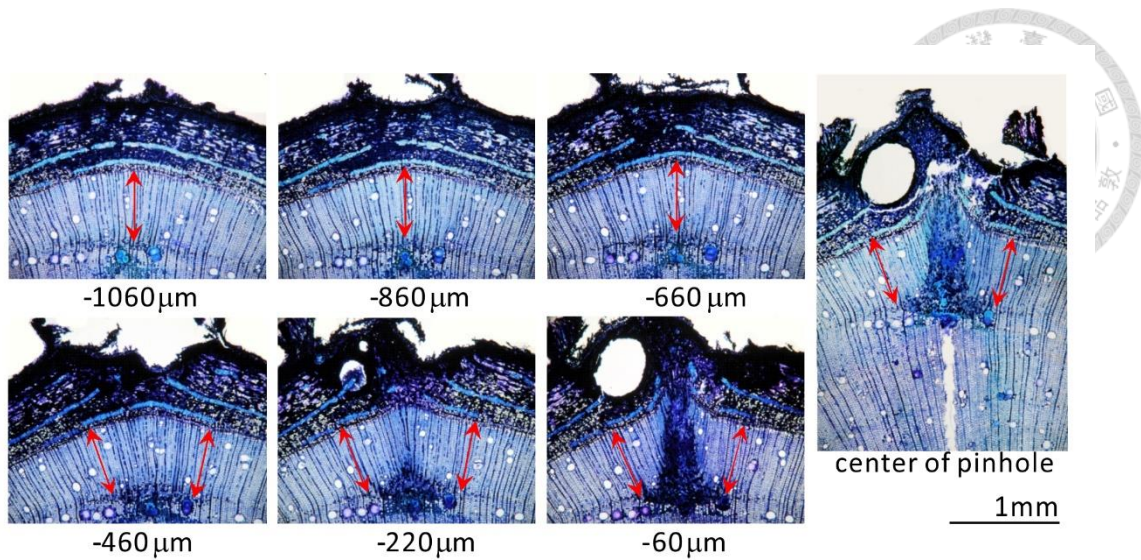
Figure A 9. The measurement of radial growth increment on the wood section marked by pinning.

The equal-length double-headed arrows indicate the growth increment after pinning. In sections which are far from the center of the pinhole, the growth increment is measured from the center of the wound to the current cambium; in sections near the pinhole, the growth increment is the average of the measurements from both wound edges. The distance of the section to the center of pinhole is labeled under the section.

96
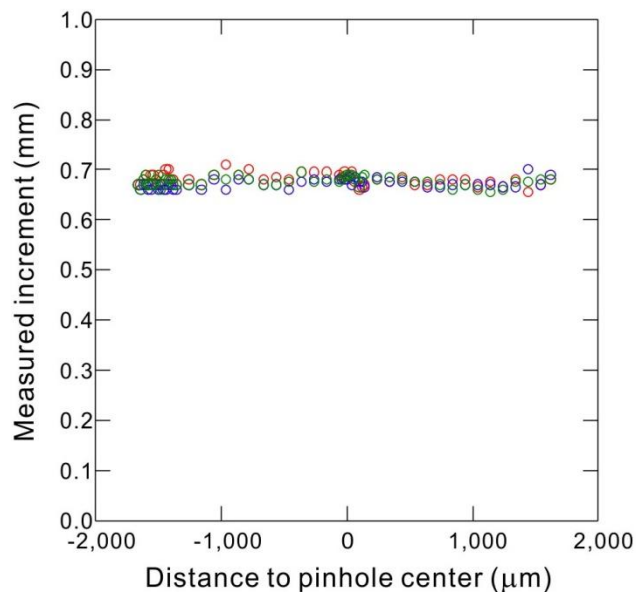
Figure A 10. Three independent measurements of radial increment via serial sections of one pinned sample.

The value of the radial growth increment is uniform in three repetitions along the pinhole, eliminating the methodological and artificial errors.
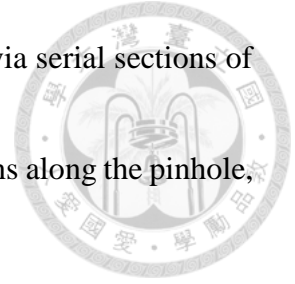
Appendix Ⅲ. Tension wood distribution in the studied seedlings

Sample preparation

For all the studied control and artificially inclined seedlings, stem segments of 3 cm long with the marked pinholes were collected and fixed in FPGA (Formalin: Propionic acid: Glycerol: 95% Alcohol: distilled water = 1: 1: 3: 7: 8). By using sliding microtome (ERMA optical works, Ltd), 20 μm thick wood sections containing pinning-induced callus were collected and stained with 1% toluidine blue O in 1% sodium borax (TBO). Whole stem sections were photographed by using a digital camera (Sony DSC-T200).

Results

Tension wood area is stained purple because of the cellulose rich G-layer, and thus can be distinguished from normal wood. For some of the control and the inclined seedlings, tension wood formed before the beginning of the experiment and they can be determined by the pinning mark. In the control upright *K. henryi* seedlings, no G-fibers were observed in the wood tissues formed after the experiment except on the B side of the half-height in the C10 seedling (Fig. A11). In contrast, in all inclined seedlings, a crescent tension wood zone containing G-fibers was observed on the upper side of the wood section (Fig. A12).
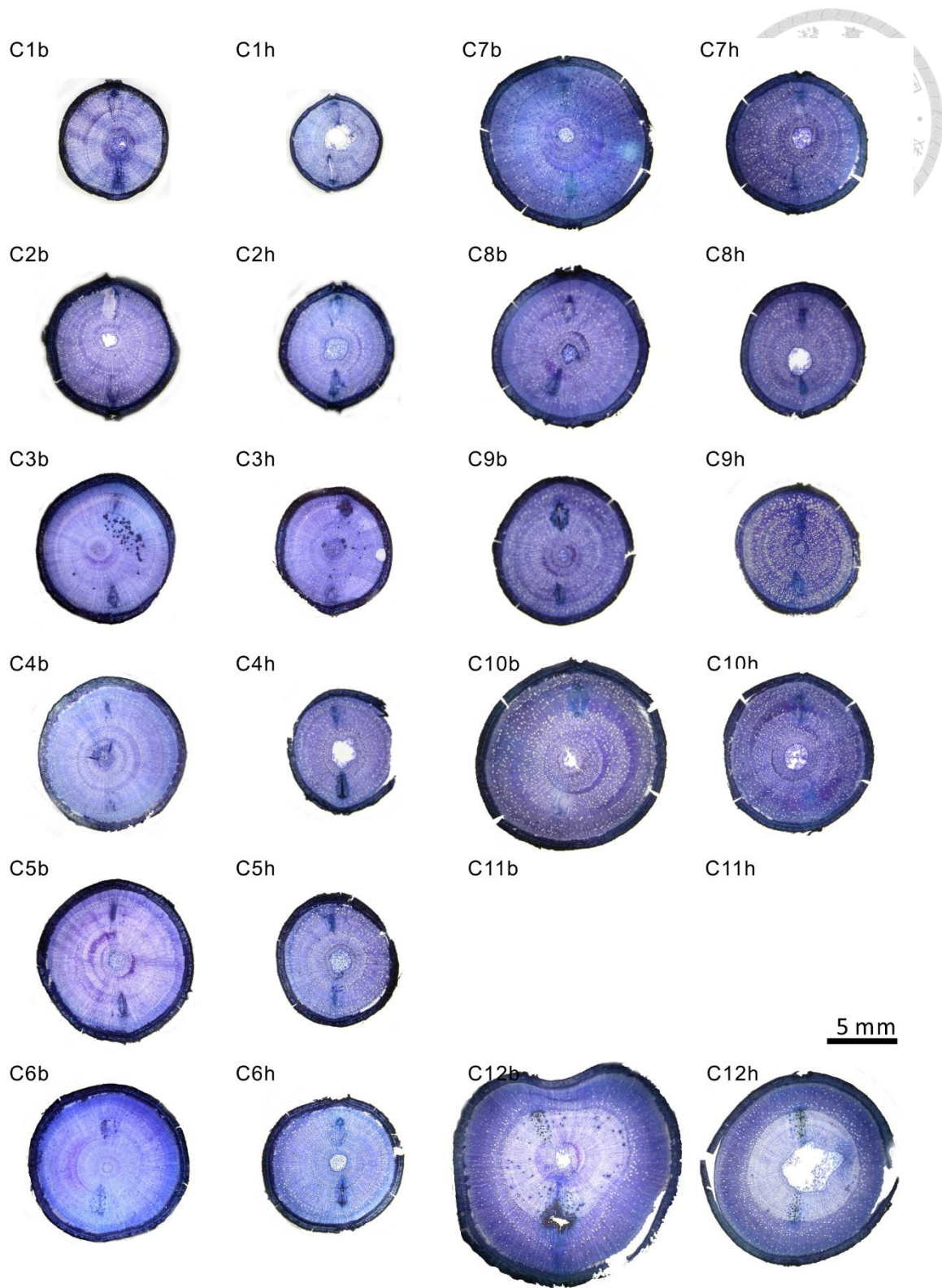
98

Figure A 11. Wood sections of the control upright seedlings (C) at the stem base (b) and the half-height (h).

T1b   T1h   T7b   T7h
T2b   T2h   T8b   T8h
T3b   T3h   T9b   T9h
T4b   T4h   T10b T10h
T5b   T5h   T11b T11h
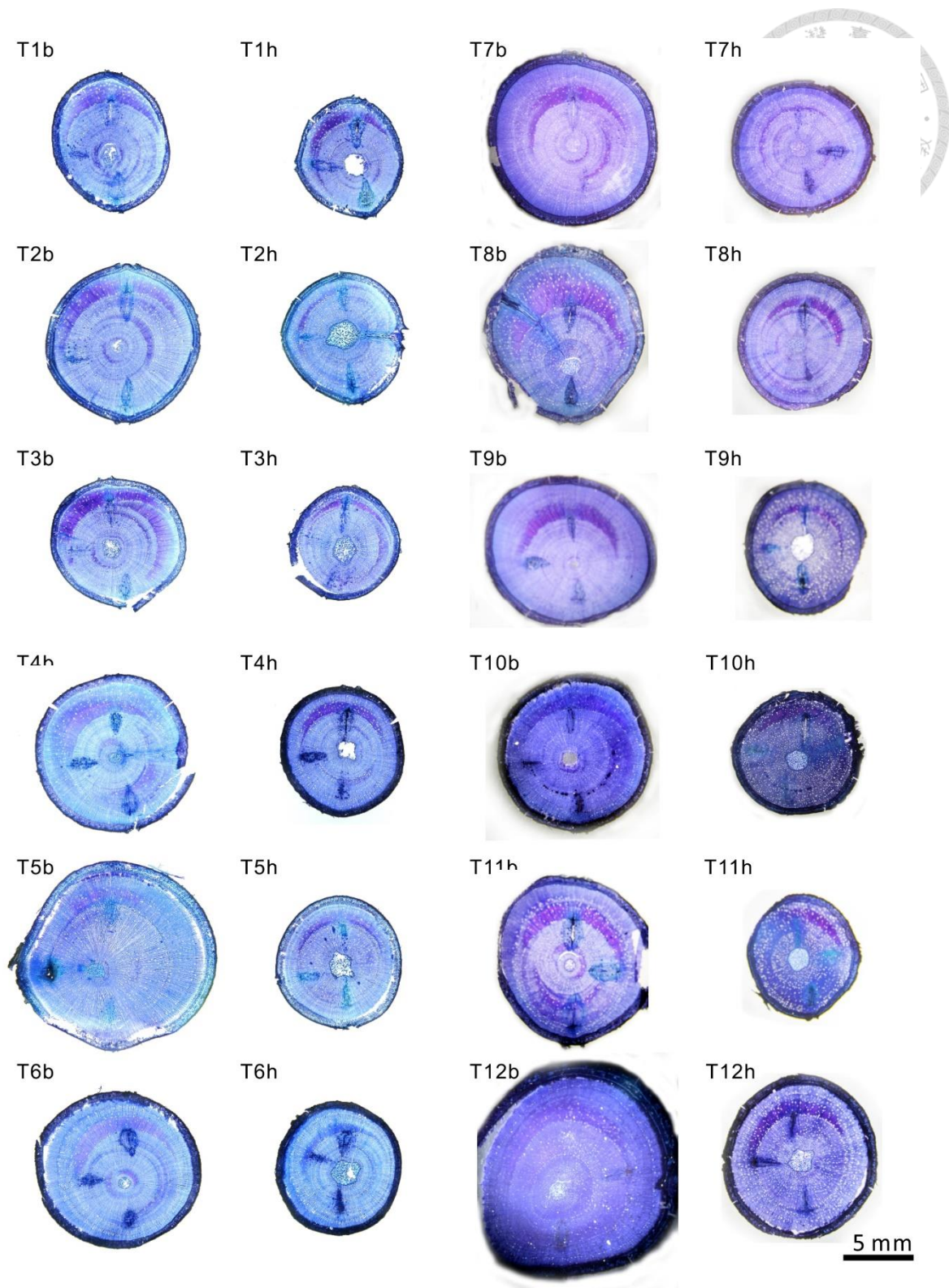T6b   T6h   T12b T12h

5 mm

Figure A 12. Wood sections of the inclined seedlings (T) at the stem base (b) and the half-height (h) showing tension wood distribution before and after the experiment.

100

Appendix Ⅳ. Cambial activity of the artificially inclined seedlings

Plant materials and sample preparation

For cambial activity observation, samples (1mm x 1mm x 2 mm) were cut from the upper side (A side) and the lower side (B side) of the inclined (control) trunk at 20 cm height above the ground, and fixed overnight with 2.5% glutaldehyde in 0.1M phosphate buffer. The samples were rinsed with phosphate buffer for 3 times to remove excessive fixative and post-fixed overnight with 1% osmium tetraoxide in 0.1M phosphate buffer. After rinsed with buffer for 3 times, the samples were dehydrated with acetone series, and then embedded in Spurr's resin (Spurr, 1969). Semi-thin sections were cut using an ultramicrotome (Ultracut E) and stained with Stevenel's blue (del Cerro et al, 1980). Photographs were taken by Leica Diaplan Microscope and Nikon D3 camera.

Results

The cambial activity was observed on the A side and the B side of all the upright seedlings (Fig. A13) and on the upper and the lower sides of all the inclined seedlings (Fig. A14) sampled on Jul. 23 (summer, C1~C3; T1~T3), Oct. 20 (autumn C4~C6; T4~T6) in 2009 and Feb. 1 (winter, C7~C9; T7~T9), Apr. 21 (spring, C10~C12; T10~T12) in 2010. Seasonal dynamic of wood formation was observed by counting cell numbers (per radial profile) of cambium, cell-enlarging xylem and wall-thickening xylem (Figs. A15, A16). In the summer, only two inclined seedlings were producing G-fiber while the others were rest. In the autumn, the cambia resumed activity on both sides of inclined and upright seedlings. In the winter, the cambial cells of all seedlings stopped dividing and entered into dormancy until the following spring when they regain activity.
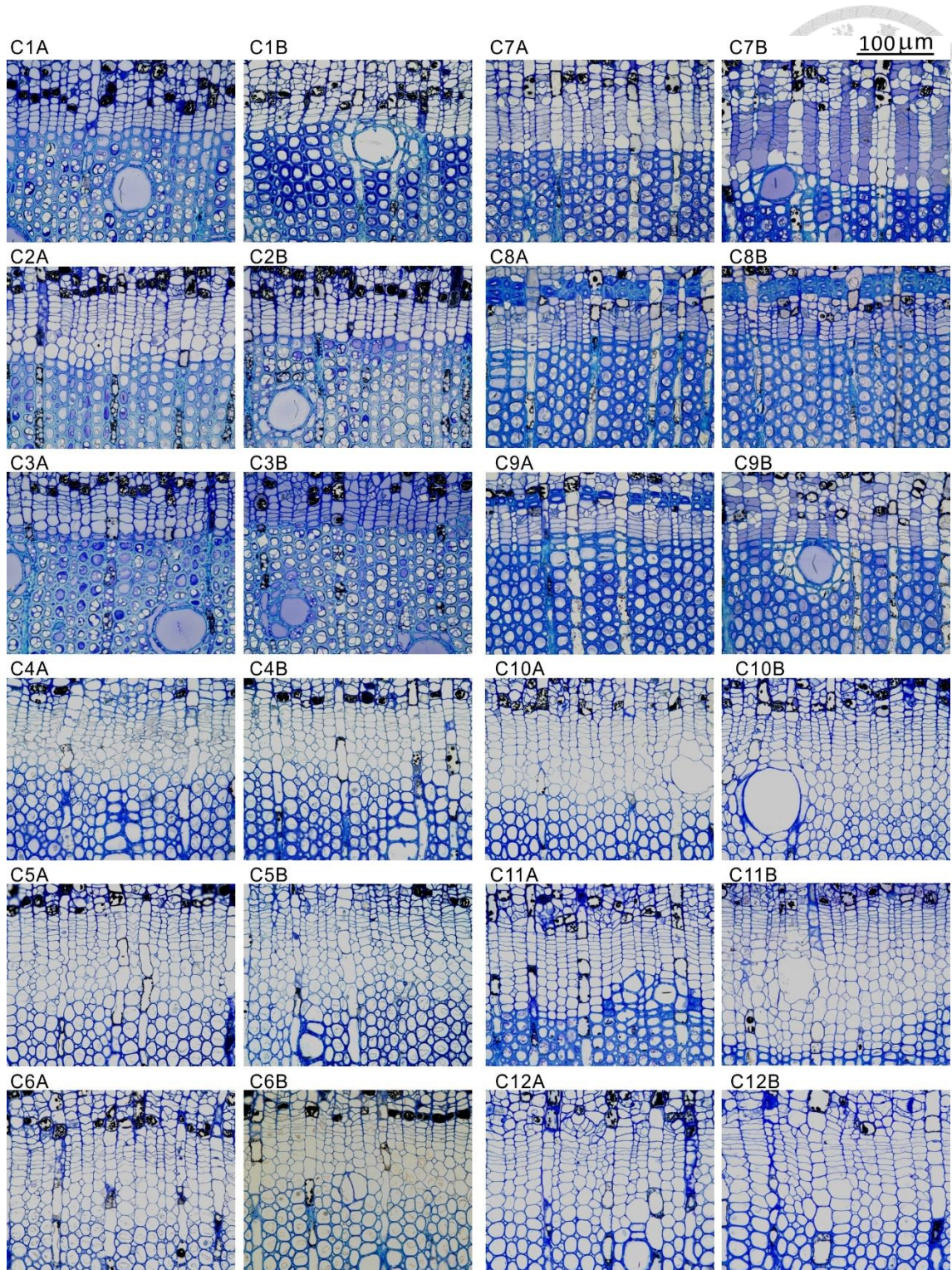
Figure A 13. Cross sections of cambial zone in the A and B side of the control upright seedlings (C)
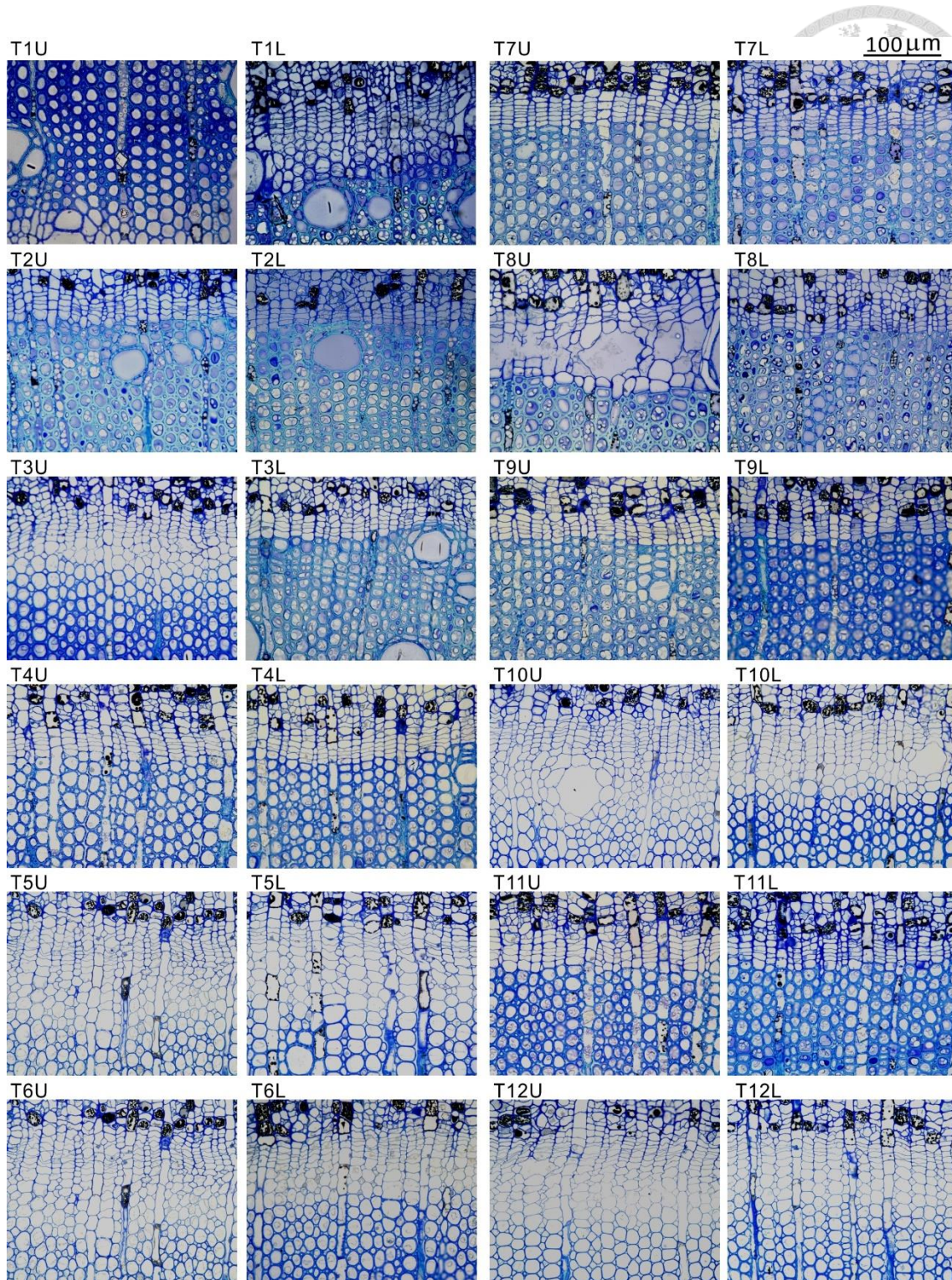
Figure A 14. Cross sections of cambial zone in the upper side (U) and the lower side (L) of the inclined seedlings (T)
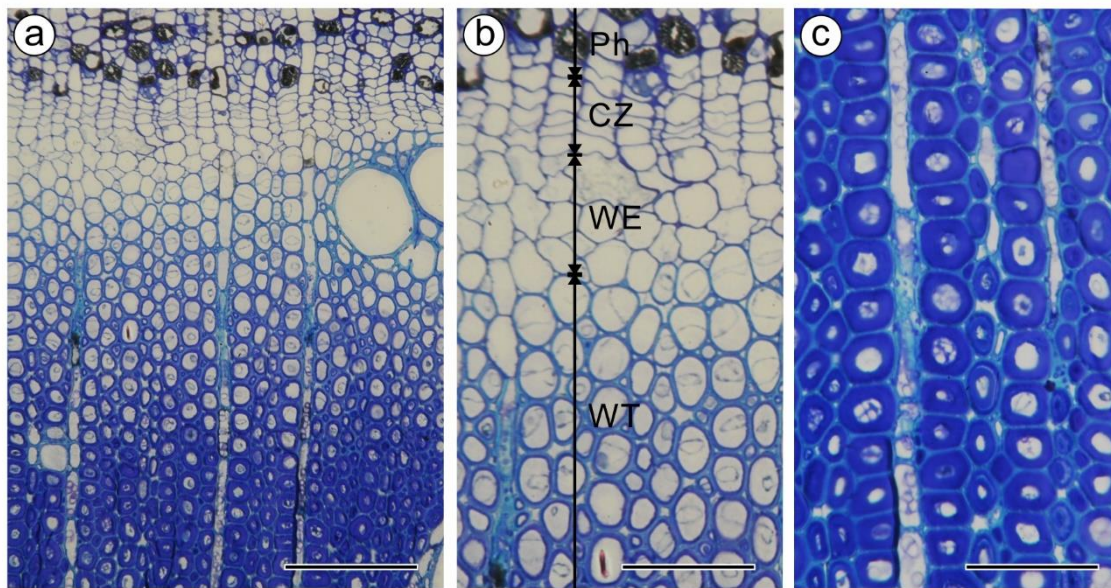
103

Figure A 15. Plastic sections showing tension wood formation in *K. henryi* seedling.
a Cross section of cambial zone and differentiating tension wood. **b** A close view showing the active cambial zone. **c** Mature G-fibers with thick G-layer in the innermost secondary wall. Bar = 100 μm in (A) and 50 μm in (B) and (C). *CZ*, cambial zone; *Ph*, phloem; *WE*, xylary cells undergoing wall enlargement and, *WT*, wall thickening
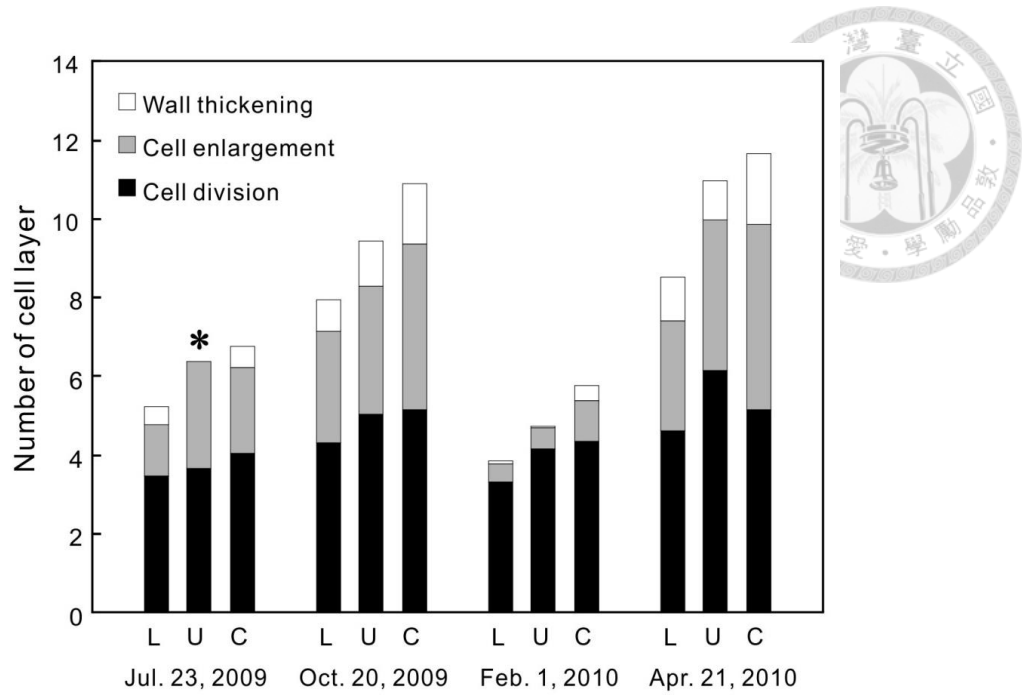
Figure A 16. Seasonal cambial activity of inclined seedlings and upright seedlings. L, the lower side; U, upper side; C, upright control. *indicates the G-layer thickening which is indiscernible under light microscope

Appendix Ⅴ. Tension wood induction in branches of *Koelreuteria henryi*

Plant materials and branch angle manipulation

For tension wood induction, on June 26, 2012, two young trees were selected and one branch each (B19 and B21) were bent down and another one each (B20 and B22) were bent up and tied to the trunk (Fig. A17). The strain measuring sites (B19-1, 3; B20-1, 3; B21-1, 2; B22-1, 2) were marked with white-out at 10 and 35 cm from the branch base. The vascular cambium was marked with a pin (0.4mm) inserting into the bark through the wood beside the measuring sites. The strains caused by the tie were measured on the surface of bark when the experiment was conducted. The branches were sampled on September 11, 2012. Unfortunately, the tree bearing B21 and B22 was blown down by a typhoon on August, the strains were only measured for the branches B19 and B20. The wood discs containing pinning marks obtained from all 4 branches were used for tension wood examination. For branches B 19 and B20, one wood disc each cut at 25 cm from the branch base (B19-2, B20-2) was also cut for tension wood examination.
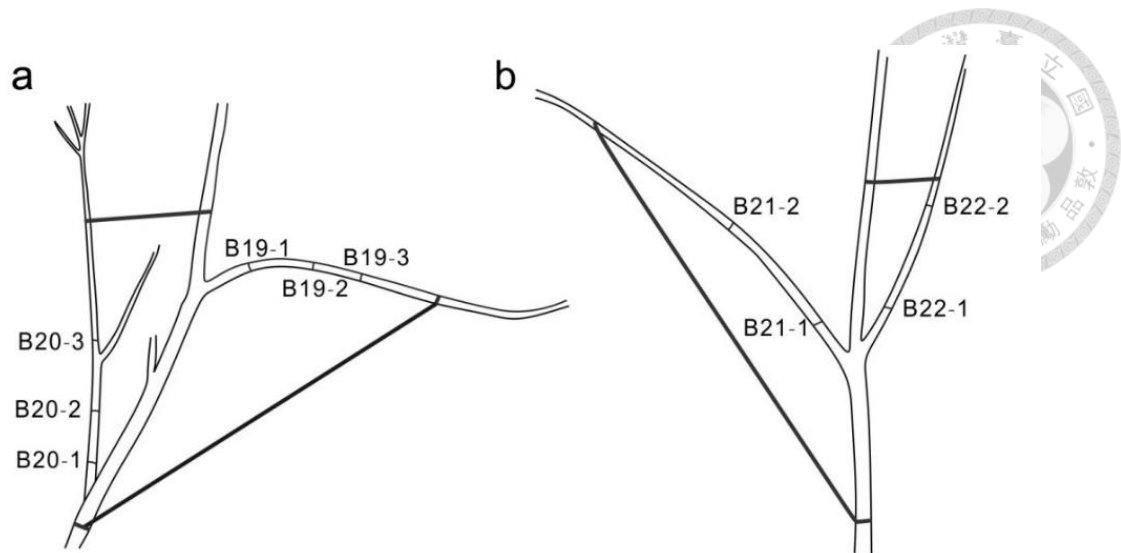
Figure A 17. The branches were tied with rope to manipulate the branch angle. B19 and B21 were bended down and B20 and B22 were bended up.

Results

Contractive strains were measured on the upper side of B19 and the lower side of B20 which were both tensile side; however, extensive strains were measured on the lower side of B19 and the upper side of B20 (Table A1).

The tension wood formed after the branches being tied could be identified with the aid of pinning marks. The formation of tension wood was affected by the pin insertion, we often found no tension wood formed around the pinhole. To avoid the interference of pin insertion, we examined an extra wood disc in between the two measuring sites in B19 and B20 (Fig. A18, A19). For branches B19 and 21 which were bending down, tension wood formed on the upper side with tensile stress; and for B20 and B22 which were

107
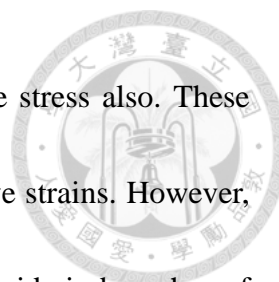
bending down, tension wood formed on the lower side with tensile stress also. These

results suggest that tension wood associated with a higher contractive strains. However,

no obvious anatomical characteristic was found on the compressive side in branches of

Koelreuteria henryi.

Table A 1. Experimental data of the branch angle manipulation study of *Koelreuteria henryi*

|	L (cm)	Strain caused by being tied		Calibration while being tied		Strain after releasing rope		Spring back strain		Strain after being cut	
		upper	lower	upper	lower	upper	lower	upper	lower	upper	lower
B19-1	10 cm	4617	-3784	0	0	-670	1074	-1334	2021	-1409	1215
B19-3	35 cm	1668	-2472	0	0	-403	984	-997	2349	-1135	5
B20-1	10 cm	-3510	4807	0	0	2540	-1577	1888	-1063	2234	-1179
B20-3	35 cm	-2287	4060	0	0	3270	-1558	2915	-1015	3525	-1107
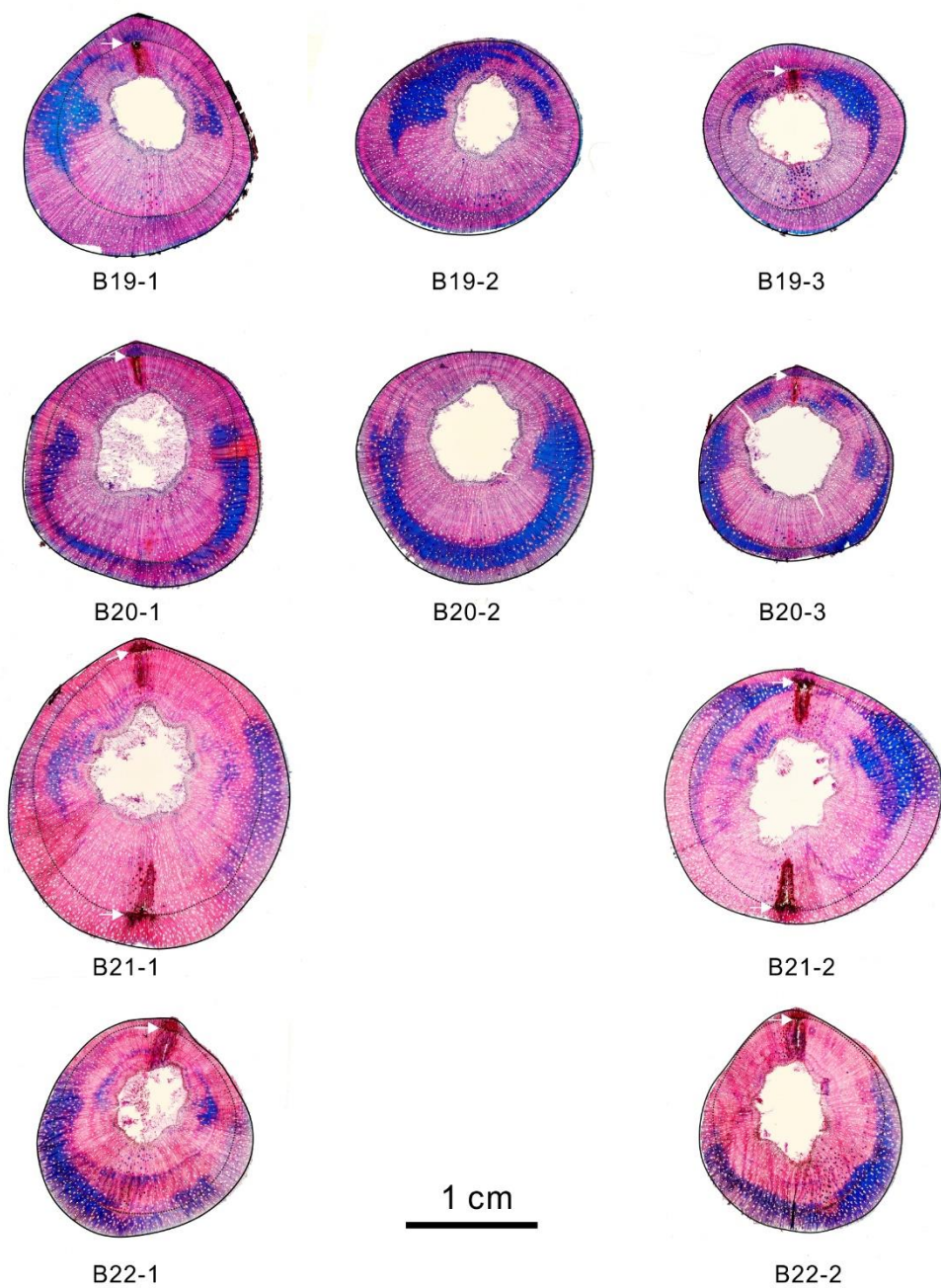
Figure A 18. Wood sections double stained with safranin O and alcian blue showing the pinning mark (white arrows) and tension wood distribution.

For branches B19 and 21 which were bending down, tension wood formed on the upper side with tensile stress; and for B20 and B22 which were bending down, tension wood formed on the lower side with tensile stress.
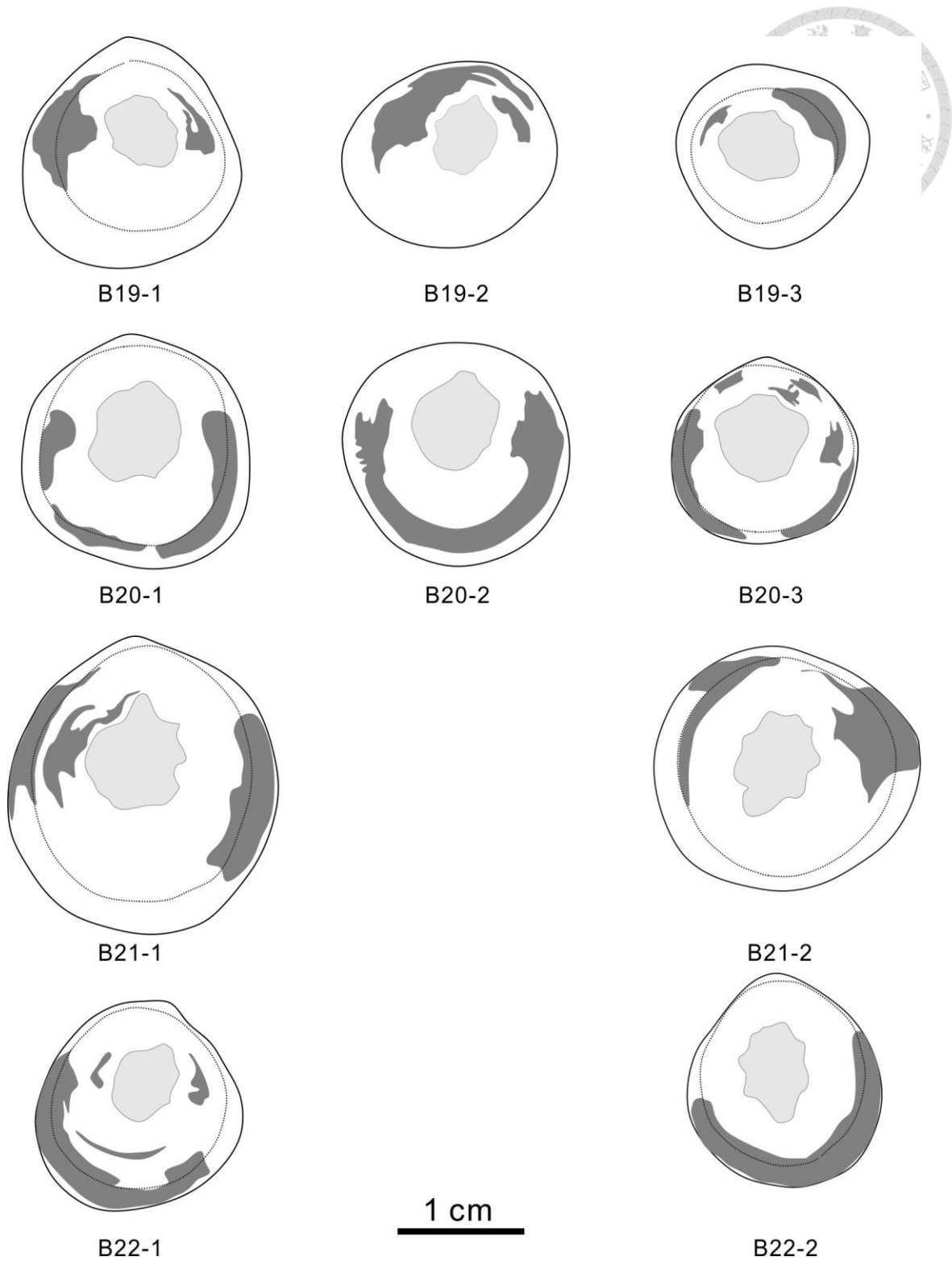
Figure A 19. Illustration showing the tension wood distribution on the tied branches.

110